

GSFC JPSS CMO
May 19, 2015
Released

**Joint Polar Satellite System (JPSS) Ground Project
Code 474
474-00090**

**Joint Polar Satellite System (JPSS)
Operational Algorithm Description
(OAD)
Document for VIIRS Geolocation
(GEO) Sensor Data Record (SDR) and
Calibration (CAL) SDR Software**

For Public Release

The information provided herein does not contain technical data as defined in the International Traffic in Arms Regulations (ITAR) 22 CFC 120.10. This document has been approved For Public Release to the NOAA Comprehensive Large Array-data Stewardship System (CLASS).



**Goddard Space Flight Center
Greenbelt, Maryland**

National Aeronautics and
Space Administration

**Joint Polar Satellite System (JPSS)
Operational Algorithm Description (OAD) Document for
VIIRS Geolocation (GEO) Sensor Data Record (SDR) and
Calibration (CAL) SDR Software
JPSS Electronic Signature Page**

Prepared By:

Bruce Guenther
JPSS Data Products and Algorithms SDR Lead
(Electronic Approvals available online at (https://jpssmis.gsfc.nasa.gov/mainmenu_dsp.cfm))

Approved By:

Gilberto Vicente
JPSS Ground Project Algorithm Integration Team (AIT) Manager
(Electronic Approvals available online at (https://jpssmis.gsfc.nasa.gov/mainmenu_dsp.cfm))

**Goddard Space Flight Center
Greenbelt, Maryland**

Preface

This document is under JPSS Ground Algorithm ERB configuration control. Once this document is approved, JPSS approved changes are handled in accordance with Class I and Class II change control requirements as described in the JPSS Configuration Management Procedures, and changes to this document shall be made by complete revision.

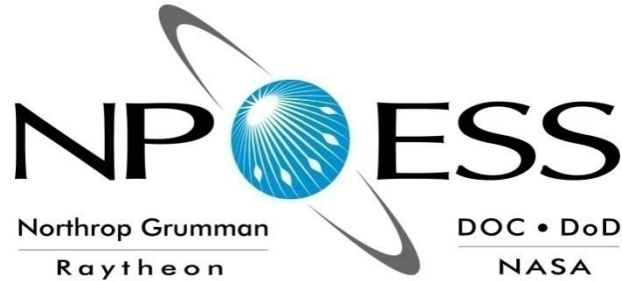
Any questions should be addressed to:

JPSS Configuration Management Office
NASA/GSFC
Code 474
Greenbelt, MD 20771

Change History Log

Revision	Effective Date	Description of Changes (Reference the CCR & CCB/ERB Approve Date)
Original	08/24/2011	This version incorporates 474-CCR-11-0105 : (This version baselines D41868, Rev A dated 09/22/2010. This is the version that was approved for NPP launch. Per NPOESS CDFCB - External, Volume V – Metadata, doc number D34862-05, this has been approved for Public Release into CLASS.) to create JPSS version, Rev-. This was approved by the JPSS Ground Algorithm ERB on August 24, 2011.
Revision A	01/18/2012	474-CCR-11-0250 : This version baselines 474-00090, Joint Polar Satellite System (JPSS) Operational Algorithm Description (OAD) Document for VIIRS Geolocation (GEO) Sensor Data Record (SDR) and Calibration (CAL) SDR Software, for the Mx 6 IDPS release. This CCR was approved by the JPSS Algorithm ERB on January 18, 2012.
Revision B	10/09/2012	474-CCR-12-0627 : This version authorizes 474-00090, Joint Polar Satellite System (JPSS) Operational Algorithm Description (OAD) Document for VIIRS Geolocation (GEO) Sensor Data Record (SDR) and Calibration (CAL) SDR Software, for the Mx 6.1 – 6.3 IDPS releases. Includes: ECR-ALG-0035 which contains Raytheon PCR030210; OAD: Implement 474-CCR-12-362 (VIIRS SDR Code and LUT Mods for scan-by-scan RSB Calibration) (ADR 4586) updated Table 19. Raytheon PCR030559, OAD: Implement 474-CCR-12-0402 (Add Mirror Side Information to VIIRS SDR Geolocation Files) (ADR 4703), updated Table 13 and section 2.2.2.28. Raytheon PCR030617; OAD: Implement 474-CCR-12-0406 (VIIRS-SDR Reflective Band Limits SZA Modified to 89 Degrees from 85 Degrees) (ADR 4277), updated Section 2.3.2.3. Raytheon PCR031579; OAD: Implement 474-CCR-12-0490 (Modify Cal Sector Data in VIIRS OBC-IP) (ADR 4743, 4744, 4745, 4820) updated Tables 3, 18 & 31. Raytheon PCR031615, OAD: Implement 474-CCR-12-0489 (Add VIIRS Scan Encoder Electronics Side Indicator to VIIRS SDR GEO QF's) (ADR 4759), updated Tables 9-13.
Revision C	05/14/2013	474-CCR-13-0948 : This version authorizes 474-00090, JPSS OAD Document for VIIRS GEO SDR and CAL SDR Software, for the Mx 7.0 IDPS release. Includes Raytheon PCR032720; 474-CCR-13-0916/ECR-ALG-0037: Update applicable OAD filenames/template/Rev/etc. for Mx7 Release.
Revision D	07/10/2013	474-CCR-13-1101 : This version authorizes 474-00090, JPSS OAD Document for VIIRS GEO SDR and CAL SDR

		Software, for the Mx 7.1 IDPS release. Includes Raytheon ECR-ALG-0039. Includes PCR033683: OAD: Implement 474-CCR-12-0730 (Create a VIIRS GEO QF When HAM/RTA Sync is Lost and For Sector Rotation) (ADRs 4767, 4776, 4777, 4795, 4981, 4992), in Tables 13 & 26. Includes PCR034044: OAD: Implement 474-CCR-13-0885 (VIIRS SDR Products Generated During WUCD Should Be Flagged) (ADR 4710), in Table 26.
Revision E	11/06/2013	474-CCR-13-1288: This version authorizes 474-00090, JPSS OAD Document for VIIRS GEO SDR and CAL SDR Software, for the Mx 8.0 IDPS release. Includes administrative changes authorized by interoffice memo and Raytheon PCR034496; OAD; PRO: 474-CCR-13-0876 Automated VIIRS RSB (Reflective Solar Band) Calibration - DR4663 by updating sections of 2.3 and most of section 2.4. Also includes Raytheon PCR034560; OAD: PRO: 474-CCR-13-1007: Add VIIRS DNB Stray Light Correction to VIIRS SDR (DR 7060), in tables 19 & 26.
Revision F	03/05/2014	474-CCR-14-1590: This version authorizes 474-00090, JPSS OAD Document for VIIRS GEO SDR and CAL SDR Software, for the Mx 8.3 IDPS release. Includes Raytheon PCR036358; CHILD: PRO: OAD: 474-CCR-13-1220: LWIR Bands Not Marked Invalid - DR 4501, in table 26.
Revision G	04/30/2014	474-CCR-14-1702: This version authorizes 474-00090, JPSS OAD Document for VIIRS GEO SDR and CAL SDR Software, for the Mx 8.4 IDPS release. Includes Raytheon PCRs (3): (1)-PCR037017; CHILD: PRO: OAD: 474-CCR-13-1362: Add VIIRS Terrain-Corrected DNB Geolocation in the Products (DR 4924), in Tables 9, 14 & 18, (2)-PCR037484; CHILD: PRO: OAD: 474-CCR-13-1244: Space View (SV) Lunar Intrusion Test in RSBAutoCal - DR 7336, in Table 34, (3)-PCR037914; Child: PRO: OAD: 474-CCR-14-1595: Geolocation Document Changes (DR 7550), in Tables 9-12.
Revision H	05/13/2015	474-CCR-15-2428: This version authorizes 474-00090, JPSS OAD Document for VIIRS GEO SDR and CAL SDR Software, for the Mx 8.9 IDPS release. Includes Raytheon PCR046789; Child: PRO: OAD: 474-CCR-15-2345: VIIRS Radiance and Reflectance/Brightness Temperature Upper Bounds & Quality Flagging Are Inconsistent - DR 7294 VIIRS SDR OAD, in Tables 1 and 27.



NATIONAL POLAR-ORBITING OPERATIONAL ENVIRONMENTAL SATELLITE SYSTEM (NPOESS)

OPERATIONAL ALGORITHM DESCRIPTION DOCUMENT FOR VIIRS GEOLOCATION (GEO) SENSOR DATA RECORD (SDR) and CALIBRATION (CAL) SDR

**SDRL No. S141
SYSTEM SPECIFICATION SS22-0096**

**RAYTHEON COMPANY
INTELLIGENCE AND INFORMATION SYSTEMS (IIS)
NPOESS PROGRAM
OMAHA, NEBRASKA**

**Copyright © 2004-2012
Raytheon Company
Unpublished Work
ALL RIGHTS RESERVED**

Portions of this work are the copyrighted work of Raytheon. However, other entities may own copyrights in this work. Therefore, the recipient should not imply that Raytheon is the only copyright owner in this work.

This data was developed pursuant to Contract Number F04701-02-C-0502 with the US Government under subcontract number 7600002744. The US Government's right in and to this copyrighted data are as specified in DFAR 252.227-7013, which was made part of the above contract.

Northrop Grumman Space & Mission Systems Corp.
Space Technology
 One Space Park
 Redondo Beach, CA 90278



**Engineering & Manufacturing Development (EMD) Phase
 Acquisition & Operations Contract**

CAGE NO. 11982

**Operational Algorithm Description
 VIIRS SDR**

Document Number: D41868
Revision: B7

Document Date: Nov 04, 2011

PREPARED BY:

 Ronson Chu *Date*
AM&S VIIRS SDR Lead

 Paul D. Siebels *Date*
IDPS PRO SW Manager

ELECTRONIC APPROVAL SIGNATURES:

 Roy Tsugawa *Date*
SEIT Lead & ACCB Chair

 Bob Hughes *Date*
Algorithm Implementation Thread Lead

 Bob Hughes *Date*
Data Product System Engineering Lead

 Stephen E. Ellefson *Date*
IDPS Processing SI Lead

Prepared by
Northrop Grumman Space Technology
 One Space Park
 Redondo Beach, CA 90278

Prepared for
Department of the Air Force
 NPOESS Integrated Program Office
 C/O SMC/CIK
 2420 Vela Way, Suite 1467-A8
 Los Angeles AFB, CA 90245-4659

Under
Contract No. F04701-02-C-0502

This document has been identified per the NPOESS Common Data Format Control Book – External Volume 5 Metadata, D34862-05, Appendix B as a document to be provided to the NOAA Comprehensive Large Array-data Stewardship System (CLASS) via the delivery of NPOESS Document Release Packages to CLASS.

Northrop Grumman Space & Mission Systems Corp. Space Technology One Space Park Redondo Beach, CA 90278		 	
Revision/Change Record			Document Number D41868
Revision	Document Date	Revision/Change Description	Pages Affected
---	8-31-04	Initial Release VIIRS Geolocation (GEO) SDR Software.	All
---	9-30-04	Initial Release VIIRS SDR Calibration Software.	All
A1	6-8-06	06Oct05 - Reflects continued Science To Operational Code Conversion combining VIIRS GEO SDR OAD and VIIRS Calibration SDR OAD since official delivery of separate documents to NGST on 15Sep05. 14Mar06 – Updated copyright on coversheet; inserted latest Unit Test dated 9Mar06 (31 pages); updated Table of Content page numbers and List of Table page numbers; addressed Omaha QA comments from Code Completion Peer Review (CCPR) on 14Mar06. 15Mar06 – Continued to edit based on Omaha QA comments, individually listing all 60 TBDs versus lumping them together per the Table they reside in; fixing Table references in the text, etc. 20Mar06 – Updated Section 1.3.3 Source Code and Test Data References. 28Mar06 – Minor edits to fix Doug Rishel CCPR comments. 29Mar06 – Changed upper right header document number to only use the originally dropped VIIRS Geolocation SDR OAD (D39300) number although this document incorporates a lot of information from the originally dropped VIIRS SDR Calibration OAD (D39553). 21Apr06 – Added viirs_decmp function information and updated TOC 11May06 – Updated for SDR Optimization modifications 08 Jun06 – Updated Document Numbers. Original VIIRS Geolocation OAD D39300. Original VIIRS Calibration OAD D39553. These 2 OADs combined into this single OAD.	All
A2	12-11-06	Add Section 2.3.1.4 for new “createRadianProducts()” method.	All
A3	2-16-07	Updated for DDPR AIs.	All
A4	5-3-07	Rename and modify Section 2.3.1.4.	All
A5	6-18-07	Updated for CCPR AIs.	All

Northrop Grumman Space & Mission Systems Corp. Space Technology One Space Park Redondo Beach, CA 90278		 	
Revision/Change Record			Document Number D41868
Revision	Document Date	Revision/Change Description	Pages Affected
A6	7-3-07	Updated for the implementation of NP-EMD.2005.510.0122_VIIRS_CAL_SD_Detailed_Code_Changes_Oct_2005 NP-EMD-2007.510.0014_VIIRS_SDR_Cal_Modif_Implement_OAD NP-EMD-2007.510.0009_VIIRS_SDR_Even_odd_subframe_design NP-EMD-2007.510.0010_VIIRS_SDR_Robust_Alg_design NP-EMD-2007.510.0012_NPP_VIIRS_CAL_EV_Detailed_Code_Changes_Feb_2007	All
A7	8-2-07	Delivered to NGST.	All
A8	9-27-07	Implemented NP-EMD-2007.510.0029_NPP_VIIRS_SDR_DNB_FirstFrameAnomaly.	All
A9	11-9-07	Added S/C Attitude to non-gridded geolocation outputs. Responded to PR comments – ECR A-122.	All
A10	12-17-07	ECR A-103, EDR-PR 1.8 CP 3, and CDFCB-X compliance updates: updated non-gridded geolocation output structures and quality flags and the SDR scan-level quality flags.	All
A11	2-22-08	Reformatted in accordance to new template. Implementation of NP-EMD.2005.510.0134, NP-EMD.2005.510.0119, NP-EMD.2005.510.0065, NP-EMD.2005.510.0067, NP-EMD.2005.510.0069, NP-EMD.2005.510.0071, NP-EMD.2005.510.0074, NP-EMD.2005.510.0081, MP-EMD.2005.510.0064, NP-EMD.2005.510.0075, NP-EMD.2005.510.0004, NP-EMD.2005.510.0012, NP-EMD.2005.510.0068, NP-EMD.2005.510.0125, NP-EMD.2006.510.0098, NP-EMD-2007.510.0011, NP-EMD-2007.510.0013. Added Bright Pixel sections. Incorporated updates from NGST comments pertaining to previous delivery. Delivered to NGST.	All
A12	2-25-08	Accept all track changes for re-baselined version.	All
A13	8-18-08	Updated in accordance with NP-EMD.2008.510.0027.	All
A14	10-17-08	Updated in accordance with NP-EMD-2008.510.0019. Remove moon_vector field from VIIRS-OBC-IP. Incorporated comments from previous delivery. Updated cover sheet and Acronym list. Delivered to NGST.	All

Northrop Grumman Space & Mission Systems Corp. Space Technology One Space Park Redondo Beach, CA 90278		 	
Revision/Change Record			Document Number D41868
Revision	Document Date	Revision/Change Description	Pages Affected
A15	11-12-08	Minor changes for PCR 18378, VIIRS SDR Refactor, to remove specific references to ProSdrViirs.	5, 7
A16	3-18-09	Incorporated comments from SDRL Delivery. Fixed definition of Moon Phase, typo in definition of SolarAzimuth, bit numbering in Scan Level Geolocation Quality Byte, and updated OBC structure definition. Updated Table 9 for IPO Issue. Prepared OAD for TIM – (All pages).	20-25, 45-47
A17	6-15-09	Incorporated TIM comments and prepared for ARB/ACCB. Updated the obc-ip output structure – PCR19290/PCR 20614. ARB actions delayed until after Sep 09, revision increment returned to header(s).	All Table 31
A18	7-06-09	PCR 15261 Removed Sensor Dependent column since all AUX items are sensor dependent. Updated the obc-ip output structure ECR 878 changes.	Table 19, Table 31
A19	7-07-09	NP-EMD.2008.510.0050 VIIRS GEO EVtimes Updates	Tables 9, 10, 11, 12, and 31, Section 2.1.2.5
A20	11-04-09	Updated for ECR-878 Changes which fixed packet info.	All
A21	01-13-10	Implemented: NP-EMD.2009.510.0047_VIIRS_GEO_DNB_AggZoneFix, NP-EMD.2009.510.0048 Rev A VIIRS Geo Quality Flags Logic Updates, NP-EMD-2009.510.0033 Rev A VIIRS SDR OAD Updates to the Geolocation Parameters Table, NP-EMD-2009.510.0031 Rev A Solar Diffuser LUT Read Update, NP-EMD-2009.510.0042 Solar Diffuser Cal SDSM Angle Fix. k Updated for 878 Changes which fixed packet info. NP-EMD-2009.510.0041 SDR Calibration Imagery Even Odd Parity Fix Code Update	All
A22	02-25-10	Implemented: NP-EMD-2009.510.0052 VIIRS Bright Pixel ID Algorithm Update	Tables 1, 2

Northrop Grumman Space & Mission Systems Corp. Space Technology One Space Park Redondo Beach, CA 90278		 	
Revision/Change Record			Document Number D41868
Revision	Document Date	Revision/Change Description	Pages Affected
A23	06-17-10	Implemented ECR-A280: NP-EMD.2010.510.0003_SDR_and_SDCal_RVS_LUT_Update NP-EMD.2010.510.0007-Rev-A_SDR_Calibration_Thermistor_LUT_Update NP-EMD.2010.510.0008_VIIRS_SDR_Calibration_OBC_Blackbody_Calibration_Update NP-EMD.2010.510.0011_SDR_Calibration_RSR_LUT_Update NP-EMD.2010.510.0012_VIIRS_SDR_Cal_DNB_Stray_Light_Quality_Flag NP-EMD.2010.510.0013_VIIRS_SDR_Cal_DG_Anomaly_Quality_Flag NP-EMD.2010.510.0021_VIIRS_SDR_Calibration_EMI_Spike_Filter NP-EMD.2010.510.0016_Solar_Diffuser_LUT_Update	All
A24	6-22-10	Updated Tables 1 & 2, coversheets, font, and format throughout document.	All
A25	7-08-10	Updated for SDRL	All
A26	8-17-10	Incorporated TM 2010.510.0004	All
A27	8-23-10	Incorporated VIIRS SDR fixes for ADCM-010	Tables 1 & 2
A28	9-16-10	Updated for TIM/ARB	All
A	9-22-10	Incorporated TIM and ARB comments in preparation for ACCB (ECR-A325)	All
B1	9-29-10	Updated for Algorithm Development Library	Section 2.0
B2	10-12-10	Updated due to document convergence, to include tech memos 2010.510.0011, 2010.510.0012, 2010.510.0013, 2010.510.0014, & 2010.510.0016,	All
B3	11-29-10	Updates for PCR025126 – Revert OBC-IP to UInt16s (Rev B3 undone in Rev B7)	All
B4	02-10-11	Updates for ISTN_VIIRS_NGST_4.19.2 & ISTN_VIIRS_NGST_4.23.1 (NP-EMD.2010.510.0094)	All
B5	06-29-11	Implemented TM NP-EMD.2011.510.0003_VIIRS_inst2sc.pdf	All
B6	09-28-11	Updated for PCR026634.	All
B7	11-04-11	Updated for PCR027965 Solar diffuser dim fixes. Undo of PCR025126. And updated for PCR027896.	All

Table of Contents

1.0 INTRODUCTION..... 1

 1.1 Objective..... 1

 1.2 Scope 1

 1.3 References 1

 1.3.3 Document References 1

 1.3.3 Source Code References 4

2.0 ALGORITHM OVERVIEW 8

 2.1 VIIRS SDR Verified RDR Description..... 11

 2.1.1 Interfaces 13

 2.1.1.1 Inputs 13

 2.1.1.2 Outputs 18

 2.1.2 Algorithm Processing..... 18

 2.1.2.1 createVerifiedRDR()..... 19

 2.1.2.2 ProViirsVerifiedRDRConverter() 19

 2.1.2.3 ViirsCalAppPacket()..... 20

 2.1.2.4 ViirsEngAppPacket()..... 20

 2.1.2.5 ViirsHrdAppPacket() 20

 2.1.3 Graceful Degradation..... 20

 2.1.3.1 Graceful Degradation Inputs 20

 2.1.3.2 Graceful Degradation Processing 20

 2.1.3.3 Graceful Degradation Outputs 20

 2.1.4 Exception Handling 20

 2.1.5 Data Quality Monitoring 20

 2.1.6 Computational Precision Requirements 21

 2.1.7 Algorithm Support Considerations 21

 2.1.8 Assumptions and Limitations 21

 2.2 VIIRS SDR Geolocation Description 21

 2.2.1 Interfaces 22

 2.2.1.1 Inputs 22

 2.2.1.2 Outputs 28

 2.2.1.2.1 Geolocation Gridded Outputs..... 37

 2.2.2 Algorithm Processing..... 39

 2.2.2.1 Main driver for Geolocation (geolocateGranule())..... 40

2.2.2.2	GEO_absolute_limit_check()	41
2.2.2.3	GEO_determine_DNB_sample_time_offsets()	42
2.2.2.4	GEO_determine_sample_time_offsets().....	42
2.2.2.5	GEO_determine_thermal_corrections()	42
2.2.2.6	GEO_determine_view_vectors().....	42
2.2.2.7	GEO_evaluate_polynomial().....	43
2.2.2.8	GEO_find_next_flag()	43
2.2.2.9	GEO_get_grid().....	43
2.2.2.10	GEO_interp_mod_unagg().....	44
2.2.2.11	GEO_interpolate_mirror_encoder()	44
2.2.2.12	GEO_interpolate_telescope_encoder().....	44
2.2.2.13	GEO_process_parameters().....	44
2.2.2.14	GEO_relative_limit_check()	44
2.2.2.15	GEO_validate_scan_encoder_data().....	44
2.2.2.16	geolocatePixel()	44
2.2.2.17	geolocateDecim()	45
2.2.2.18	geolocateFullFromDecim().....	45
2.2.2.19	calcModFromImg().....	45
2.2.2.20	createInterpRctngls()	45
2.2.2.21	initGeoDataStructs()	45
2.2.2.22	storeGranule().....	45
2.2.2.23	fixSatAngles().....	45
2.2.2.24	quadInterp()	45
2.2.2.25	geolocateAllRecPix().....	46
2.2.2.26	interpLocations()	46
2.2.2.27	interpAngles().....	46
2.2.2.28	Geolocation Quality Flag Logic	46
2.2.2.29	Create Degree GEO Products	46
2.2.3	Graceful Degradation.....	46
2.2.3.1	Graceful Degradation Inputs	47
2.2.3.2	Graceful Degradation Processing	47
2.2.3.3	Graceful Degradation Outputs	47
2.2.4	Exception Handling	47
2.2.5	Data Quality Monitoring	47
2.2.6	Computational Precision Requirements	47

- 2.2.7 Algorithm Support Considerations 48
- 2.2.8 Assumptions and Limitations 48
 - 2.2.8.1 Sci2Ops Issues 48
 - 2.2.8.2 Numerical Computation Considerations..... 48
 - 2.2.8.3 Additional Assumptions..... 48
 - 2.2.8.4 Additional Limitations 49
- 2.3 VIIRS SDR Calibration Description 49
 - 2.3.1 Interfaces 51
 - 2.3.1.1 Inputs 51
 - 2.3.1.2 Outputs 52
 - 2.3.1.2.1 Definitions of the Calibration VIIRS SDR Outputs 54
 - 2.3.1.2.2 VIIRS On-Board Calibrator Intermediate Product 58
 - 2.3.2 Algorithm Processing..... 64
 - 2.3.2.1 Sub-frame Offset Compensation 65
 - 2.3.2.2 Robust Algorithm Design 66
 - 2.3.2.3 Earth View Radiometric Calibration Error Handling 66
 - 2.3.2.4 calibrateSDR() 66
 - 2.3.2.5 PreprocessRDR() and PreprocessDNB()..... 66
 - 2.3.2.6 SDRSetup()..... 66
 - 2.3.2.7 Combine_Reduced_Quality_Flags()..... 66
 - 2.3.2.8 Calibrate_Emissive_Bands()..... 66
 - 2.3.2.9 Find_SV_Scan_Index()..... 67
 - 2.3.2.10 Calibrate_Reflective_Bands() 67
 - 2.3.2.11 Calibrate_DayNight_Bands() 67
 - 2.3.2.12 Aggregate_750M_DG()..... 67
 - 2.3.2.13 viirs_decomp() 67
 - 2.3.3 Graceful Degradation..... 67
 - 2.3.3.1 Graceful Degradation Inputs 67
 - 2.3.3.2 Graceful Degradation Processing 67
 - 2.3.3.3 Graceful Degradation Outputs 68
 - 2.3.4 Exception Handling 68
 - 2.3.5 Data Quality Monitoring 68
 - 2.3.6 Computational Precision Requirements 68
 - 2.3.7 Algorithm Support Considerations 68
 - 2.3.8 Assumptions and Limitations 68

- 2.3.8.1 I/O Timeliness 68
- 2.3.8.2 Sci2Ops Issues 69
- 2.3.8.3 Numerical Computation Considerations..... 69
- 2.3.8.4 Additional Assumptions..... 69
- 2.3.8.5 Additional Limitations 69
- 2.4 VIIRS SDR Reflective Solar Band (RSB) Automated Calibration (RSBAutoCal)
 - Description..... 70
 - 2.4.1 Interfaces 70
 - 2.4.1.1 Inputs 70
 - 2.4.1.2 Outputs for RSBAutoCal Data Processing Unit 72
 - 2.4.2 Algorithm Processing 73
 - 2.4.2.1 Automated Reflective Solar Band Calibration Data Processing Logic..... 73
 - 2.4.2.2 Calibration Symbols and Units 74
 - 2.4.2.3 Reflective Calibration Core Equations 76
 - 2.4.2.4 Emissive Calibration Core Equations..... 77
 - 2.4.2.5 Day Night Band Calibration Core Equations 78
 - 2.4.2.6 Solar Diffuser View Data Processing Core Equations 78
 - 2.4.2.7 Event Processing 78
 - 2.4.2.7.1 Solar Event Processing Flow 79
 - 2.4.2.7.1.1 calcOrbitalMedianAndSmoothH..... 79
 - 2.4.2.7.1.2 calcOrbitalMedianAndSmoothRsbF 80
 - 2.4.2.7.1.3 calcOrbitalMedianAndSmoothDnbLgsGain 80
 - 2.4.2.7.1.4 calcOrbitalMedianAndSmoothDnbDarkSignal..... 80
 - 2.4.2.7.1.5 calcOrbitalMedianAndSmoothDnbGainRatios) 80
 - 2.4.3 Graceful Degradation..... 81
 - 2.4.3.1 Graceful Degradation Inputs 81
 - 2.4.3.2 Graceful Degradation Processing 81
 - 2.4.3.3 Graceful Degradation Outputs 81
 - 2.4.4 Exception Handling 81
 - 2.4.5 Data Quality Monitoring 81
 - 2.4.6 Computational Precision Requirements 81
 - 2.4.7 Algorithm Support Considerations 81
 - 2.4.8 Assumptions and Limitations 81
- 2.5 VIIRS SDR Bright Pixel Description 81
 - 2.5.1 Interfaces 82
 - 2.5.1.1 Inputs 82

2.5.1.2	Outputs	82
2.5.2	Algorithm Processing	83
2.5.2.1	Estimating % Scattered Light	83
2.5.2.2	“Calculation Unreliable” Flag	85
2.5.2.3	Creation of Non-Saturated Scene	85
2.5.2.4	Common Adjacency Use In Bright Pixel	87
2.5.2.5	Data Convolution	87
2.5.3	Graceful Degradation	88
2.5.3.1	Graceful Degradation Inputs	88
2.5.3.2	Graceful Degradation Processing	88
2.5.3.3	Graceful Degradation Outputs	88
2.5.4	Exception Handling	88
2.5.5	Data Quality Monitoring	88
2.5.6	Computational Precision Requirements	88
2.5.7	Algorithm Support Considerations	88
2.5.8	Assumptions and Limitations	88
3.0	GLOSSARY/ACRONYM LIST	89
3.1	Glossary	89
3.2	Acronyms	92
4.0	OPEN ISSUES	93

List of Figures

Figure 1 IPO Model Interface to INF and DMS (Calibration) 8
 Figure 2 VIIRS Verified RDR Flow Diagram 9
 Figure 3 VIIRS Geolocation Flow Diagram 10
 Figure 4 VIIRS Calibration Flow Diagram 10
 Figure 5 Instrument Engineering Order and Product Order Illustration..... 12
 Figure 6 Create Verified VIIRS RDR Flow Diagram 19
 Figure 7 Geolocation Processing Chain 22
 Figure 8 geolocateGranule() Flow Diagram 41
 Figure 9 GEO_determine_view_vectors() Block Diagram (Geolocation)..... 43
 Figure 10 Calibration Processing Chain 50
 Figure 11 Radiometric Calibration Main Program Flow 65
 Figure 12 High level RSBAutoCal Data Processing Main Program Flow 74
 Figure 13 Detailed Solar Event Processing Program Flow 79

List of Tables

Table 1 Document References 1

Table 2 Source Code References..... 5

Table 3 Verified VIIRS RDR Engineering Packet Data Inputs 13

Table 4 Verified VIIRS RDR Science Packet Data Inputs 16

Table 5 Verified VIIRS RDR Calibration Packet Data Inputs 17

Table 6 VIIRS Geolocation Inputs..... 22

Table 7 S/C Ephemeris and Attitude Data 23

Table 8 Geolocation Parameter Inputs 23

Table 9 DNB Geolocation Output Structure 29

Table 10 MOD Geolocation Output Structure 31

Table 11 Unaggregated MOD Geolocation Output Structure 33

Table 12 IMG Geolocation Output Structure..... 34

Table 13 Scan Level Geolocation Quality Bytes 36

Table 14 Pixel Level Geolocation Quality Byte 36

Table 15 Map Data Set (mds_type) (Geolocation) 37

Table 16 Gridded Geolocation Moderate Output (Geolocation) 38

Table 17 Gridded Geolocation Imagery Output (Geolocation)..... 39

Table 18 Earth View Radiometric Calibration Unit Inputs 51

Table 19 Earth View Radiometric Calibration Parameter & LUT Inputs 51

Table 20 Outputs from the Earth View Radiometric Calibration Unit (Calibration) 53

Table 21 Imagery Resolution SDR 54

Table 22 Moderate Resolution SDR 54

Table 23 Day/Night Band SDR 55

Table 24 Imagery Resolution Scaled SDR 55

Table 25 Moderate Resolution Scaled SDR 56

Table 26 Scan Quality Byte 57

Table 27 Pixel Quality Byte..... 57

Table 28 RDR Scan Quality Int..... 57

Table 29 Reduced Quality Flag Byte 58

Table 30 VIIRS SDR Header 58

Table 31 OBC IP Output 58

Table 32 VIIRS SDR Calibration Data Quality Monitoring 68

Table 33 RSBAutoCal Data Processing Unit Inputs (Calibration)..... 71

Table 34 RSBAutoCal Data Processing Unit Calibration Parameter Input Files 71

Table 35 RSBAutoCal: Table Output 72

Table 36 Calibration Symbols and Units 74

Table 37 Reflective Calibration Core Equations (Calibration)..... 76

Table 38 Emissive Calibration Core Equations (Calibration) 77

Table 39 Day Night Band Calibration Core Equations (Calibration) 78

Table 40 Solar Diffuser View Data Processing Core Equations (Calibration)..... 78

Table 41 VIIRS Bright Pixel Algorithm Inputs 82

Table 42 VIIRS Bright Pixel Output Files 83

Table 43 Glossary 89

Table 44 Acronyms 92

Table 45 List of TBD/TBR 93

1.0 INTRODUCTION

1.1 Objective

The purpose of the Operational Algorithm Description (OAD) document is to express, in computer-science terms, the remote sensing algorithms that produce the National Polar-Orbiting Operational Environmental Satellite System (NPOESS) end-user data products. These products are individually known as Raw Data Records (RDRs), Temperature Data Records (TDRs), Sensor Data Records (SDRs) and Environmental Data Records (EDRs). In addition, any Intermediate Products (IPs) produced in the process are also described in the OAD.

The science basis of an algorithm is described in a corresponding Algorithm Theoretical Basis Document (ATBD). The OAD provides a software description of that science as implemented in the operational ground system -- the Data Processing Element (DPE).

The purpose of an OAD is two-fold:

1. Provide initial implementation design guidance to the operational software developer.
2. Capture the “as-built” operational implementation of the algorithm reflecting any changes needed to meet operational performance/design requirements.

An individual OAD document describes one or more algorithms used in the production of one or more data products. There is a general, but not strict, one-to-one correspondence between OAD and ATBD documents.

1.2 Scope

The scope of this document is limited to the description of the core operational algorithm(s) required to create the GEO, CAL, Solar Diffuser, and Bright Pixel products for the VIIRS SDR. It provides a general overview and is intended to supplement in-line software documentation and interface control documentation for maintenance of the operational software. The theoretical basis for these algorithms is described Section 3.3 of the ATBD documents, VIIRS Geolocation Algorithm Theoretical Basis Document (ATBD), 474-00053 and VIIRS Radiometric Calibration Algorithm Theoretical Basis Document ATBD, 474-00027.

1.3 References

1.3.3 Document References

The science and system engineering documents relevant to the algorithms described in this OAD are listed in Table 1.

Table 1 Document References

Document Title	Document Number/Revision	Revision Date
VIIRS Geolocation Unit Software Architecture	Y2479a Ver. 5 Rev. 5	31 Aug 2004
VIIRS Geolocation Unit Detailed Interface Control Document	Y3243 Ver. 5 Rev. 3	31 Aug 2004
VIIRS Geolocation Unit Detailed Data Dictionary	Y3248 Ver. 5 Rev. 3	31 Aug 2004
VIIRS Geolocation Unit Detailed Design	Y3245 Ver. 5 Rev. 4	31 Aug 2004
VIIRS Geolocation Algorithm Theoretical Basis Document (ATBD)	474-00053	Latest

Document Title	Document Number/Revision	Revision Date
JPSS Environmental Data Record (EDR) Production Report (PR) for NPP	474-00012	Latest
JPSS Environmental Data Record (EDR) Interdependency Report (IR) for NPP	474-00007	Latest
JPSS Data Format Control Book – Internal Volume III – Retained Intermediate Product Formats (IDFCB) – Block 1.2.3	474-00020-03-B0123 IDFCB Vol III	Latest
NPP Mission Data Format Control Book and App A (MDFCB)	429-05-02-42-02_MDFCB	Latest
JPSS Common Data Format Control Book - External - Block 1.2.3 (All Volumes)	474-00001-01-B0123 CDFCB-X Vol I 474-00001-02-B0123 CDFCB-X Vol II 474-00001-03-B0123 CDFCB-X Vol III 474-00001-04-01-B0123 CDFCB-X Vol IV Part 1 474-00001-04-02-B0123 CDFCB-X Vol IV Part 2 474-00001-04-03-B0123 CDFCB-X Vol IV Part 3 474-00001-04-04-B0123 CDFCB-X Vol IV Part 4 474-00001-05-B0123 CDFCB-X Vol V 474-00001-06-B0123 CDFCB-X Vol VI 474-00001-08-B0123 CDFCB-X Vol VIII	Latest
JPSS Common Data Format Control Book - External - Block 1.2.4 (All Volumes)	474-00001-01-B0124 CDFCB-X Vol I 474-00001-02-B0124 CDFCB-X Vol II 474-00001-03-B0124 CDFCB-X Vol III 474-00001-04-01-B0124 CDFCB-X Vol IV Part 1 474-00001-04-02-B0124 CDFCB-X Vol IV Part 2 474-00001-04-03-B0124 CDFCB-X Vol IV Part 3 474-00001-04-04-B0124 CDFCB-X Vol IV Part 4 474-00001-05-B0124 CDFCB-X Vol V 474-00001-06-B0124 CDFCB-X Vol VI 474-00001-08-B0124 CDFCB-X Vol VIII	Latest
NPP Command and Telemetry (C&T) Handbook	D568423 Rev. C	30 Sep 2008
JPSS CGS Data Processor Inter-subsystem Interface Control Document (DPIS ICD) Vol I – IV	IC60917-IDP-002	Latest
Operational Algorithm Description Document for Common Geolocation	474-00091	Latest
VIIRS Radiometric Calibration Component Software Architecture	Y2479b Ver. 5 Rev. 5	30 Sep 2004
VIIRS Radiometric Calibration Component Interface Control Document	Y3242 Ver. 5 Rev. 2	11 Aug 2004

Document Title	Document Number/Revision	Revision Date
VIIRS Radiometric Calibration Component Data Dictionary	Y3273 Ver. 5 Rev. 3	11 Aug 2004
VIIRS Radiometric Calibration Unit Level Detailed Design	Y2490 Ver. 5 Rev. 4	30 Sep 2004
VIIRS Radiometric Calibration Algorithm Theoretical Basis Document ATBD	474-00027	Latest
VIIRS Radiometric Calibration Equations	D36966 Rev. 1	02 Aug 2004
Joint Polar Satellite System (JPSS) Program Lexicon	470-00041	Latest
NGST/SE technical memo – VIIRS_CAL_SD_Detailed_Code_Changes_Oct_2005	NP-EMD.2005.510.0122 Rev. ---	12 Oct 2005
NGST/SE technical memo – VIIRS_SDR_Cal_Modif_Implement_OAD	NP-EMD-2007.510.0014 Rev. ---	14 Feb 2007
NGST/SE technical memo – VIIRS_SDR_Even_odd_subframe_design	NP-EMD-2007.510.0009 Rev. ---	14 Feb 2007
NGST/SE technical memo – VIIRS_SDR_Robust_Alg_design	NP-EMD-2007.510.0010 Rev. ---	14 Feb 2007
NGST/SE technical memo – NPP_VIIRS_CAL_EV_Detailed_Code_Changes_Feb_2007	NP-EMD-2007.510.0012 Rev. ---	14 Feb 2007
NGST/SE technical memo – NPP_VIIRS_SDR_DNB_FirstFrameAnomaly	NP-EMD-2007.510.0029 Rev. ---	23 Apr 2007
NGST/SE technical memo – viirsLUTconfigMethod	NP-EMD.2005.510.0134 Rev. ---	12 Oct 2005
NGST/SE technical memo – RevA_viirsCAL_sdIO_description	NP-EMD.2005.510.0119 Rev. A	11 Jun 2007
NGST/SE technical memo – EM061405_viirsCAL_moon_in_SV	NP-EMD.2005.510.0065 Rev. ---	14 Dec 2005
NGST/SE technical memo – EM052405_viirsRDR_HDF_description	NP-EMD.2005.510.0067 Rev. ---	24 May 2005
NGST/SE technical memo – EM061005_viirsCAL_evIO_description	NP-EMD.2005.510.0069 Rev. ---	06 Oct 2005
NGST/SE technical memo – EM061005_viirsCAL_sdIO_description	NP-EMD.2005.510.0071 Rev. ---	06 Oct 2005
NGST/SE technical memo – EM060305VIIRS_CAL_EV_Detailed_Code_Changes	NP-EMD.2005.510.0074 Rev. ---	02 Jun 2005
NGST/SE technical memo – VIIRS_CAL_testProc	NP-EMD.2005.510.0081 Rev. ---	25 Jul 2005
NGST/SE technical memo – cal_Sdcode_change_Description	NP-EMD.2005.510.0064 Rev. ---	03 Jun 2005
NGST/SE technical memo – EM060305VIIRS_CAL_SD_Detailed_Code_Changes	NP-EMD.2005.510.0075 Rev. ---	03 Jun 2005
NGST/SE technical memo – EM050106Parameters-M	NP-EMD.2005.510.0004 Rev. ---	06 Jan 2005
NGST/SE technical memo – VIIRS_GEO_OADtables_memo	NP-EMD.2005.510.0012 Rev. ---	17 Jan 2005
NGST/SE technical memo – VIIRS_CAL_Sdcode_changes_011905	NA	19 Jan 2005
NGST/SE technical memo – EM060605_viirsGEO_IP_description	NP-EMD.2005.510.0068 Rev. ---	06 Jun 2005
NGST/SE technical memo – EM101005_geo_OADupdates_Rev_A	NP-EMD.2005.510.0125 Rev. A	30 Nov 2005
NGST/SE technical memo – NPP_Geo_AtmosphericCorrectionSZAcac	NP-EMD.2006.510.0098 Rev. ---	15 Dec 2006
NGST/SE technical memo – Rev.A_VIIRS_SDR_BrightPixel_ID_design_Rev_A	NP-EMD-2007.510.0011 Rev. A	11 May 2007
NGST/SE technical memo – VIIRS_SDR_BrightPixel_ID_Implement_OAD	NP-EMD-2007.510.0013 Rev. ---	14 Feb 2007
NGST/SE technical memo – VIIRS_GEO_BugFixes	NP-EMD.2008.510.0044 Rev. ---	03 Jul 2008
NGST/SE technical memo – VIIRS_GEO_OAD_Updates	NP-EMD.2008.510.0027 Rev. A	19 Aug 2008
NGST/SE technical memo – SDSM_OAD_Update	NP-EMD-2008.510.0019 Rev. ---	20 Mar 2008

Document Title	Document Number/Revision	Revision Date
NGAS/A&DP technical memo – SDSM_OAD_Update	NP-EMD-2009.510.0006	21 Jan 2009
NGST/SE technical memo –VIIRS GEO EvtimesUpdates	NP-EMD-2008.510.0050	29 Oct 2008
NGAS/SE technical memo – Direction for Setting the VIIRS Pixel Level SDR Quality flag for VIIRS SDR Calibration	NP-EMD.2009.510.0038	24 Jun 2009
NGAS/SE technical memo – VIIRS Geo Quality Flags Logic Updates	NP-EMD.2009.510.0048 Rev A	12 Oct 2009
NGAS/SE technical memo – VIIRS SDR OAD Updates to the Geolocation Parameters Table	NP-EMD.2009.510.0033 Rev A	12 Oct 2009
NGAS/SE technical memo – Solar Diffuser LUT Read Update	NP-EMD.2009.510.0031 Rev A	03 Dec 2009
NGAS/SE technical memo – Solar Diffuser Cal SDSM Angle Fix	NP-EMD.2009.510.0042	23 Jul 2009
NGAS/SE technical memo – Solar Diffuser Cal SDSM Angle Fix	NP-EMD.2009.510.0047	15 Sep 2009
VIIRS Bright Pixel ID Algorithm Update	NP-EMD-2009.510.0052	09 Oct 2009
NGAS/SE technical memo – SDR/SDCal RVS Update	NP-EMD-2010.510.0003	10 Feb 2010
NGAS/SE technical memo – VIIRS SDR Cal Thermistor Update	NP-EMD-2010.510.0007 Rev-A	22 Mar 2010
NGAS/SE technical memo – VIIRS SDR OBC Cal Update	NP-EMD-2010.510.0008	24 Feb 2010
NGAS/SE technical memo – VIIRS SDR Cal RSR Update	NP-EMD-2010.510.0011	26 Feb 2010
NGAS/SE technical memo – VIIRS SDR Cal DNB Stray Light QF	NP-EMD-2010.510.0012	05 Mar 2010
NGAS/SE technical memo – VIIRS SDR Cal DG Anomaly QF	NP-EMD-2010.510.0013	12 Mar 2010
NGAS/SE technical memo – VIIRS Solar Diffuser LUT Update	NP-EMD-2010.510.0016	05 Mar 2010
NGAS/SE technical memo – VIIRS SDR Cal EMI Spike Filter	NP-EMD-2010.510.0021	16 Mar 2010
NGAS/SE technical memo – VIIRS_SDR_SD_Calibration_Off_During_Manuever	NP-EMD-2010.510.0004	11 Feb 2010
NGST/SE technical memos: LUT_OAD_Drop_History_Corrections LUT_Format_Corrections PC_OAD_Last_Drop_Corrections PC_Format_Corrections SAD_Formatand Usage_Corrections	NPOESS GJM-2010.510.0011 NPOESS GJM-2010.510.0012 NPOESS GJM-2010.510.0013 NPOESS GJM-2010.510.0014 NPOESS GJM-2010.510.0016	21 Sep 2010 21 Sep 2010 22 Sep 2010 22 Sep 2010 22 Sep 2010
NGST/SE technical memo – VIIRS_SDR-GEO_CODE_LUT_Update_Dec_2010	NP-EMD.2010.510.0094	01 Dec 2010
NGST/SE technical memo – VIIRS_inst2sc.pdf	NP-EMD.2011.510.0003	21 Feb 2011
Joint Polar Satellite System (JPSS) Common Ground System (CGS) IDPS PRO Software User's Manual Part 2	UG60917-IDP-026 Rev -	Latest

1.3.3 Source Code References

The science and operational code and associated documentation relevant to the algorithms described in this OAD are listed in Table 2.

Table 2 Source Code References

Reference Title	Reference Tag/Revision	Revision Date
VIIRS SDR --- Science-grade Software	ISTN_VIIRS_NGST_2.9	30 Sep 2004
NGST/SE technical memo – EM050106Parameters-M	NP-EMD.2005.510.0004 Rev. ---	06 Jan 2005
VIIRS SDR --- Operational-grade Software	Build 1.3 (OAD D39553 Rev ---)	30 Sep 2004
NGST/SE technical memo – VIIRS_CAL_Sdcode_changes_011905	NA [Build 1.3]	19 Jan 2005
VIIRS SDR --- Science-grade Software	ISTN_VIIRS_NGST_2.9.1	27 Jul 2005
NGST/SE technical memo – EM052405_viirsRDR_HDF_description	NP-EMD.2005.510.0067 Rev. --- [Build 1.3]	24 May 2005
NGST/SE technical memo – EM061405_viirsCAL_moon_in_SV	NP-EMD.2005.510.0065 Rev. --- [Build 1.3]	14 Dec 2005
NGST/SE technical memo – EM061005_viirsCAL_evIO_description	NP-EMD.2005.510.0069 Rev. --- [Build 1.3]	06 Oct 2005
NGST/SE technical memo – EM061005_viirsCAL_sdIO_description	NP-EMD.2005.510.0071 Rev. --- [Build 1.3]	06 Oct 2005
NGST/SE technical memo – cal_Sdcode_change_Description	NP-EMD.2005.510.0064 Rev. --- [Build 1.3]	03 Jun 2005
NGST/SE technical memo – EM060305VIIRS_CAL_SD_Detailed_Code_Changes	NP-EMD.2005.510.0075 Rev. --- [Build 1.3]	03 Jun 2005
NGST/SE technical memo – EM060605_viirsGEO_IP_description	NP-EMD.2005.510.0068 Rev. --- [Build 1.3]	06 Jun 2005
NGST/SE technical memo – VIIRS_CAL_testProc	NP-EMD.2005.510.0081 Rev. --- [Build 1.3]	25 Jul 2005
NGST/SE technical memo – VIIRS_CAL_SD_Detailed_Code_Changes_Oct_2005	NP-EMD.2005.510.0122 Rev. --- [Build 1.3]	12 Oct 2005
NGST/SE technical memo – EM060305VIIRS_CAL_EV_Detailed_Code_Changes	NP-EMD.2005.510.0074 Rev. --- [Build 1.3]	02 Jun 2005
VIIRS SDR --- Operational-grade Software	Build 1.4 (follow-on)	27 Jul 2005
VIIRS SDR --- Science-grade Software (GEO)	ISTN_VIIRS_NGST_2.7.2 (ECR-A080C)	01 Dec 2005
VIIRS SDR --- Science-grade Software	ISTN_VIIRS_NGST_2.9.2	06 Dec 2005
NGST/SE technical memo – viirsLUTconfigMethod	NP-EMD.2005.510.0134 Rev. --- [Build 1.4]	12 Oct 2005
NGST/SE technical memo –viirsCAL_sdIO_description	NP-EMD.2005.510.0119 [Build 1.4]	12 Oct 2005
VIIRS SDR --- Science-grade Software	ISTN_VIIRS_NGST_2.9.3	06 Apr 2006
VIIRS SDR --- Operational-grade Software	Build 1.4 (follow-on)	06 Apr 2006
Combined CAL and GEO OADs (D39300) into D41868	Build 1.4 (D41868 Rev A1)	08 Jun 2006
NGST/SE technical memo – NPP_Geo_AtmosphericCorrectionSZacalc	NP-EMD.2006.510.0098 Rev. --- [Build 1.4]	15 Dec 2006
VIIRS SDR --- Operational-grade Software	Build 1.5 (OAD Revs A3-A8)	01 Jan 2007
NGST/SE technical memo – VIIRS_SDR_Even_odd_subframe_design	NP-EMD.2007.510.0009 Rev. --- [Build 1.5]	14 Feb 2007
NGST/SE technical memo – VIIRS_SDR_Robust_Align_design	NP-EMD.2007.510.0010 Rev. --- [Build 1.5]	14 Feb 2007
NGST/SE technical memo – Rev.A_VIIRS_SDR_BrightPixel_ID_design_Rev_A	NP-EMD.2007.510.0011 Rev. A [Build 1.5]	11 May 2007
NGST/SE technical memo – NPP_VIIRS_CAL_EV_Detailed_Code_Changes_Feb_2007	NP-EMD.2007.510.0012 Rev. --- [Build 1.5]	14 Feb 2007

Reference Title	Reference Tag/Revision	Revision Date
NGST/SE technical memo – VIIRS_SDR_BrightPixel_ID_Implement_OAD	NP-EMD.2007.510.0013 Rev. --- [Build 1.5]	14 Feb 2007
NGST/SE technical memo – VIIRS_SDR_Cal_Modif_Implement_OAD	NP-EMD.2007.510.0014 Rev. --- [Build 1.5]	14 Feb 2007
NGST/SE technical memo – NPP_VIIRS_SDR_DNB_FirstFrameAnomaly	NP-EMD.2007.510.0029 Rev. --- [Build 1.5]	23 Apr 2007
NGST/SE technical memo – RevA_viirsCAL_sdIO_description	NP-EMD.2005.510.0119 Rev. A [Build 1.5]	11 Jun 2007
VIIRS SDR --- Science-grade Software	ISTN_VIIRS_NGST_2.9.4	13 Aug 2007
VIIRS SDR operational software	B1.5.x.1 (OAD Revs A9-A16)	01 Oct 2007
NGST/SE technical memo – SDSM_OAD_Update	NP-EMD-2008.510.0019 Rev. --- [Build 1.5.x.1]	20 Mar 2008
VIIRS SDR --- Science-grade Software	ISTN_VIIRS_NGST_2.9.5	14 May 2008
VIIRS Geolocation – Science-grade Software	ISTN_VIIRS_NGST_4.10 (ECR-A157)	18 Jun 2008
NGST/SE technical memo – VIIRS_GEO_BugFixes	NP-EMD.2008.510.0044 Rev. --- [Build 1.5.x.1]	03 Jul 2008
VIIRS SDR --- Science-grade Software (Model 'E' LUT update)	ISTN_VIIRS_NGST_2.9.7	08 Aug 2008
VIIRS_SDR_DNB_Calibration_Saturation_Value_Bug_Fix (PCR019689)	NP-EMD.2009.510.0006- [Build Post-X-C] (No update to OAD required)	31 Mar 2009
PCR019290	Build Post-X-E (OAD Rev-A17)	23 Apr 2009
VIIRS SDR --- Science-grade Software	ISTN_VIIRS_NGST_2.9.8	25 Jul 2009
NGAS/SE technical memo – Direction for Setting the VIIRS Pixel Level SDR Quality flag for VIIRS SDR Calibration (PCR20858)	NP-EMD.2009.510.0038--Build 1.5 Sensor Characterization Build SC 3 (No OAD updates)	01 Sep 2009
VIIRS SDR --- Science-grade Software (Calibration)	ISTN_VIIRS_NGST_4.18	11 Nov 2009
VIIRS SDR --- Science-grade Software (Geo)	ISTN_VIIRS_NGST_4.19	11 Nov 2009
VIIRS SDR operational software Includes Tech Memos (not listed in Table 1): NP-EMD.2009.510.0071_VIIRS_SDR_Cal_14bit_Conversion (PCR22051) NP-EMD-2009.510.0041_SDR_Cal_Imagery_Even_Odd_Parity_Fix (PCR21468) NP-EMD-2009.510.0044_VIIRS_Calibration_3rd_Order_Coefficient_Fix (PCR21467) NP-EMD.2009.510.0028_RevB_VIIRS_GEO_MissingEncoderRobustness (PCR20616)	Build 1.5 Sensor Characterization Build SC 6 (OAD Rev A21)	20 Jan 2010
VIIRS SDR Bright Pixel Identification science algorithm drop 4.21	ISTN_VIIRS_NGST_4.21 (ECR A-259B)	14 Dec 2009
NP-EMD-2009.510.0052 VIIRS Bright Pixel ID Algorithm Update (PCR021472)	Build 1.5 Sensor Characterization Build SC 8 (OAD Rev A22)	25 Feb 2010
VIIRS SDR --- Science-grade Software (Geo)	ISTN_VIIRS_NGST_4.19.1 (ECR-A280A)	07 Apr 2010
VIIRS SDR --- Science-grade Software (Calibration) includes: NP-EMD-2010.510.0003 – SDR/SDCal RVS Update NP-EMD-2010.510.0007 revA – VIIRS SDR Cal Thermistor Update	ISTN_VIIRS_NGST_4.23	09 Apr 2010

Reference Title	Reference Tag/Revision	Revision Date
NP-EMD-2010.510.0008 – VIIRS SDR OBC Cal Update NP-EMD-2010.510.0011 – VIIRS SDR Cal RSR Update NP-EMD-2010.510.0012 – VIIRS SDR Cal DNB Stray Light QF NP-EMD-2010.510.0013 – VIIRS SDR Cal DG Anomaly QF NP-EMD-2010.510.0016 – VIIRS Solar Diffuser LUT Update NP-EMD-2010.510.0021 – VIIRS SDR Cal EMI Spike Filter		
VIIRS SDR operational software	Build 1.5 Sensor Characterization Build SC 11 (OAD Rev A23)	16 Jun 2010
SDRL	(OAD Rev A25)	08 Jul 2010
PCRs 19655, 22912, 22913 (TM 2010.510.0004)	Build 1.5 Sensor Characterization Build SC 13 (OAD Rev A26)	17 Aug 2010
ACCB	OAD Rev A	22 Sep 2010
VIIRS SDR Algorithm Development Library	Mx1.5.4.00 (OAD Rev B1)	29 Sep 2010
Convergence Update (No code updates)	Mx1.5.4.00 (OAD Rev B2)	12 Oct 2010
PCR025126 Revert OBCIP to UIn16s	Mx1.5.5_A (OAD Rev B3)	29 Oct 2010
VIIRS SDR --- Science-grade Software (Calibration) includes: VIIRS_SDR-GEO_CODE_LUT_Update_Dec_2010 (PCRs 025836 & 026160)	ISTN_VIIRS_NGST_4.19.2, ISTN_VIIRS_NGST_4.23.1 Mx1.5.5_A (OAD Rev B4)	01 Dec 2010 & 29 Jun 2011 (OAD)
VIIRS SDR --- Science-grade Software (Calibration) includes: NP-EMD.2011.510.0003_VIIRS_inst2sc.pdf4 PCRs026129 & 026130	ISTN_VIIRS_NGST_4.19.3, Mx1.5.5_E (OAD Rev B5)	08 Mar 2011 & 29 Jun 2011 (OAD)
PCR026634 (OAD update for ADL)	(OAD Rev B6)	28 Sep 2011
PCR027965 (& undo of PCR025126) and PCR027896	(OAD Rev B7)	04 Nov 2011
OAD transitioned to JPSS Program – this table is no longer updated.		

2.0 ALGORITHM OVERVIEW

To begin data processing, the VIIRS SDR algorithms (Verified RDR, Geolocation and Calibration) are initiated or retasked by the Infrastructure (INF) Subsystem Software Item (SI). The INF SI provides tasking information to the VIIRS SDR algorithms indicating which granule number and version to process. The Data Management Subsystem (DMS) SI provides data storage and retrieval capability. A library of C++ classes is used to implement the SI interfaces (for more information refer to document UG60917-IDP-026 particularly sections regarding PRO Common processing and the IPO Model). The VIIRS SDR algorithms are identified as a persistent retaskable process. When it completes processing for a specified granule, instead of shutting down, the algorithm requests new tasking data in order to process another granule. Figure 1 shows the IPO (Input, Processing, Output) model interface to INF and DMS for calibration only but the Verified RDR and Geolocation algorithms follow the same IPO model.

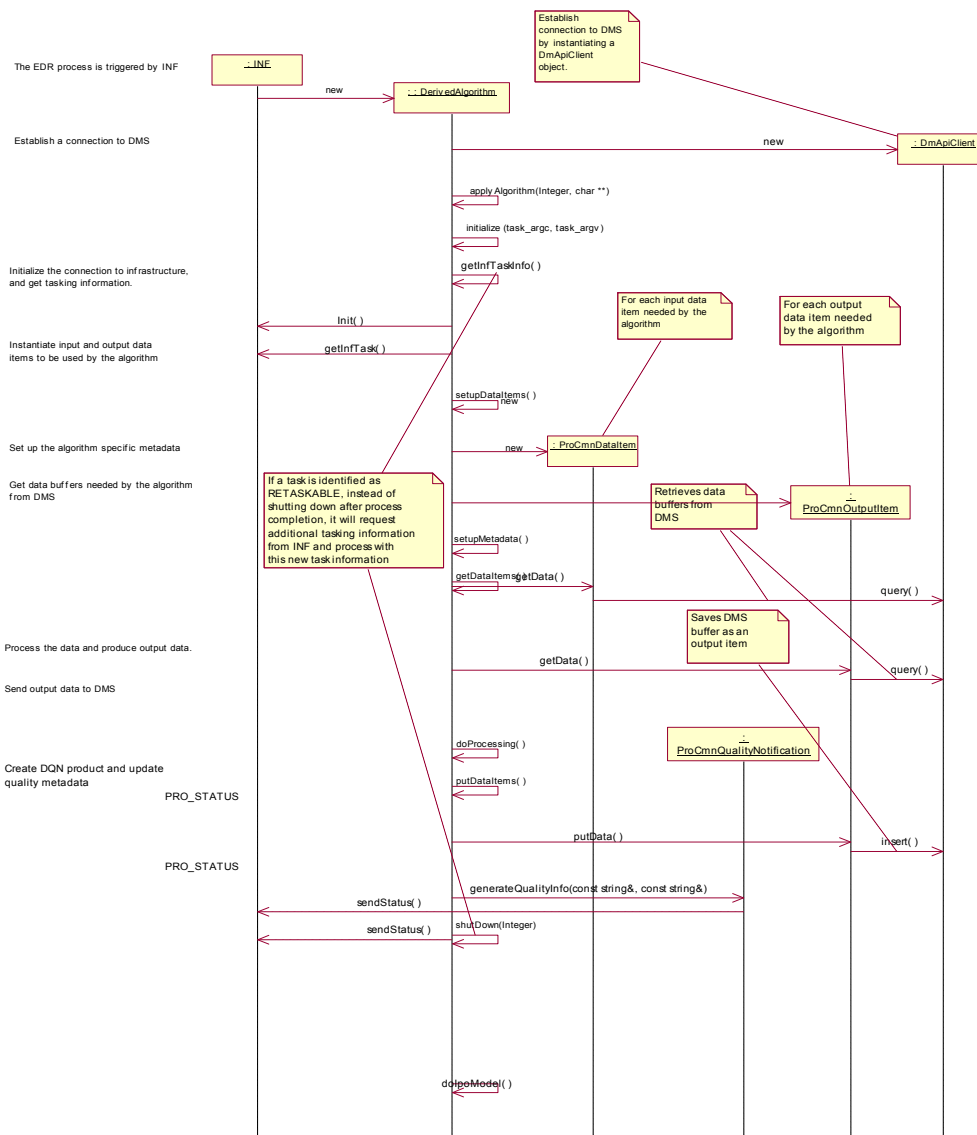


Figure 1 IPO Model Interface to INF and DMS (Calibration)

When the VIIRS SDR algorithms are called, they first initialize values such as routine name and software version number, then call `setupDataItems()` to create data items handlers for retrieving input data from, and storing output data to, DMS. Next, `doPtrAssignmentToInputAndOutput()` assigns pointers to input and output data items. The Verified RDR algorithm, `ProSdrViirsVerifiedRDR`, produces the Verified RDR. The geolocation algorithm, `ProSdrViirsGeo` controls the execution and processing of the geolocation outputs.

In the `ProSdrViirsGeo` algorithm, consecutive calls are made to the `GEO` method, `geolocateGranule`, with appropriate resolution parameter structures to produce `GEO` products in the following order (first to last): imagery (non-terrain corrected and terrain corrected items); moderate (non-terrain corrected and terrain corrected items); moderate unaggregated; DNB.

The `ProSdrViirsCal` algorithm calls the Radiometric Calibration routine to produce TOA radiances, reflectances (reflective bands only), and brightness temperatures (emissive bands only) for each pixel in the imagery bands, moderate bands, and day/night band .

Finally, outputs are checked for data quality, and select outputs are scaled before all output data items are written to DMS. A flow diagram of the VIIRS SDR algorithms is provided in Figure 2, Figure 3 and Figure 4 for clarification.

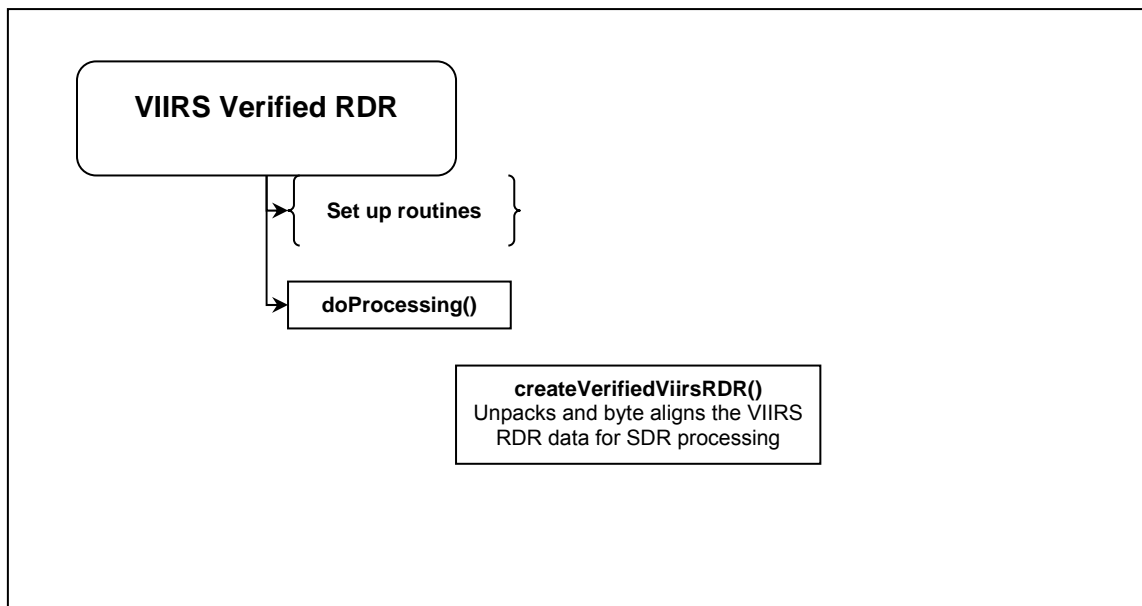


Figure 2 VIIRS Verified RDR Flow Diagram

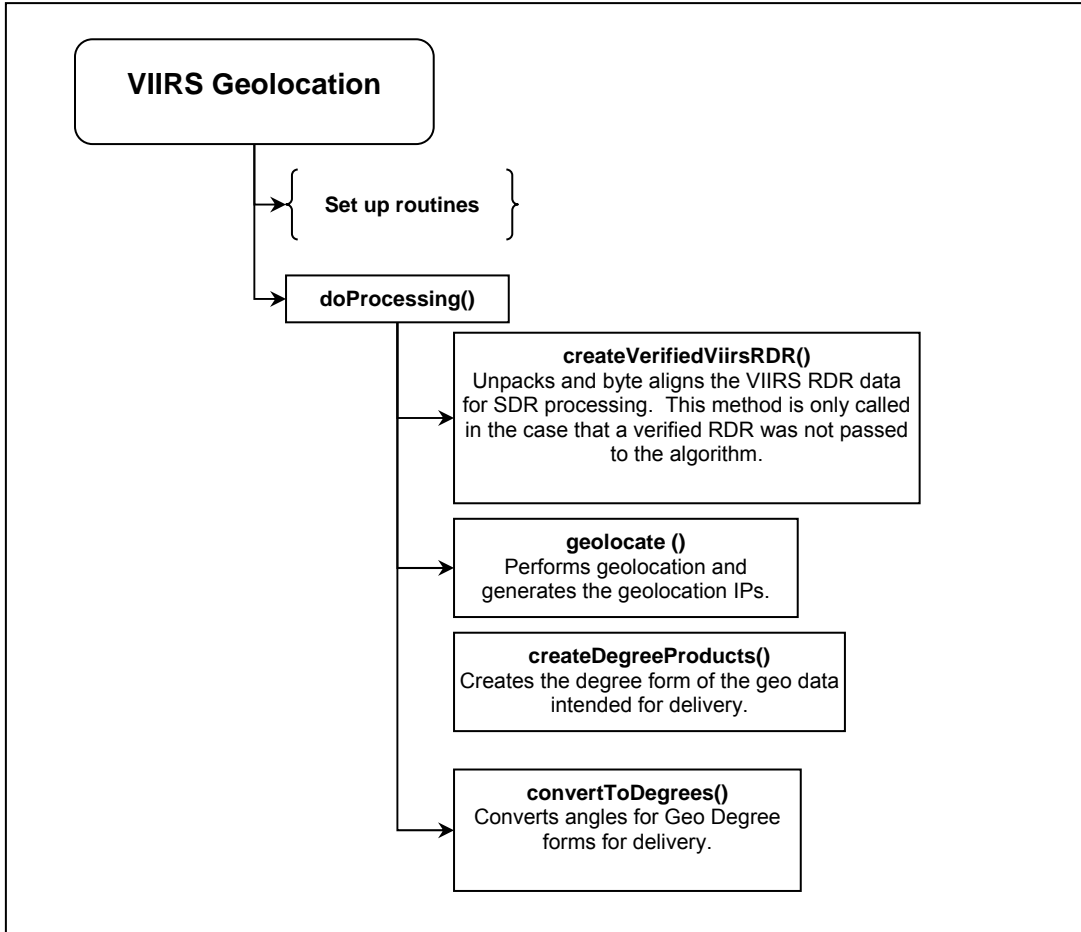


Figure 3 VIIRS Geolocation Flow Diagram

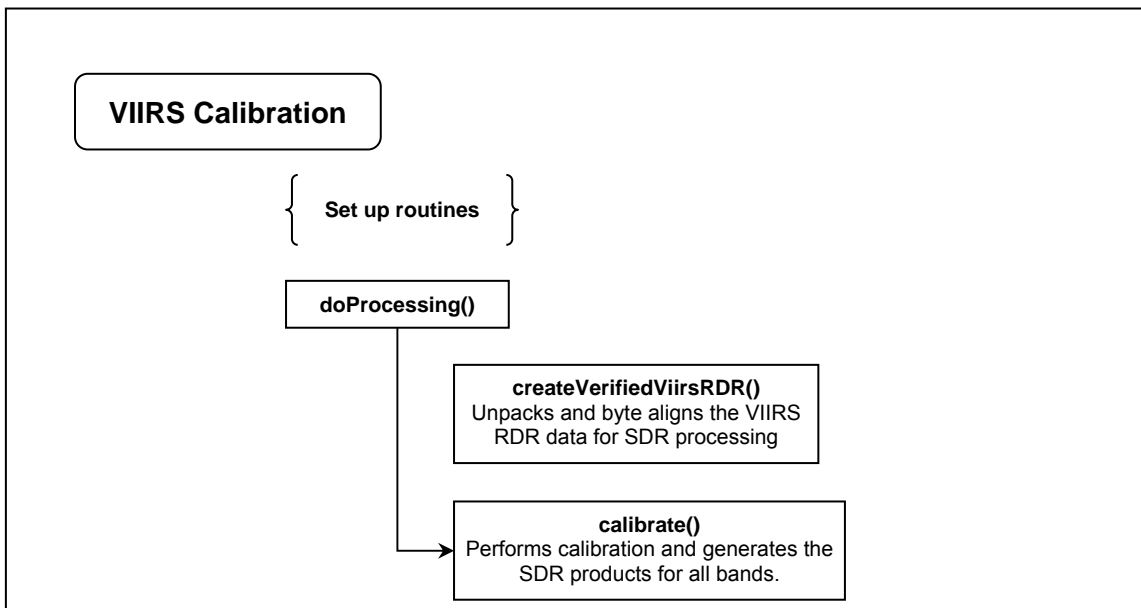


Figure 4 VIIRS Calibration Flow Diagram

2.1 VIIRS SDR Verified RDR Description

Before the geolocation or calibration components can be run the RDR packets must be assembled into what is called the Verified RDR. The RDR packets must first be decompressed. There are four stages of decompression. All stages are lossless. The stages in order of application on the compression side for the earth-view (EV) data are:

- Removal of unused bits
- Piecewise linear offset for dual-gain bands only
- Differential Encoding using a predictor band
- Universal Source Encoder for Space (USES), an industry standard for lossless encoding.

The decompression reverses the compression steps and is therefore applied in the reverse of the order listed above. The decompressed EV packets are then assembled into matrices in the order needed by the calibration algorithm. The calibration views must also be assembled into matrices called granules. The granules have n full scans (either $n_{scan}=47$ or 48 in the current configuration). The scans are assembled from first to last in time, with increasing scan line indices corresponding to later times. This is referred to as the in-track index. The detector focal plane arrays (FPA) are positioned so that detector 1 is at the leading edge of the FPA in the track direction. Unfortunately, this is the opposite of what is needed to produce the verified RDR with the scan lines increasing in the in-track direction. Therefore, the order of the detectors must be reversed in creating granules from packets. The numbering of the detectors on the FPA is referred to as Instrument Engineering Order (IEO). The reversed ordering that is used in the verified RDR (as well as the SDR and EDR) is referred to as Product Order (PO). All look-up tables that have per detector values should be in Product Order. Figure 5 provides an illustration of the different detector ordering.

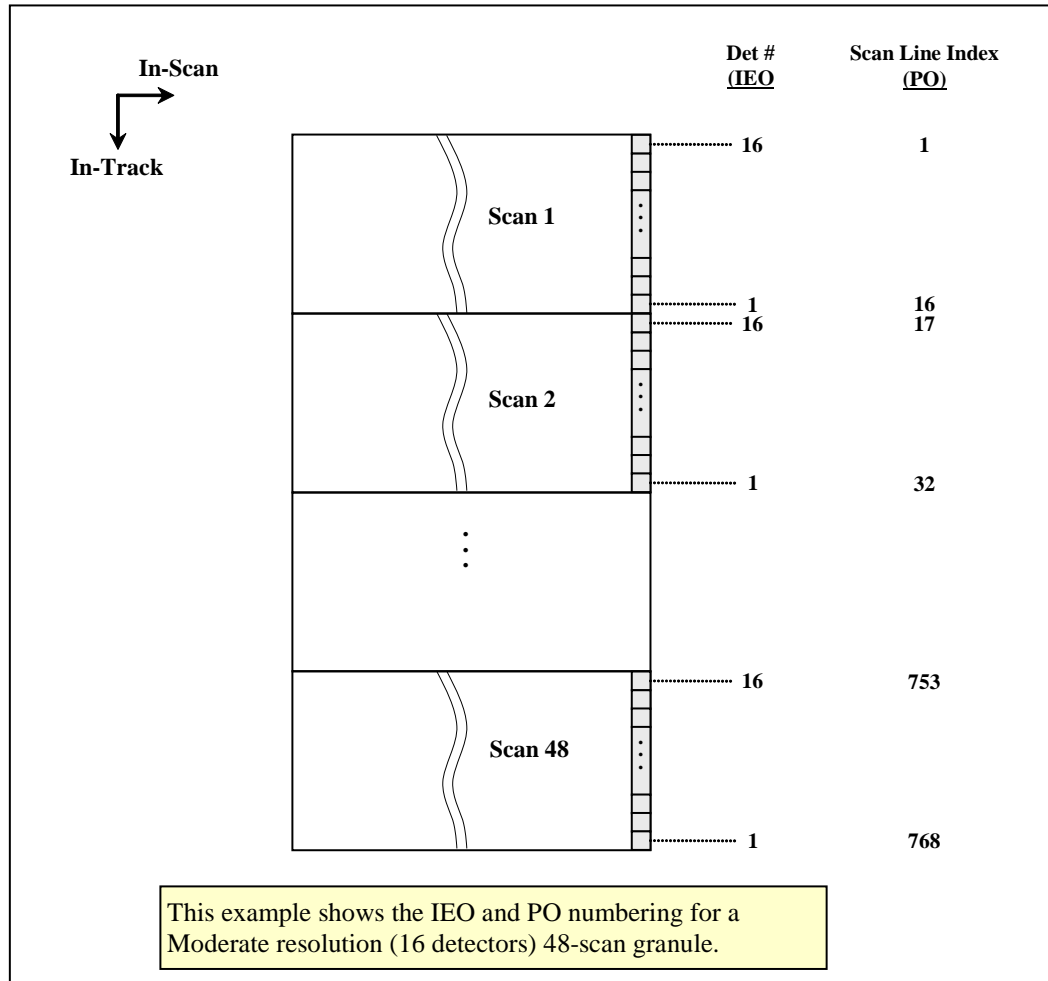


Figure 5 Instrument Engineering Order and Product Order Illustration

The other dimension is in the scan direction, referred to as the scan index, and has increasing indices from start of scan to end of scan. The imagery bands (I1 to I5) have 6400 samples in the scan index for the EV verified RDR. The dual gain moderate resolution bands (M1 to M5, M7 and M13) have 6304 samples and the other moderate resolution bands have 3200. The DNB has 4064 EV samples in-scan.

The Cal views have 96 samples in scan for imagery bands I1 to I5, and 48 samples in-scan for the moderate resolution bands. The number of samples per view for the DNB band is 64 except for Aggregation Modes 34 and 35 when it is 16. The DNB aggregation mode in the Cal view changes every two scans, cycling over aggregation Modes 1 to 36 in 72 scans. The DNB Cal data is split between the four FPAs used by the DNB: HGA, HGB, MGS, and LGS. Because the M16 detectors use TDI, it contains calibration data for both M16A and M16B detectors. The EV data, however, is aggregated before transmission for M16, so there is no separate A and B data in the verified RDR. When the Verified RDR granule arrays are created, fill values must be put in pixels where there is missing data.

Verified engineering application packet data is also produced and byte aligned as part of this process.

For the geolocation algorithm the Verified Spacecraft E&A RDR is generated from the RDR packets. This is S/C Ephemeris and Attitude RDR data that has been byte aligned. This process is done as part of the geolocation algorithm. The onboard S/C ephemeris and attitude data (in APID 11) includes: spacecraft ECR (GPS ECEF) position vectors (X, Y, Z components in meters), ECR velocity vectors (X, Y, Z components in meters per second) and attitude quaternion data (4 dimensionless numbers). The attitude quaternion data are used to create a quaternion matrix providing unambiguous rotation from J2000 ECI coordinates to spacecraft coordinates.

2.1.1 Interfaces

2.1.1.1 Inputs

The VIIRS Verified RDR process takes as input the VIIRS RDR data as shown in Table 3, Table 4, and Table 5.

Table 3 Verified VIIRS RDR Engineering Packet Data Inputs

Input	Type/ Dimensions	Description	Units/ Valid Range	Fill Value
startIETusec	Int64/ (nscans)	IET time at the start of the scan which is the number of microseconds since 1/1/1958	IET microseconds	MISS_IN T64
startTAIsec	Float64/ (nscans)	TAI time at the start of the scan which is the number of seconds since 1/1/1958	TAI seconds	MISS_FL OAT64
mirror_side	uint8/ (nscans)	mirror side in optical path – “0” for side 1 and “1” for side 2	Unitless/ [0 1]	MISS_UI NT8
dpp_config	uint8/ (nscans)(128)	digital PreProcessor Configuration	Unitless/ Count	MISS_UI NT8
mf_ao_blkhd_px_nz	int16/ (nscans)	MF_AO_BLKHD_PX_NZ Therm 44	Unitless/ Count	MISS_IN T16
mf_ao_blkhd_nx_pz	int16/ (nscans)	MF_AO_BLKHD_NX_PZ Therm 45	Unitless/ Count	MISS_IN T16
mf_stopassy_baff_nz	int16/ (nscans)	On Baffle NZ of Apert Stop Assy between HAM and FM2 Therm 14	Unitless/ Count	MISS_IN T16
mf_fold_mir_bkhd_ct	int16/ (nscans)	MF_FOLD MIRROR BLKHD Center Therm 6	Unitless/ Count	MISS_IN T16
mf_tel_blkhd_py	int16/ (nscans)	Mainframe Telescope Bulkhead Therm 33, RT16 (Node 1022 in Radiometry Model)	Unitless/ Count	MISS_IN T16
ap_lw_cca	int16/ (nscans)	Long wave IR CCA Information stored in the Engineering packet.	Unitless/ Count	MISS_IN T16
ap_sm_cca	int16/ (nscans)	Short/Med wave IR CCA information stored in the Engineering packet.	Unitless/ Count	MISS_IN T16
ap_vn_cca	int16/ (nscans)	Visible/Near IR CCA information stored in the Engineering packet	Unitless/ Count	MISS_IN T16
ct_prec_tref_mux1ca1	int16/ (nscans)	Precision Thermistor Cal Ref Resistor 1	Unitless/ Count	MISS_IN T16
ct_prec_tref_mux1ca2	int16/ (nscans)	Precision Thermistor Cal Ref Resistor 2	Unitless/ Count	MISS_IN T16
ct_prec_tref_mux1ca3	int16/ (nscans)	Precision Thermistor Cal Ref Resistor 3	Unitless/ Count	MISS_IN T16
ft_lw_cfpa_hi_rsl	int16/ (nscans)	focal plane Temperature Controller Long Wave IR CFPA high resolution temperature	degrees Kelvin/ 70 – 89K Note 1	MISS_IN T16

Input	Type/ Dimensions	Description	Units/ Valid Range	Fill Value
ft_lw_cfpa_lo_rsl	int16/ (nscans)	focal plane Temperature Controller Long Wave IR CFPA wide range temperature	degrees Kelvin/ 52 – 330K Note 1	MISS_IN T16
ft_sm_cfpa_hi_rsl	int16/ (nscans)	focal plane Temperature Controller Short Midwave IR CFPA high resolution temperature	degrees Kelvin/ 70 – 89K Note 1	MISS_IN T16
ft_sm_cfpa_lo_rsl	int16/ (nscans)	focal plane Temperature Controller Short Midwave IR CFPA wide range temperature	degrees Kelvin/ 51- 330K Note 1	MISS_IN T16
ft_vis_nir_fpa	int16/ (nscans)	focal plane Temperature Controller Visual/Near IR fpa	degrees Kelvin/ 245- 319K Note 1	MISS_IN T16
m1_asp_offset	int16/ (nscans)(2)(16)	moderate band 1 Analog Signal Processor offset	Unitless	MISS_IN T16
m2_asp_offset	int16/ (nscans)(2)(16)	moderate band 2 Analog Signal Processor offset	Unitless	MISS_IN T16
m3_asp_offset	int16/ (nscans)(2)(16)	moderate band 3 Analog Signal Processor offset	Unitless	MISS_IN T16
m4_asp_offset	int16/ (nscans)(2)(16)	moderate band 4 Analog Signal Processor offset	Unitless	MISS_IN T16
m5_asp_offset	int16/ (nscans)(2)(16)	moderate band 5 Analog Signal Processor offset	Unitless	MISS_IN T16
m6_asp_offset	int16/ (nscans)(2)(16)	moderate band 6 Analog Signal Processor offset	Unitless	MISS_IN T16
m7_asp_offset	int16/ (nscans)(2)(16)	moderate band 7 Analog Signal Processor offset	Unitless	MISS_IN T16
m8_asp_offset	int16/ (nscans)(2)(16)	moderate band 8 Analog Signal Processor offset	Unitless	MISS_IN T16
m9_asp_offset	int16/ (nscans)(2)(16)	moderate band 9 Analog Signal Processor offset	Unitless	MISS_IN T16
m10_asp_offset	int16/ (nscans)(2)(16)	moderate band 10 Analog Signal Processor offset	Unitless	MISS_IN T16
m11_asp_offset	int16/ (nscans)(2)(16)	moderate band 11 Analog Signal Processor offset	Unitless	MISS_IN T16
m12_asp_offset	int16/ (nscans)(2)(16)	moderate band 12 Analog Signal Processor offset	Unitless	MISS_IN T16
m13_asp_offset	int16/ (nscans)(2)(16)	moderate band 13 Analog Signal Processor offset	Unitless	MISS_IN T16
m14_asp_offset	int16/ (nscans)(2)(16)	moderate band 14 Analog Signal Processor offset	Unitless	MISS_IN T16
m15_asp_offset	int16/ (nscans)(2)(16)	moderate band 15 Analog Signal Processor offset	Unitless	MISS_IN T16
m16a_asp_offset	int16/ (nscans)(2)(16)	moderate band 16 Analog Signal Processor offset	Unitless	MISS_IN T16
m16b_asp_offset	int16/ (nscans)(2)(16)	day/night band Analog Signal Processor offset	Unitless	MISS_IN T16
i1_asp_offset	int16/ (nscans)(2)(32)	imagery band 1 Analog Signal Processor offset	Unitless	MISS_IN T16
i2_asp_offset	int16/ (nscans)(2)(32)	imagery band 2 Analog Signal Processor offset	Unitless	MISS_IN T16
i3_asp_offset	int16/ (nscans)(2)(32)	imagery band 3 Analog Signal Processor offset	Unitless	MISS_IN T16
i4_asp_offset	int16/ (nscans)(2)(32)	imagery band 4 Analog Signal Processor offset	Unitless	MISS_IN T16
i5_asp_offset	int16/ (nscans)(2)(32)	imagery band 5 Analog Signal Processor offset	Unitless	MISS_IN T16

Input	Type/ Dimensions	Description	Units/ Valid Range	Fill Value
bb_tmps	int16/ (nscans)(6)	black body temperatures, OT shutdown=315K	degrees Kelvin/ 243 to 336 K Note 1	MISS_IN T16
ham_tmp1	int16/ (nscans)	half angle mirror T1 prec therm 07, radiatively coupled	degrees Celsius/ -30 to 65 °C Note 1	MISS_IN T16
ham_tmp2	int16/ (nscans)	half angle mirror T2 prec therm 08, radiatively coupled	degrees Celsius/ -30 to 65 °C Note 1	MISS_IN T16
mf_nadir_rad_nxp	int16/ (nscans)	mainframe Nadir radiator nxpy	degrees Celsius/ -25 to 65 °C Note 1	MISS_IN T16
mf_scan_cavity_nxp	int16/ (nscans)	mainframe scan cavity nx pz therm 46	degrees Celsius/ -25 to 60°C Note 1	MISS_IN T16
mf_scan_cavity_baf_nz	int16/ (nscans)	mainframe scan cavity baffle NZ prec therm 10	degrees Celsius/ -25 to 60°C Note 1	MISS_IN T16
mf_scan_cavity_baf_pz	int16/ (nscans)	mainframe scan cavity baffle PZ prec therm 9 temperature	degrees Celsius/ -25 to 60°C Note 1	MISS_IN T16
mf_scan_cavity_bknd_n	int16/ (nscans)	mainframe scan cavity bulkhead ny therm 8	degrees Celsius/ -25 to 60°C Note 1	MISS_IN T16
dp_dnb_cca	int16/ (nscans)	digital preprocessor DNB cca thermistor 60	degrees Celsius/ -25 to 60°C Note 1	MISS_IN T16
dp_dpp_cca	int16/ (nscans)	digital preprocessor DPP cca thermistor 61	degrees Celsius/ -25 to 60°C Note 1	MISS_IN T16
dp_fpie_clk_cca	int16/ (nscans)	digital preprocessor focal plane interface electronics clk cca thermistor 51	degrees Celsius/ -25 to 60°C Note 1	MISS_IN T16
power_supply1	int16/ (nscans)	power supply 1 thermistor 52	degrees Celsius/ -25 to 60°C Note 1	MISS_IN T16
power_supply2	int16/ (nscans)	power supply 2 thermistor 53	degrees Celsius/ -25 to 60°C Note 1	MISS_IN T16
se_a_cca	int16/ (nscans)	scan control electronics A cca thermistor 31	degrees Celsius/ -25 to 60°C Note 1	MISS_IN T16
se_b_cca	int16/ (nscans)	scan control electronics B cca thermistor 12	degrees Celsius/ -25 to 60°C Note 1	MISS_IN T16

Input	Type/ Dimensions	Description	Units/ Valid Range	Fill Value
sdsd_position	Uint8/ (nscans)	SDSM position 0=home, 1=SD view and 2=sun view	Unitless/ 0- 2	MISS_UI NT8
sdsd_samples	int16/ [nscans] [n_sdsd_samples(5)] [n_sdsd_detectors(8)]	SDSM Samples	Volts/ -2.5 to 2.5 V Note 1	MISS_IN T16
sdsd_preamp	int16/ [nscans]	SDSM Preamp Thermistor 57	degrees Celsius/ -70 to 120°C Note 1	MISS_IN T16
tel_enc	uint16/ [nscans x (num. of TEL enc. Pulses)]	contains the raw encoder values for each scan in the granule	Scan time counter ticks/[0 – 65535]	MISS_IN T16
ham_enc	uint16/ [nscans x (num. Of HAM enc. Pulses)]	contains the raw encoder values for each scan in the granule	Scan time counter ticks/[0 – 65535]	MISS_IN T16
tel_start_enc	uint16 / [nscans]	Telescope start of scan encoder value (15-bit encoder)	15-bit encoder ticks/ [0 – 32768]	MISS_IN T16
ham_start_enc	uint16 / [nscans]	Half angle mirror start of scan encoder value (15-bit encoder)	15-bit encoder ticks/ [0 – 32768]	MISS_IN T16
act_scans	int32/ 1	number of actual scans	N/A/ 0 – 16	MISS_IN T32
scan_mode	char8/ [nscans]	sensor mode of each scan	N/A/ [Day Night Other]	MISS_UI NT8
Mode	uint8/ 1	scan mode	NA/ 0=night, 1=day, 2=mixed	MISS_UI NT8
bgnTime	int64/ 1	begin boundary of the granule	IET	MISS_IN T64
endTime	int64/ 1	end boundary of the granule	IET	MISS_IN T64
first_scan	int64/ 1	IET of the first scan	IET	MISS_IN T64
last_scan	int64/ 1	IET of the last scan	IET	MISS_IN T64
sensor_softver	uint8/ [16]	sensor software version	N/A	MISS_UI NT8
Sensor	uint8/ [8]	VIIRS sensor ID	N/A	MISS_UI NT8
sensor_model	int32/ 1	1=EDU, 2=FU1 (Flight Unit), FU2, FU3	N/A	MISS_IN T32
dnb_sequence	Uint8/ [nscans]	DNB sequence number	Unitless/ 1 to 36	MISS_UI NT8

Note: The field is a digital count. Units/Valid Range are after polynomial conversion.

Table 4 Verified VIIRS RDR Science Packet Data Inputs

Input	Type Dimensions	Description	Units Range	Fill Value
Image Band				
IETusec	Int64 [48]	IET start of the scan	Microseconds since Jan 1, 1958	MISS_INT64_FI LL
earthview	UInt16 / [1536][6400]	each pixel of the scan	12 bit count 0 – 4095	MISS_UINT16_ FILL

Input	Type Dimensions	Description	Units Range	Fill Value
Single Gain Moderate Band				
IETusec	Int64 [48]	IET start of the scan	Microseconds since Jan 1, 1958	MISS_INT64_FILL
earthview	UINT16 [768][3200]	each pixel of the scan	12 bit count 0 – 4095	MISS_UINT16_FILL
Dual Gain				
IETusec	Int64 [48]	IET start of the scan	Microseconds since Jan 1, 1958	MISS_INT64_FILL
earthview	UInt16 [768][6304]	each pixel of the scan	12 bit count 0 – 4095	MISS_UINT16_FILL
gain	UInt8 [768][6304]	the gain for each pixel	0 or 1	MISS_UINT8_FILL
DNB				
IETusec	Int64 [48]	IET start of the scan	Microseconds since Jan 1, 1958	MISS_INT64_FILL
earthview	UInt16 [768][4064]	each pixel of the scan	13 or 14 bit count 0 – 16383	MISS_UINT16_FILL
gain	UInt8 [768][4064]	the gain for each pixel	0, 2, or 3	MISS_UINT8_FILL

Table 5 Verified VIIRS RDR Calibration Packet Data Inputs

Input	Type Dimensions	Description	Units Range	Fill Value
Image Band				
sv_calib	UInt16 [1536][96]	space view calibration source	counts 0 – 32767	MISS_UINT16_FILL
bb_calib	UInt16 [1536][96]	black body calibration source	counts 0 – 32767	MISS_UINT16_FILL
sd_calib	UInt16 [1536][96]	solar diffuser calibration source	counts 0 – 32767	MISS_UINT16_FILL
Single Gain Moderate Band				
sv_calib	UInt16 [768][48]	space view calibration source	counts 0 – 32767	MISS_UINT16_FILL
bb_calib	UInt16 [768][48]	black body calibration source	counts 0 – 32767	MISS_UINT16_FILL
sd_calib	UInt16 [768][48]	solar diffuser calibration source	counts 0 – 32767	MISS_UINT16_FILL
Dual Gain / DN Bands				
sv_calib	UInt16 [768][48]	space view calibration source	counts 0 – 32767	MISS_UINT16_FILL
bb_calib	UInt16 [768][48]	black body calibration source	counts 0 – 32767	MISS_UINT16_FILL
sv_calib	UInt16 [768][48]	solar diffuser calibration source	counts 0 – 32767	MISS_UINT16_FILL
sv_calib_gain	UInt8 [768][48]	gain state for the space view calibration	counts 0 – 1	MISS_UINT8_FILL
bb_calib_gain	UInt8 [768][48]	gain state for the black body calibration	counts 0 – 1	MISS_UINT8_FILL
sd_calib_gain	UInt8/ [768][48]	gain state for the solar diffuser calibration	counts 0 – 1	MISS_UINT8_FILL
DNB				
sv_calib	UInt16 [768][64]	space view calibration source	counts 0 – 32767	MISS_UINT16_FILL
bb_calib	UInt16 [768][64]	black body calibration source	counts 0 – 32767	MISS_UINT16_FILL
sv_calib	UInt16 [768][64]	solar diffuser calibration source	counts 0 – 32767	MISS_UINT16_FILL

2.1.1.2 Outputs

The internal output of the VIIRS Verified RDR is a byte-aligned version of the VIIRS RDR.

2.1.2 Algorithm Processing

This is the derived algorithm for the VIIRS SDR Verified RDR algorithm and is a subclass of the `AutoGeneratedProSdrViirsVerifiedRdr` and `ProCmnAlgorithm` classes. The derived algorithm class creates a list of input data items read from DMS and passes required data into the algorithm. All output data items are written to DMS once the algorithm finishes processing this data.

VIIRS Science RDRs contain the science, CAL and engineering application packets that are required for SDR processing of a tasked granule. In addition to the tasked granule, the RDR information from the previous and following granule also need to be processed in order to accurately calibrate dual gain bands. Not all of the data in the RDRs are needed for SDR processing. A Verified RDR contains only the data from an RDR that is required for the SDR processing of a tasked granule. The data has been extracted, unpacked and byte aligned from the CCSDS application packets contained in the RDR. In other words, a Verified RDR is a byte-aligned RDR. This unpacked and byte-aligned data is assigned to the internal verified RDR structure, which is not in the same structure that the packet data came in (for efficiency reasons), and VIIRS SDR processing uses the data from that structure to do further processing. Figure 6 shows the Create Verified VIIRS RDR Flow.

The first sample from each of the 16 DNB detector outputs reported in the Earth View and the three calibration views (Space, Blackbody and Solar Diffuser) is anomalous for each VIIRS scan. The main cause for this anomaly was found to be due to a problem in the startup portion of the CCD timing. This timing problem may be fixed in the hardware for Flight Unit 2; however, for Flight Unit 1, this DNB anomaly should be removed during the VIIRS SDR process by placing fill integer 0 values in the RDR data for the DNB Earth View and the three calibration views. This VIIRS DNB First Frame anomaly was fixed per

NP-EMD-2007.510.0029_NPP_VIIRS_SDR_DNB_FirstFrameAnomaly.

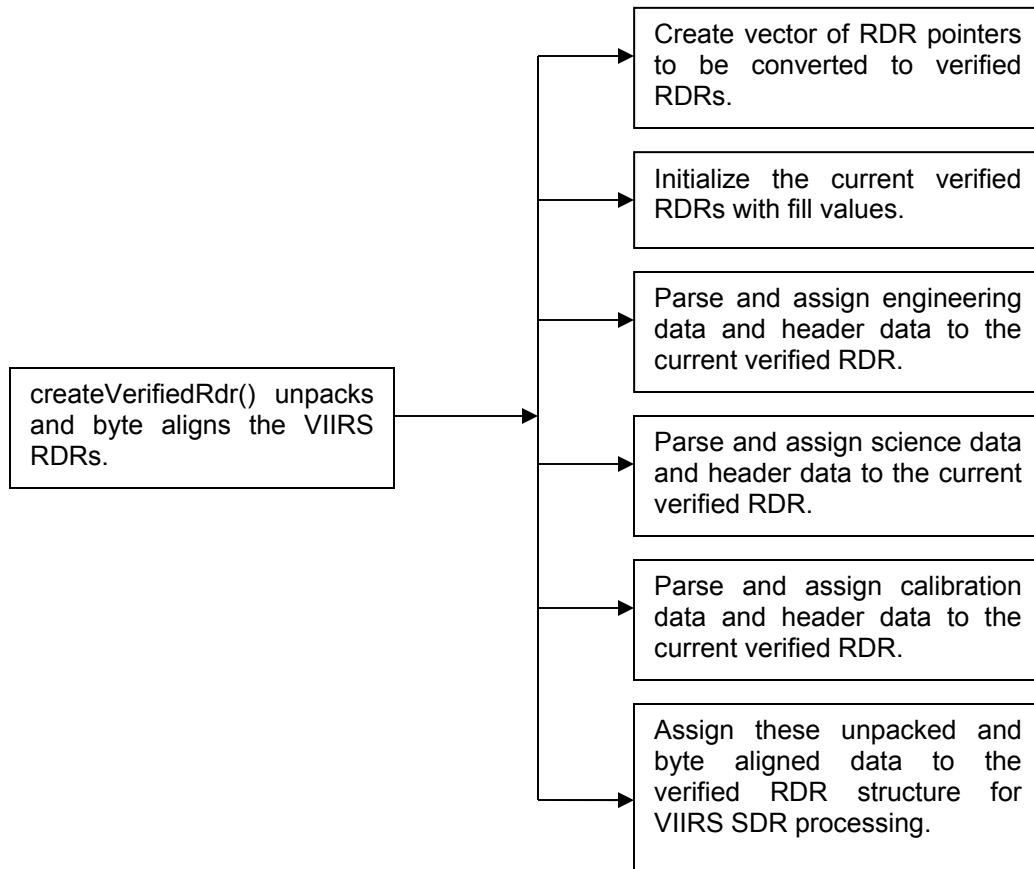


Figure 6 Create Verified VIIRS RDR Flow Diagram

2.1.2.1 createVerifiedRDR()

createVerifiedRDR() creates a VIIRS Verified RDR structure for the current, previous, and following granules and calls ProViirsVerifiedRDRConverter::convert() to fill the Verified RDRs with unpacked and byte-aligned engineering, science, and CAL data. The Verified RDR number of actual scans is validated and the granule mode (day, night, mixed) is determined.

2.1.2.2 ProViirsVerifiedRDRConverter()

ProViirsVerifiedRDRConverter() retrieves the engineering, science, and CAL packets by APID from the VIIRS RDRs and calls the appropriate methods (ViirsEngAppPacket::parsePkts(), ViirsSciAppPacket::parsePkts(), ViirsEngCalPacket::parsePkts()) to unpack and byte align the data which is stored in the VIIRS Verified RDR. To ensure that every granule starts at a scan 1 and that missing scans are treated appropriately, scan ids are turned into offsets from the minimum scan id in the granule.

2.1.2.3 ViirsCalAppPacket()

The ViirsCalAppPacket class contains methods to retrieve and decompress the CAL packet data in the VIIRS RDR. It loops through the space view, black body, and solar diffuser CAL data and decompresses the views for each detector of each band. Universal Source Encoder for Space (USES) (viirs_decmp()) is used for this purpose. This is also referred to Rice compression (after its creator or Modified NCSA (National Center for Supercomputing Applications) code. This class also converts the CCSDS time to IET time.

2.1.2.4 ViirsEngAppPacket()

The ViirsEngAppPacket class contains methods to unpack and byte align engineering packet data in the VIIRS RDR. This class also retrieves and converts the CCSDS time to IET time.

2.1.2.5 ViirsHrdAppPacket()

The ViirsHrdAppPacket class contains methods to retrieve and decompress the science packet data in the VIIRS RDR. This class also converts the CCSDS time to IET time and fills in the start of scan trigger time for the RDR.

2.1.3 Graceful Degradation

The VIIRS Verified RDR procedure contains no graceful degradation.

2.1.3.1 Graceful Degradation Inputs

None.

2.1.3.2 Graceful Degradation Processing

None.

2.1.3.3 Graceful Degradation Outputs

None.

2.1.4 Exception Handling

No exception handling is performed in the VIIRS Verified RDR process.

2.1.5 Data Quality Monitoring

No data quality monitoring is performed in the VIIRS Verified RDR process.

2.1.6 Computational Precision Requirements

There are no computational precision requirements for the VIIRS Verified RDR process.

2.1.7 Algorithm Support Considerations

The DMS and INF must be running before the algorithm is executed.

2.1.8 Assumptions and Limitations

The VIIRS Verified RDR requires as input raw data packets transmitted from the satellite.

2.2 VIIRS SDR Geolocation Description

The purpose of the VIIRS GEO software is to provide Earth location and related spatial information for each of the samples in the Raw Data Record (RDR) belonging to the moderate resolution radiometric bands (aggregated and unaggregated), the fine resolution imagery bands, and the Day/Night Band (DNB). The output GEO data fields include geodetic latitude, longitude and derived products such as satellite zenith and azimuth angles, range to the satellite, solar zenith and azimuth angles, and (for the DNB) both lunar zenith and azimuth angles. The VIIRS GEO algorithm processes the engineering VIIRS RDR and Spacecraft Ephemeris and Attitude (E&A) RDRs, as well as external support data sets to generate the GEO data fields. The Earth location fields, which include the geodetic latitude, longitude and height, are computed using rigorous models of the Earth and VIIRS instrument pointing. The algorithm computes the earth location by first determining each pixel's line-of-sight (LOS) vector by constructing dynamic models of the VIIRS instrument using the engineering and spacecraft RDR data. Each detector's LOS vector is then intersected with the rotating WGS84 ellipsoid to obtain geodetic latitude and longitude. If terrain correction is to be performed, then the LOS intersection with the terrain-adjusted surface (geoid plus height over the geoid) is computed to output a terrain corrected geodetic latitude, longitude and height. The GEO products are held in internal memory to be input to the radiometric CAL module before they are written out to the Data Management Subsystem (DMS). For a list of GEO products to be produced, please refer to Section 2.2.1.2. The Geolocation Processing Chain is shown in Figure 7.

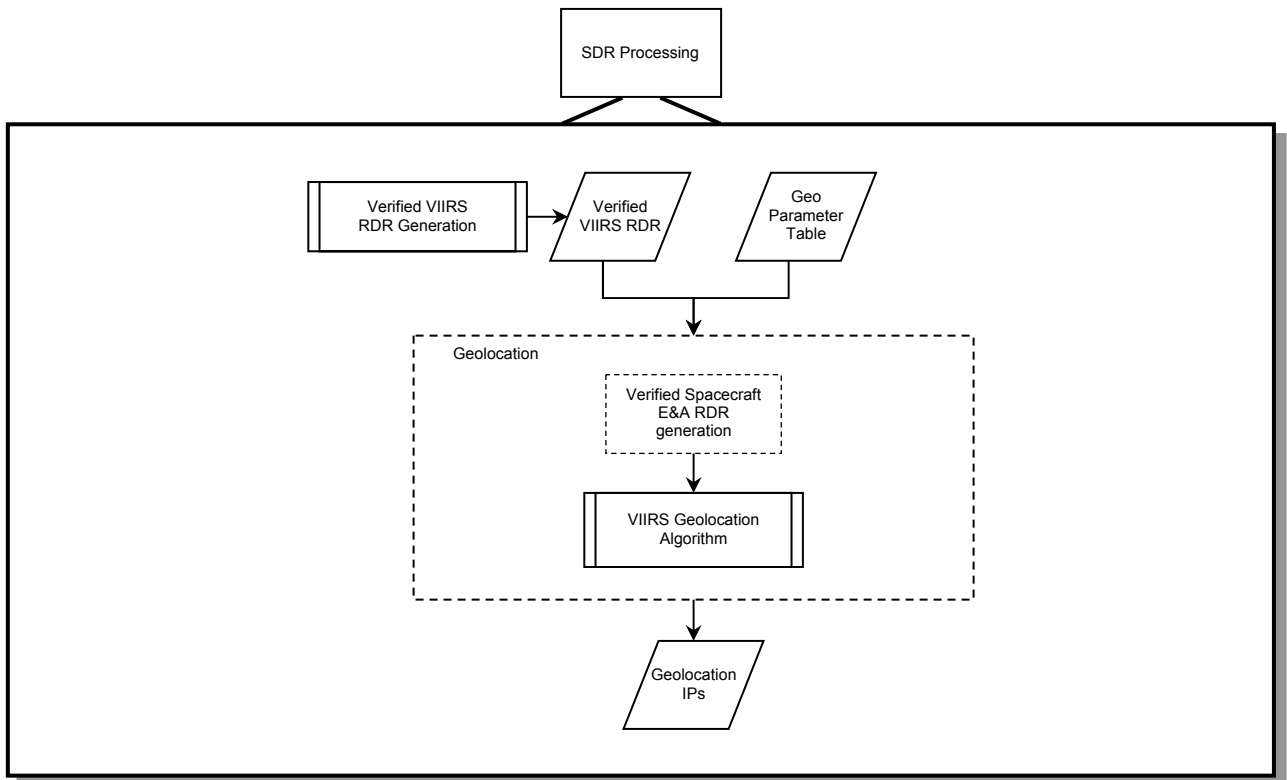


Figure 7 Geolocation Processing Chain

2.2.1 Interfaces

2.2.1.1 Inputs

Table 6 lists the VIIRS GEO SDR inputs which are further detailed within Tables 7, and 8. The rotating telescope assembly (RTA) encoder data and half angle mirror (HAM) encoder data is used by the Geolocation algorithm to construct models of the RTA and HAM rotation as a function of time. The scan timing information is used to relate the VIIRS spatial elements to the models of both the dynamic components of the instrument (RTA and HAM) and the S/C. Some parameters listed in this table are not used by GEO but must remain in the data structure for sizing purposes. Table 7 contains a list of the S/C ephemeris and attitude data used to construct a model of the platform position, velocity, and orientation as a function of time. Table 8, Geolocation Parameter Inputs, contains instrument constants that include focal plane, band, and detector locations which are used to generate corrections applicable to each detector (channel) in a spatial element.

Table 6 VIIRS Geolocation Inputs

Input	Object/Format	Description
Verified VIIRS RDR	Binary	VIIRS Engineering RDR packets that have been byte aligned.
Verified Spacecraft E&A RDR	Binary	S/C Ephemeris and Attitude RDR data that has been byte aligned.

Input	Object/Format	Description
Geolocation Parameter Table	Binary	File containing information specific for processing each resolution – 1 for each resolution.

Table 7 S/C Ephemeris and Attitude Data

Input	Type/ Dimensions	Description	Units/ Valid Range	Fill Value
ietTime	Int64[NUM_EPH_RPTS]	IET time of the ephemeris data	Microseconds since 1/1/1958	None
pos	float32[NUM_EPH_RPTS][3]	ECEF (Earth Centered Earth Fixed)	Meters -7.25E6 to 7.25E6	None
vel	float32[NUM_EPH_RPTS][3]	ECEF	meters/sec -7.55E3 to 7.55E3	None
ietTime	Int64[NUM_ATT_RPTS]	IET time of the attitude data	Microseconds since 1/1/1958	None
quat	float32[NUM_ATT_RPTS][4]	Quaternion of Control Frame relative to J2000.0	Quaternion [-1 to +1]	None

Table 8 Geolocation Parameter Inputs

Input	Type/ Dimensions	Description	Units/ Valid Range	Fill Value
revision	UInt8/ (1,10)	Revision number for the parameter file (1-D array, 10 bytes in length).	Unitless/ N/A	None
band_number	Int32/ 1	Band number to geolocate (0 is the ideal band). This parameter is used to index other band dependent parameters.	Unitless/ [0 to 22]	None
latch_to_center	float64/ 1	Used to calculate sample time from frame time. This specifies the fraction of the frame time that is used to compute the sample time, e.g., latch_to_center = 0.5 means that the sample time is computed at the center of the frame time.	Unitless/ [0 – 1.0]	None
t_reset	float64/ 1	Time to reset the sample, otherwise called the readout time. This is computed by subtracting the integration time from the frame time. If the readout occurs at the beginning of the frame time (before the integration time), then a negative t_reset should be used in the parameter file to adjust the sample time equations appropriately.	Seconds [-2.3e-5 - 2.3e-5]	None
N_samp	UInt16/ Max Band Number (MBN) + 1	Factor used to determine the number of samples per frame for each band (0 is the ideal band).	Unitless/ [1 – 2]	None

Input	Type/ Dimensions	Description	Units/ Valid Range	Fill Value
focal_length	float64/ MBN+1	Instrument focal length for each band. This parameter is tied to the Mag parameter. If the system Mag is used, then the system focal length should be used. Likewise, if the Mag of the Aft Optics is used, then the Aft Optics focal length should be used.	Meters/ [0.270 - 1.15]	None
det_space_track	float64/ MBN+1	Detector center spacing in the track direction (0 is the ideal band)	Meters/ Range for IMG: [0.000508 – 0.000511] Range for MOD: [0.001016 – 0.001022]	None
det_space_scan	float64/ MBN+1	Detector center spacing in the scan direction (0 is the ideal band). This parameter currently set to zero for all bands since the scan offset is accounted for by a timing offset.	Meters/ ≥ 0	None
DNB_space_track	float64/ 32	DNB detector center spacing in the track direction. Aggregation zone dependent, listed in order from Zone 0 to 31, where Aggregation Zone 0 is nadir.	Meters/ [0.000484 - 0.001016]	None
DNB_space_scan	float64/ 32	DNB detector center spacing in the scan direction. Aggregation zone dependent, listed in order from Zone 0 to 31, where aggregation Zone 0 is nadir. This parameter currently set to zero for all zones since the scan offset is accounted for by a timing offset.	Meters/ ≥ 0	None
det_position	float64/ (MBN+1, 2)	Band center x and y offset pairs with respect to the optical center (0 is the ideal band). This value is the average shift of all detector locations within the band from the nominal location (overall bias per band).	Meters/ Range Dim 1 (scan): [0 to 0.000177] IMG [0 to 0.000354] MOD [0 to 0.000015] DNB Range Dim 2 (track): [0 to 0.000508] IMG [0 to 0.001016] MOD [0 to 0.000024] DNB	None
band_position	float64/ MBN+1	Scan IFOV offsets of band trailing edges with respect to the optical center (0 is the ideal band)	MOD IFOV/ [-22 to 22]	None
earth_view_delay	float64/ 1	The delay following the start of scan (referenced to the encoder clock reset) to the start of the first Earth View (EV) sample. This parameter specifies the dropped samples to allow for electronic settling before EV sampling.	Seconds/ Real number	None
detector_sampling_rate	float64/ 1	Sampling rate for MOD, IMG and DNB resolution detectors.	Seconds/ [0.000003 – 0.0009]	None
scan_length	float64/ 1	Scan period (Length of VIIRS scan)	Seconds/ [1.77 – 1.80]	None

Input	Type/ Dimensions	Description	Units/ Valid Range	Fill Value
agg_zone_bounds	int32/ (1,5)	Upper bounds for the MOD and IMG resolution along-scan aggregation zones. For the MOD res. case, specification of a Negative value for the first zone forces software to geolocate unaggregated MOD pixels. Capability required for CalVal. Note that N_frame should be consistent with choice made here.	Frame number/ fixed set of values for IMG and MOD	None
DNB_aggregation	int32/ (32,2)	The first column is the number of samples occurring in each DNB aggregation zone, and the second column is the number of along-scan photosites per pixel for that zone. Values are listed from aggregation zone 0 to 31, where Zone 0 is nadir.	Unitless/ fixed set of values	None
DNB_ag_zone_bounds	Int32/ (64, 3)	Frame number limits for the 32 DNB aggregation zones from start of scan through nadir to end of scan, and the associated DNB aggregation zone indices. Columns 0 & 1 are the lower and upper frame numbers per zone, respectively. Column 2 contains the associated aggregation zone index, where Index 0 corresponds to nadir and Index 31 the edge of scan.	<u>Units:</u> Col 0 & 1: Frame Num Col 2: Agg Zone Index <u>Valid Range:</u> Col 0 & 1: [0 4063] Col 2: [0 – 31]	None
scan_ang_coef_tel	float64/ 1	Scan angle coefficient for telescope	Unitless/ Real number	None
scan_ang_coef_mirr	float64/ 1	Scan angle coefficient for HAM	Unitless/ Real number	None
scan_ang_offsets	float64/ (1,2)	Scan angle offsets for computing the sample scan angle for mirror side 1 (element 0) and side 2 (element 1).	Radians/ [0 - 2 π]	None
enc_scale	float64/ 1	Scale factor for converting 14-bit encoders to 16-bit representation	Unitless/ Fixed Value	None
mirr_abs_limit	float64/ (1,2)	Mirror encoder time stamp absolute limits in units of Scan-Time counter ticks. This parameter determines the valid range for the mirror encoder delta time stamp readings (specifies the acceptable stable scan rate range by limiting the delta timestamp readings).	Scan-time counter ticks/ [875 – 885]	None
mirr_del_limit	float64/ 1	Mirror encoder time stamp delta limits in units of Scan-Time counter ticks. This parameter specifies the maximum allowable difference between adjacent mirror encoder delta time stamp readings (limits the instantaneous changes in scan rate).	Scan-time counter ticks/ ≤ 10	None

Input	Type/ Dimensions	Description	Units/ Valid Range	Fill Value
tel_abs_limit	float64/ (1,2)	Telescope encoder time stamp absolute limits in units of Scan-Time counter ticks. This parameter determines the valid range for the telescope encoder delta time stamp readings (specifies the acceptable stable scan rate range by limiting the delta timestamp readings).	Scan-time counter ticks/ [875 – 885]	None
tel_del_limit	float64/ 1	Telescope encoder time stamp delta limits in units of Scan-Time counter ticks. This parameter specifies the maximum allowable difference between adjacent telescope encoder delta time stamp readings (limits the instantaneous changes in scan rate).	Scan-time counter ticks ≤10	None
sample_impulse_mirr	int32 / 1	Mirror encoder pulses between each encoder sample (= 2)	Encoder pulses/ Fixed Value	None
sample_impulse_tel	int 32/ 1	Telescope encoder pulses between each encoder sample (= 4)	Encoder pulses/ Fixed Value	None
A_bit_adj	int32/ (1,2)	Offset to convert from pseudo 15-bit to 16-bit encoders, depending on if the Start-of-Scan15-bit encoder is even or odd [even adjust / odd adjust]	16-bit encoder ticks/ [0 to 1]	None
B_HAM_adj	int32/ (1,2)	Offset for converting HAM encoders to absolute encoders depending on the HAM side [HAM A adjust / HAM B adjust]	16-bit encoder ticks/ [0 to 2 ¹⁶]	None
t_encoder	float64/ 1	Encoder data scale factor to convert from scan time counter ticks to time.	Microseconds per scan time counter tick/ [0.495624 – 0.495688]	None
mirr_side1_range	float64/ (1,2)	Mirror side 1 angle range	Radians/ [- π – π]	None
alpha	float64/ 1	Mirror wedge angle α is the non-parallelism of the HAM in the along-scan axis, and creates an along-scan offset between scans from mirror sides 1 and 2.	Radians/ < 9.7e-5	None
beta	float64/ 1	Mirror wedge angle β is the non-parallelism of the HAM in the along-track axis, and creates an along-track offset.	Radians/ < 9.7e-5	None
gammaa	float64/ 1	Misalignment of the mirror plane-of-symmetry (defined as the plane midway between the two mirror surfaces) to the rotation axis (HAM motor axis)	Radians/ [-4.85e-5 to 4.85e-5]	None
T_inst2sc	float64/ (3,3)	3x3 Instrument to Spacecraft frame transformation matrix	Unitless/ Real numbers	None
T_mirr2inst	float64/ (3,3)	3x3 Mirror to Instrument frame transformation matrix	Unitless/ Real numbers	None

Input	Type/ Dimensions	Description	Units/ Valid Range	Fill Value
T_aft2inst	float64/ (3,3)	3x3 AFT to Instrument frame transformation matrix (this matrix includes Focal plane to AFT frame transformation, which is a 3x3 rotation matrix with the scan velocity lag angle)	Unitless/ [-1 to 1]	None
T_inst2SD	float64/ (3,3)	3x3 Instrument to Solar Diffuser frame transformation matrix	Unitless/ [-2 to 2]	None
T_tel2inst	float64/ (3,3)	3x3 Telescope to Instrument frame transformation matrix	Unitless/ Real numbers	None
num_thermistor	int32/ 1	Number of thermistors currently used for thermal correction.	N/A [0 – 26]	None
thermistor_id	Uint8/ (26,40)	ID of thermistors used for temperature corrections. Each ID or name corresponds to a set of thermistor coefficients listed in the thermistor_coefs parameter. The number of items listed here should equal num_thermistor.	Unitless/ N/A	None
thermistor_coefs	float64/ (26,6)	Set of coefficients used in a conversion polynomial to derive a temperature from thermistor readings. Each set corresponds to a thermistor name (see thermistor_id). The number of items entered here should equal num_thermistor. (This parameter allows for 6 coefficients per thermistor).	Unitless/ Real numbers	None
Mag	float64/ (3, 3)	3x3 telescope magnification matrix, where the matrix contains the term 1/m. This parameter is coupled with the focal_length parameter (see focal_length description).	Unitless/ [0 – 1]	None
basis_in	float64/ (3,3)	3x3 telescope entrance basis matrix	Unitless/ [0 – 1]	None
basis_out	float64/ (3,3)	3x3 telescope exit basis matrix	Unitless/ [0 – 1]	None
poly_coef_mirr	float64/ (1,5)	Polynomial coefficients for mirror encoder-to-angle conversion. Assumes linear relationship, so only first two coefficients are populated.	Elem. 0: Radians Elem. 1: radians per 16-bit encoder ticks/ Real numbers	None
poly_coef_tel	float64/ (2,5)	Polynomial coefficients for telescope encoder-to-angle conversion. Assumes linear relationship, so only first two coefficients are populated.	Elem. 0: Radians Elem. 1: radians per 16-bit encoder ticks/ Real numbers	None
tel_ref	float64/ 1	Telescope reference angle	Radians/ [- π to π]	None
band_type	Int32	Identifies band type: moderate (0), imagery (1), or DNB (2)	Unitless/ [0 – 2]	None
num_detectors	Int32	Number of detectors per band (depends on band type).	Unitless/ [16 – 32]	None
poly_degree	int32/ 1	Degree of the polynomial for mirror encoder-to-angle conversion	Unitless/ [1 – 4]	None

Input	Type/ Dimensions	Description	Units/ Valid Range	Fill Value
N_frame	Unit16	Number of frames per scan (depends on band type)	Unitless/ [3200 – 6400]	None
MIN_COS_VIEW	float64/ 1	This parameter specifies the sensor zenith angle limit used for flagging pixels as being near the limb. If the sensor zenith angle is greater than MIN_COS_VIEW, the pixels are flagged as being Near Limb	Unitless/ [0 – PI]	None

2.2.1.2 Outputs

The VIIRS SDR GEO code produces six non-gridded GEO products (DNB, MOD, MOD Unagg, IMG, MOD terrain corrected, IMG terrain corrected) and two gridded GEO products (MOD and IMG). For the six non-gridded GEO products, the data is output in both radians and degrees. Either the radians geo product or the degrees geo product can be used by downstream algorithms. The two gridded GEO outputs are used for internal processing only. The default grid projection used by the Operational code is polar stereographic projection. The gridded GEO outputs are used for the remapping of Imagery EDRs and can be used for remapping from the VIIRS SDR to any map projection. See Sections 2.2.1.2.1 and 2.2.1.2.2 for associated geolocation output data. All relevant Metadata associated with these output items is defined in the CDFCB-X, Volume V.

Each non-gridded product contains the granule scan and pixel level data, as shown in Tables 9 through 12. Note that for MOD and IMG, the same structures are used for both terrain corrected and non-terrain corrected products. In the terrain corrected products, the latitude and longitude, and all of the pixel level products are adjusted for terrain.

Granule-Level quality flags (QF) (Automatic Quality and the Percent Missing) (note that these are two of the name/value pair metadata QFs) apply to IMG, MOD and DNB bands and are defined below: Automatic Quality QF:

- 1) HAM/RTA Encoder Flag: If the encoder flags are set to bad or degraded, Automatic QF should be triggered.
- 2) HAM/RTA Encoder Flag: If the encoder data is missing, Automatic QF should be triggered.
- 3) Missing E&A Flag: If E&A data is missing, Automatic QF should be triggered.
- 4) SAA flag - Automatic QF should NOT be triggered as this does not affect the geo quality,
- 5) Eclipse flag - Automatic QF should NOT be triggered as this does not affect the geo quality.
- 6) Bad pointing QF and Percent out of Bounds - if this is triggered Automatic QF should be triggered.
- 7) Bad terrain and invalid solar angles QF - if these are triggered; the Automatic QF should be triggered.

Percent Missing QF:

This quality flag is a percentage summary of:

- 1) geo Scan Quality=missing, OR
- 2) scan-level Missing ephemeris or attitude QF is anything other than nominal (there are 4 options)

Table 9 DNB Geolocation Output Structure

Output	Type/Dimensions	Description	Units/Valid Range	Fill Value
Scan Start Time	Int64[VIIRS_RDR_SCANS]	Scan start time, defined at the leading edge of the first Earth View frame in IET	Microseconds 0 ≤ scanStartTime ≤ 1.00E+38	-999
Scan Mid Time	Int64[VIIRS_RDR_SCANS]	Mid Time of Scan in IET	Microseconds 0 ≤ scanMidTime ≤ 1.00E+38	-999
Latitude	Float32[DNB_VIIRS_SDR_ROWS] [DNB_VIIRS_SDR_COLS]	Geodetic latitude of the VIIRS pixels	Degrees -90° ≤ Latitude ≤ 90° (positive to the North)	-999.9
Latitude_TC	Float32[DNB_VIIRS_SDR_ROWS] [DNB_VIIRS_SDR_COLS]	Terrain corrected latitude of the VIIRS pixels	Degrees -90° ≤ Latitude ≤ 90° (positive to the North)	-999.9
Longitude	Float32[DNB_VIIRS_SDR_ROWS] [DNB_VIIRS_SDR_COLS]	Geodetic longitude of the VIIRS pixels	Degrees -180° ≤ Longitude ≤ 180° (positive to the East of Greenwich)	-999.9
Longitude_TC	Float32[DNB_VIIRS_SDR_ROWS] [DNB_VIIRS_SDR_COLS]	Terrain corrected longitude of the VIIRS pixels	Degrees -180° ≤ Longitude ≤ 180° (positive to the East of Greenwich)	-999.9
SolarZenith	Float32[DNB_VIIRS_SDR_ROWS] [DNB_VIIRS_SDR_COLS]	Solar zenith angle relative to the VIIRS pixels measured from the local vertical	Degrees 0° ≤ SolarZenith ≤ 180°	-999.9
SolarAzimuth	Float32[DNB_VIIRS_SDR_ROWS] [DNB_VIIRS_SDR_COLS]	solar azimuth angle relative to the VIIRS pixels and measured from the local North towards East	Degrees -180° ≤ SolarAzimuth ≤ 180°	-999.9

Output	Type/Dimensions	Description	Units/Valid Range	Fill Value
satZen	Float32[DNB_VIIRS_SDR_ROWS] [DNB_VIIRS_SDR_COLS]	S/C zenith angle relative to the VIIRS pixels measured from the local vertical	Degrees 0° <= satZen <= 180°	-999.9
satAzm	Float32[DNB_VIIRS_SDR_ROWS] [DNB_VIIRS_SDR_COLS]	S/C azimuth angle relative to the VIIRS pixels and measured from the local North towards East	Degrees -180° <= satAzm <= 180°	-999.9
LunarZenith	Float32[DNB_VIIRS_SDR_ROWS] [DNB_VIIRS_SDR_COLS]	Lunar zenith angle relative to the VIIRS pixels measured from the local vertical	Degrees 0° <= LunarZenith <= 180°	-999.9
LunarAzimuth	Float32[DNB_VIIRS_SDR_ROWS] [DNB_VIIRS_SDR_COLS]	Lunar azimuth angle relative to the VIIRS pixels and measured from the local North towards East	Degrees -180° <= LunarAzimuth <= 180°	-999.9
Height	Float32[DNB_VIIRS_SDR_ROWS] [DNB_VIIRS_SDR_COLS]	Difference between ellipsoid and geoid heights	Meters -150 <= Height <= 150	-999.9
Height_TC	Float32[DNB_VIIRS_SDR_ROWS] [DNB_VIIRS_SDR_COLS]	Ellipsoid-geoid separation for non-Terrain corrected Geo, and the height is the terrain height above MSL for terrain corrected Geo	Meters -150 <= Height <= 150	-999.9
Range	Float32[DNB_VIIRS_SDR_ROWS] [DNB_VIIRS_SDR_COLS]	The distance from the ground position represented by the pixel to the S/C	Meters 800000 <= Range <= 2000000	-999.9
S/C Position	Float32[VIIRS_RDR_SCANS][3]	S/C Position in ECR coordinates at mid-scan time	Meters -7.46E+06 <= Position <= 7.46E+06	-999.9
S/C Velocity	Float32[VIIRS_RDR_SCANS][3]	S/C Velocity in ECR coordinates at mid-scan time	Meters/sec -6600 <= Velocity <= 6600	-999.9
S/C Attitude	Float32[VIIRS_RDR_SCANS][3]	S/C Attitude (roll, pitch, yaw) computed at mid-scan time. The roll, pitch, and yaw angles can be used to create a direction cosine matrix that rotates the S/C coordinates to the Orbit Frame coordinates ¹ .	Arcseconds -648000 <= Attitude <= 648000	-999.9

¹ The Orbit Frame is defined as follows: the Orbit Frame z-axis is determined from the ECR position of the spacecraft. The initial vector is from the ECR position of the spacecraft to geodetic nadir. The ECR geodetic nadir vector is converted to ECI J2000 and converted to a unit vector. The ECR S/C velocity vector is converted to ECI J2000 coordinates, and the y-axis of the Orbit Frame is determined by calculating the following vector cross product: Orbit Frame z-axis X S/C velocity vector in ECI J2000. The result is

Output	Type/Dimensions	Description	Units/Valid Range	Fill Value
S/C Solar Zenith	Float32[VIIRS_RDR_SCANS]	Solar zenith angle with respect to the solar diffuser reference frame z-axis, where the SD z-axis is normal to the SD surface.	Degrees 0 <= scSunZen <= 180	-999.9
S/C Solar Azimuth	Float32[VIIRS_RDR_SCANS]	Solar azimuth angle measured counterclockwise about the solar diffuser reference frame z-axis with respect to the solar diffuser x-axis (with positive z-axis towards the observer)	Degrees -180 <= scSunZen <= 180	-999.9
moon_phase	Float32	Angle between ray vector from the moon to earth and ray vector of moon to sun.	Degrees 0 <= moon_phase <= 180	-999.9
mi_frac	Float32	Fraction of the moon illuminated (expressed as percent)	No units 0.0 <= mi_frac <= 100	-999.9
scan_mode	Uint8[VIIRS_RDR_SCANS]	The VIIRS operational mode, reported at the scan level. (Refer to Table 30.)	None 0=Night; 1=Day	255
mode	Uint8	The VIIRS operational mode, reported at the granule level. (Refer to Table 30.)	None 0=Night; 1=Day; 2=Mixed	255
act_scans	Int32	Actual number of VIIRS scans that were used to create this granule.	0 <= act_scans <= 48	-999
QF1_SCAN_VIIRSSDRGEO	Uint8[VIIRS_RDR_SCANS]	Scan-level quality flags	See QF1 in Table 13	None
QF2_SCAN_VIIRSSDRGEO	Uint8[VIIRS_RDR_SCANS]	Scan-level quality flags	See QF2 in Table 13	None
QF2_VIIRSSDRGEO	Int8[DNB_VIIRS_SDR_ROWS] [DNB_VIIRS_SDR_COLS]	Pixel Level Quality flags	See Table 14	None
QF2_VIIRSSDRGEO_TC	Int8[DNB_VIIRS_SDR_ROWS] [DNB_VIIRS_SDR_COLS]	Pixel Quality flags (terrain corrected)	See Table 14	None

Table 10 MOD Geolocation Output Structure

Output	Type/Dimensions	Description	Units/Valid Range	Fill Value
--------	-----------------	-------------	-------------------	------------

then converted to a unit vector. The Orbit Frame x-axis is computed by taking the vector cross product of the y-axis and z-axis (y-axis X z-axis).

Output	Type/Dimensions	Description	Units/Valid Range	Fill Value
Scan Start Time	Int64[VIIRS_RDR_SCANS]	Scan start time, defined at the leading edge of the first Earth View frame in IET	Microseconds 0 <= scanStartTime <= 1.00E+38	-999
Scan Mid Time	Int64[VIIRS_RDR_SCANS]	Mid Time of Scan in IET	Microseconds 0 <= scanStartTime <= 1.00E+38	-999
Latitude	Float32[MOD_VIIRS_SDR_ROWS] [MOD_VIIRS_SDR_COLS]	Geodetic latitude of the VIIRS pixels	Degrees -90° <= Latitude <= 90° (positive to the North)	- 999.9
Longitude	Float32[MOD_VIIRS_SDR_ROWS] [MOD_VIIRS_SDR_COLS]	Geodetic longitude of the VIIRS pixels	Degrees -180° <= Longitude <= 180° (positive to the East of Greenwich)	- 999.9
SolarZenith	Float32[MOD_VIIRS_SDR_ROWS] [MOD_VIIRS_SDR_COLS]	Solar zenith angle relative to the VIIRS pixels measured from the local vertical	Degrees 0 <= SolarZenith <= 180	- 999.9
SolarAzimuth	Float32[MOD_VIIRS_SDR_ROWS] [MOD_VIIRS_SDR_COLS]	solar azimuth angle relative to the VIIRS pixels and measured from the local North towards East	Degrees -180 <= SolarAzimuth <= 180	- 999.9
satZen	Float32[MOD_VIIRS_SDR_ROWS] [MOD_VIIRS_SDR_COLS]	S/C zenith angle relative to the VIIRS pixels measured from the local vertical	Degrees 0° <= satZen <= 180°	- 999.9
satAzm	Float32[MOD_VIIRS_SDR_ROWS] [MOD_VIIRS_SDR_COLS]	S/C azimuth angle relative to the VIIRS pixels and measured from the local North towards East	Degrees -180 <= satAzm <= 180	- 999.9
Height	Float32[MOD_VIIRS_SDR_ROWS] [MOD_VIIRS_SDR_COLS]	Ellipsoid-geoid separation for non-terrain corrected Geo, and the height is the terrain height above the MSL for terrain corrected Geo	Meters -150 <= Height <= 150	- 999.9
Range	Float32[MOD_VIIRS_SDR_ROWS] [MOD_VIIRS_SDR_COLS]	The distance from the ground position represented by the pixel to the S/C	Meters 800000<= Range <=2000000	- 999.9
S/C Position	Float32[VIIRS_RDR_SCANS][3]	S/C Position in ECR coordinates at mid-scan time	Meters -7.46E+06 <= Position <=7.46E+06	- 999.9
S/C Velocity	Float32[VIIRS_RDR_SCANS][3]	S/C Velocity in ECR coordinates at mid-scan time	Meters/sec -6600<= Velocity <=6600	- 999.9
S/C Attitude	Float32[VIIRS_RDR_SCANS][3]	S/C Attitude (roll, pitch, yaw) computed at mid-scan time. The roll, pitch, and yaw angles can be used to create a direction cosine matrix that rotates the S/C coordinates to the Orbit Frame coordinates (see Footnote 1).	Arcseconds -648000 <= Attitude <= 648000	- 999.9
S/C Solar Zenith	Float32[VIIRS_RDR_SCANS]	Solar zenith angle with respect to the solar diffuser reference frame z-axis, where the SD z-axis is normal to the SD surface.	Degrees 0 <= scSunZen <= 180	- 999.9

Output	Type/Dimensions	Description	Units/Valid Range	Fill Value
S/C Solar Azimuth	Float32[VIIRS_RDR_SCANS]	Solar azimuth angle measured counterclockwise about the solar diffuser reference frame z-axis with respect to the solar diffuser x-axis (with positive z-axis towards the observer)	Degrees -180 <= scSunZen <= 180	- 999.9
scan_mode	Uint8[VIIRS_RDR_SCANS]	The VIIRS operational mode, reported at the scan level. (Refer to Table 30.)	None 0=Night; 1=Day	255
mode	Uint8	The VIIRS operational mode, reported at the granule level. (Refer to Table 30.)	None 0=Night; 1=Day; 2=Mixed	255
act_scans	Int32	Actual number of VIIRS scans that were used to create this granule.	0 <= act_scans <= 48	-999
scanQuality	Uint8[VIIRS_RDR_SCANS]	Scan-level quality flags	See QF1 in Table 13	none
Scan_Quality1	Uint8[VIIRS_RDR_SCANS]	Scan-level quality flags	See QF2 in Table 13	None
pixelQuality	Int8[MOD_VIIRS_SDR_ROWS][MOD_VIIRS_SDR_COLS]	Pixel-level quality flags	See Table 14	none

Table 11 Unaggregated MOD Geolocation Output Structure

Output	Type/Dimensions	Description	Units/Valid Range	Fill Value
Scan Start Time	Int64[VIIRS_RDR_SCANS]	Scan start time, defined at the leading edge of the first Earth View frame in IET	Microseconds 0 <= scanStartTime <= 1.00E+38	-999
Scan Mid Time	Int64[VIIRS_RDR_SCANS]	Mid Time of Scan in IET	Microseconds 0 <= scanStartTime <= 1.00E+38	-999
Latitude	Float32[MOD_VIIRS_SDR_ROWS][MOD_UA_VIIRS_SDR_COLS]	Geodetic latitude of the VIIRS pixels	Degrees -90° <= Latitude <= 90° (positive to the North)	- 999.9
Longitude	Float32[MOD_VIIRS_SDR_ROWS][MOD_UA_VIIRS_SDR_COLS]	Geodetic longitude of the VIIRS pixels	Degrees -180° <= Longitude <= 180° (positive to the East of Greenwich)	- 999.9
SolarZenith	Float32[MOD_VIIRS_SDR_ROWS][MOD_UA_VIIRS_SDR_COLS]	Solar zenith angle relative to the VIIRS pixels measured from the local vertical	Degrees 0 <= SolarZenith <= 180	- 999.9
SolarAzimuth	Float32[MOD_VIIRS_SDR_ROWS][MOD_UA_VIIRS_SDR_COLS]	solar azimuth angle relative to the VIIRS pixels and measured from the local North towards East	Degrees -180 <= SolarAzimuth <= 180	- 999.9
satZen	Float32[MOD_VIIRS_SDR_ROWS][MOD_UA_VIIRS_SDR_COLS]	S/C zenith angle relative to the VIIRS pixels measured from the local vertical	Degrees 0° <= satZen <= 180°	- 999.9
satAzim	Float32[MOD_VIIRS_SDR_ROWS][MOD_UA_VIIRS_SDR_COLS]	S/C azimuth angle relative to the VIIRS pixels and measured from the local North towards East	Degrees -180 <= satAzim <= 180	- 999.9

Output	Type/Dimensions	Description	Units/Valid Range	Fill Value
Height	Float32[MOD_VIIRS_SDR_ROWS] [MOD_UA_VIIRS_SDR_COLS]	Difference between ellipsoid and geoid heights	Meters -150 <= Height <= 150	- 999.9
Range	Float32[MOD_VIIRS_SDR_ROWS] [MOD_UA_VIIRS_SDR_COLS]	The distance from the ground position represented by the pixel to the S/C	Meters 800000<= Range <=2000000	- 999.9
S/C Position	Float32[VIIRS_RDR_SCANS][3]	S/C Position in ECR coordinates at mid-scan time	Meters -7.46E+06 <= Position <=7.46E+06	- 999.9
S/C Velocity	Float32[VIIRS_RDR_SCANS][3]	S/C Velocity in ECR coordinates at mid-scan time	Meters/sec -6600<= Velocity <=6600	- 999.9
S/C Attitude	Float32[VIIRS_RDR_SCANS][3]	S/C Attitude (roll, pitch, yaw) computed at mid-scan time. The roll, pitch, and yaw angles can be used to create a direction cosine matrix that rotates the S/C coordinates to the Orbit Frame coordinates (see Footnote 1).	-648000 <= Attitude <= 648000	- 999.9
S/C Solar Zenith	Float32[VIIRS_RDR_SCANS]	Solar zenith angle with respect to the solar diffuser reference frame z-axis, where the SD z-axis is normal to the SD surface.	Degrees 0 <= scSunZen <= 180	- 999.9
S/C Solar Azimuth	Float32[VIIRS_RDR_SCANS]	Solar azimuth angle measured counterclockwise about the solar diffuser reference frame z-axis with respect to the solar diffuser x-axis (with positive z-axis towards the observer)	Degrees -180 <= scSunZen <= 180	- 999.9
scan_mode	Uint8[VIIRS_RDR_SCANS]	The VIIRS operational mode, reported at the scan level. (Refer to Table 30.)	None 0=Night; 1=Day	255
mode	Uint8	The VIIRS operational mode, reported at the granule level. (Refer to Table 30)	None 0=Night; 1=Day; 2=Mixed	255
act_scans	Int32	Actual number of VIIRS scans that were used to create this granule.	0 <= act_scans <= 48	-999
scanQuality	Uint8[VIIRS_RDR_SCANS]	Scan-level quality flags	See QF1 in Table 13	none
Scan_Quality1	Uint8[VIIRS_RDR_SCANS]	Scan-level quality flags	See QF2 in Table 13	None
pixelQuality	Int8[MOD_VIIRS_SDR_ROWS] [MOD_UA_VIIRS_SDR_COLS]	Pixel-level quality flags	See Table 14	none

Table 12 IMG Geolocation Output Structure

Output	Type/Dimensions	Description	Units/Valid Range	Fill Value
Scan Start Time	Int64[VIIRS_RDR_SCANS]	Scan start time, defined at the leading edge of the first Earth View frame in IET	Microseconds 0 <= scanStartTime <= 1.00E+38	-999
Scan Mid Time	Int64[VIIRS_RDR_SCANS]	Starting Time of Scan in IET	Microseconds 0 <= scanStartTime <= 1.00E+38	-999

Output	Type/Dimensions	Description	Units/Valid Range	Fill Value
Latitude	Float32[IMG_VIIRS_SDR_ROWS] [IMG_VIIRS_SDR_COLS]	Geodetic latitude of the VIIRS pixels	Degrees -90° <= Latitude <= 90° (positive to the North)	-999.9
Longitude	Float32[IMG_VIIRS_SDR_ROWS] [IMG_VIIRS_SDR_COLS]	Geodetic longitude of the VIIRS pixels	Degrees -180° <= Longitude <= 180° (positive to the East of Greenwich)	-999.9
SolarZenith	Float32[IMG_VIIRS_SDR_ROWS] [IMG_VIIRS_SDR_COLS]	Solar zenith angle relative to the VIIRS pixels measured from the local vertical	Degrees 0 <= SolarZenith <= 180	-999.9
SolarAzimuth	Float32[IMG_VIIRS_SDR_ROWS] [IMG_VIIRS_SDR_COLS]	solar azimuth angle relative to the VIIRS pixels and measured from the local North towards East	Degrees -180 <= SolarAzimuth <= 180	-999.9
satZen	Float32[IMG_VIIRS_SDR_ROWS] [IMG_VIIRS_SDR_COLS]	S/C zenith angle relative to the VIIRS pixels measured from the local vertical	Degrees 0° <= satZen <= 180°	-999.9
satAzm	Float32[IMG_VIIRS_SDR_ROWS] [IMG_VIIRS_SDR_COLS]	S/C azimuth angle relative to the VIIRS pixels and measured from the local North towards East	Degrees -180 <= satAzm <= 180	-999.9
Height	Float32[IMG_VIIRS_SDR_ROWS] [IMG_VIIRS_SDR_COLS]	Ellipsoid-geoid separation for non-terrain corrected Geo, and the height is the terrain height above the MSL for terrain corrected Geo	Meters -150 <= Height <= 150	-999.9
Range	Float32[IMG_VIIRS_SDR_ROWS] [IMG_VIIRS_SDR_COLS]	The distance from the ground position represented by the pixel to the S/C	Meters 800000 <= Range <= 2000000	-999.9
S/C Position	Float32[VIIRS_RDR_SCANS][3]	S/C Position in ECR coordinates at mid-scan time	Meters -7.46E+06 <= Position <= 7.46E+06	-999.9
S/C Velocity	Float32[VIIRS_RDR_SCANS][3]	S/C Velocity in ECR coordinates at mid-scan time	Meters/sec -6600 <= Velocity <= 6600	-999.9
S/C Attitude	Float32[VIIRS_RDR_SCANS][3]	S/C Attitude (roll, pitch, yaw) computed at mid-scan time. The roll, pitch, and yaw angles can be used to create a direction cosine matrix that rotates the S/C coordinates to the Orbit Frame coordinates (see Footnote 1).	Arcseconds -648000 <= Attitude <= 648000	-999.9
S/C Solar Zenith	Float32[VIIRS_RDR_SCANS]	Solar zenith angle with respect to the solar diffuser reference frame z-axis, where the SD z-axis is normal to the SD surface.	Degrees 0 <= scSunZen <= 180	-999.9
S/C Solar Azimuth	Float32[VIIRS_RDR_SCANS]	Solar azimuth angle measured counterclockwise about the solar diffuser reference frame z-axis with respect to the solar diffuser x-axis (with positive z-axis towards the observer)	Degrees -180 <= scSunZen <= 180	-999.9
scan_mode	Uint8[VIIRS_RDR_SCANS]	The VIIRS operational mode, reported at the scan level. (Refer to Table 30.)	None 0=Night; 1=Day	255

Output	Type/Dimensions	Description	Units/Valid Range	Fill Value
mode	UInt8	The VIIRS operational mode, reported at the granule level. (Refer to Table 30)	None 0=Night; 1=Day; 2=Mixed	255
act_scans	Int32	Actual number of VIIRS scans that were used to create this granule.	0 <= act_scans <= 48	-999
scanQuality	UInt8[VIIRS_RDR_SCANS]	Scan-level quality flags	See QF1 in Table 13	None
Scan_Quality1	UInt8[VIIRS_RDR_SCANS]	Scan-level quality flags	See QF2 in Table 13	None
pixelQuality	Int8[IMG_VIIRS_SDR_ROWS][IMG_VIIRS_SDR_COLS]	Pixel-level quality flags	See Table 14	None

Table 13 Scan Level Geolocation Quality Bytes

Byte	Bit	Flag Description	Result
QF1	0-1	Interpolation Stage	0: Nominal – E&A data available 1: Missing data <= Small gap 2: Small gap < Missing data <= Granule boundary 3: Missing data > Granule boundary
	2-3	HAM/RTA Encoder Flag	0: Good data – all encoder data is valid 1: Bad data – either HAM encoders, RTA encoders or both corrupted for the entire scan 2: Degraded data – either HAM encoders, RTA encoders or both are corrupted within the scan. 3: Missing data – Missing encoder data for the scan (dropped engineering packets)
	4	Above South Atlantic Anomaly	0: False 1: True
	5	Solar Eclipse	0: False 1: True
	6	Lunar Eclipse (DNB only)	0: False 1: True
	7	HAM Side	0: Mirror Side A 1: Mirror Side B
QF2	0-1	Scan Controller Electronics (SCE) Side	0: Side A on 1: Side B on 2: Invalid State
	2-4	Geo Scan Start State Flag	0: Nominal 1: Non-Nominal HAM start 2: HAM/RTA Sync Loss 3: Sector Rotation
	5-7	Spare	N/A

Table 14 Pixel Level Geolocation Quality Byte

Bit	Flag Description	Result
0	Input Quality indicates whether any of the S/C ephemeris or attitude data is invalid or the encoder data is invalid	0: Input valid 1: Input invalid

1	Pointing indicates that the sensor Line of Sight does not intersect the geoid, is near the limb, or has invalid sensor angles.	0: Pointing good 1: Pointing bad
2	Terrain indicates that the algorithm could not obtain a valid terrain value.	0: Terrain good 1: Terrain bad
3	Solar Angle indicates that the solar angles are good or bad.	0: Solar angle valid 1: Solar angle invalid

2.2.1.2.1 Geolocation Gridded Outputs

In addition to the Granule and Scan level data specified in Tables 9 – 12, each gridded product contains map data defined in Table 15, plus the pixel level data listed in Table 16 and Table 17.

Table 15 Map Data Set (mds_type) (Geolocation)

Output	Type/Dimensions	Description	Units/Valid Range	Fill Value
grid_type	Int16	identifies which map projection is being used	11=std Mercator, cylindrical, coaxial 21=Polar Stereographic, Northern Hemisphere 25=Polar Stereographic, Southern Hemisphere 31=Lambert Conformal Conic, Tangent cone, Northern Hemisphere 35=Lambert Conformal Conic, Tangent cone, Southern Hemisphere 41=Lambert Conformal Conic, Secant cone, Northern Hemisphere 45=Lambert Conformal Conic, Secant cone, Southern Hemisphere 51=Cylindrical Equidistant 61=Northern Polar Azimuthal Equidistant 65=Southern Polar Azimuthal Equidistant	none
wedge_rotation	Int16	used for Lambert Conformal Conic, position of the empty wedge	1=up,2=left,3=down,4=right	none
mds_num	Int32	id number of mds, not used by NPOESS system	unitless	none
stan_lat1	Float64	first std latitude	radians/-pi/2 to +pi/2	none
stan_lat2	Float64	2 nd std latitude, needed for Lambert Conformal Conics, secant cone projections	radians/-pi/2 to +pi/2	none
base_lon	Float64	base longitude of the X-Y coordinate system	radians/-pi to +pi	none
grid_inc_constant	Float64	determines scaling and grid sizes	unitless	none

Output	Type/Dimensions	Description	Units/Valid Range	Fill Value
grid_inc_c2	Float64	2 nd constant of same purpose, needed in cylindrical equidistant	unitless	none
grid_exponent	Float64	needed for Lambert projections	unitless	none
grid_constant_A	Float64	needed for Lambert projections	unitless	none
max_row	Float64	max grid row number	established at time MDS is created	none
max_col	Float64	max grid column number	established at time MDS is created	none
upr_left_lat	Float64	latitude of grid upper left corner	radians/-pi/2 to +pi/2	none
upr_left_lon	Float64	longitude of grid upper left corner	radians/-pi to +pi	none
lwr_right_lat	Float64	latitude of grid lower right corner	radians/-pi/2 to +pi/2	none
lwr_right_lon	Float64	longitude of grid lower right corner	radians/-pi to +pi	none
upr_left_x	Float64	x coordinate of upper left corner	established at time MDS is created	none
upr_left_y	Float64	y coordinate of upper left corner	established at time MDS is created	none
lwr_right_x	Float64	x coordinate of lower right corner	established at time MDS is created	none
lwr_right_y	Float64	y coordinate of lower right corner	established at time MDS is created	none
split_lon	Float64	longitude on both sides of empty sector for all lamberts	radians/-pi to +pi	none
costanlat	Float64	cosine tangent of latitude	unitless	none
latsml	Float64	smallest latitude in the MDS	radians/-pi/2 to +pi/2	none
latbig	Float64	largest latitude in the MDS	radians/-pi/2 to +pi/2	none
lonqml	Float64/[2]	smallest longitude in the MDS (need 2 because there might be 2 longitude ranges in the MDS, which happens when the MDS spans 180 degrees longitude)	radians/-pi to +pi	none
lonbig	Float64/[2]	biggest longitude in the MDS, need 2 for the same reason as lonqml	radians/-pi to +pi	none
num_lonrange	Int16	number of longitude ranges in MDS	always either 1 or 2	none

Table 16 Gridded Geolocation Moderate Output (Geolocation)

Output	Type/Dimensions	Description	Units/Valid Range	Fill Value
grow	Float64/[M_VIIRS_SDR_ROWS][M_VIIRS_SDR_COLS]	row location in grid	unitless	ERR_FLOAT64_FILL
gcol	Float64/[M_VIIRS_SDR_ROWS][M_VIIRS_SDR_COLS]	column location in grid	unitless	ERR_FLOAT64_FILL
ctr_grow	Float64/[MOD_GEOLOC_ROWS][MOD_GEOLOC_COLS]	center coordinate of interpolation	unitless	ERR_FLOAT64_FILL

Output	Type/Dimensions	Description	Units/Valid Range	Fill Value
		rectangle		
ctr_gcol	Float64/ [MOD_GEOLOC_ROWS][MOD_GEOLOC_COLS]	center coordinate of interpolation rectangle	unitless	ERR_FLOAT64_FILL
gmds	mgs_type	map data set structure	N/A	N/A

Table 17 Gridded Geolocation Imagery Output (Geolocation)

Output	Type/Dimensions	Description	Units/Valid Range	Fill Value
grow	Float64/ [I_VIIRS_SDR_ROWS][I_VIIRS_SDR_COLS]	row location in grid	unitless	ERR_FLOAT64_FILL
gcol	Float64/ [I_VIIRS_SDR_ROWS][I_VIIRS_SDR_COLS]	column location in grid	unitless	ERR_FLOAT64_FILL
ctr_grow	Float64 [IMG_GEOLOC_ROWS][IMG_GEOLOC_COLS]	center coordinate of interpolation rectangle	unitless	ERR_FLOAT64_FILL
ctr_gcol	Float64/ [IMG_GEOLOC_ROWS][IMG_GEOLOC_COLS]	center coordinate of interpolation rectangle	unitless	ERR_FLOAT64_FILL
gmds	mgs_type	map data set structure	N/A	N/A

2.2.2 Algorithm Processing

IDPS designed and developed a library of functions called common GEO that are used by all of the SDRs to calculate geodetic latitude and longitude as well as solar and lunar geometries. ProSdrCmnGeo methods are to: retrieve attitude and ephemeris information; retrieve moon vectors; determine the nadir latitude and longitude values of the scan; determine the ellipsoid intersect and satellite angles for each pixel and get terrain correction GEO values for each pixel. For more details regarding the common GEO library of functions, please refer to the ProSdrCmnGeo OAD, D41869.

Geolocation is performed using a combination of sensor specific functions and the Common Geolocation library of functions. The main driver for the geolocation algorithm is called geolocateGranule(). Consecutive calls to this driver are issued for each band type: DNB, Imagery, and Moderate. The Day/Night Band is processed first, followed by Imagery (ellipsoid and terrain corrected), and Moderate (ellipsoid and terrain corrected, and unaggregated Moderate). In order to meet latency requirements, the operational Geolocation code has implemented an interpolation scheme for computing ellipsoid geolocation. For DNB and Imagery resolution, ellipsoid geolocation is determined by performing full geolocation on a subset of pixels. The lat/long values for this subset of points are converted to a polar stereographic grid, and then quadratic interpolation is used to determine the geolocation for the remaining pixels. The results from the interpolation are then converted back to lat/long values. The terrain corrected product for Imagery is generated from the ellipsoid product for each lat/long pixel. The Moderate resolution ellipsoid product is created from the Imagery ellipsoid product by averaging four imagery pixels that surround each Moderate pixel. This averaging is done to compute the MOD ellipsoid geo for

all pixels except for a subset of pixels near nadir, where full geolocation is performed (see Section 2.2.2.19 for more details). The resulting Moderate geolocation is then used to generate the terrain corrected product, as well as the unaggregated Moderate product. The unaggregated product is produced by a quadratic interpolation scheme that has been implemented as part of the code optimization for latency improvement.

2.2.2.1 Main driver for Geolocation (`geolocateGranule()`)

The main driver for geolocation is called `geolocateGranule()`. It calls the function `initGeoDataStructs()` to initialize the processing parameters, validate the scan encoder data, determine the thermal correction matrix, and to determine the band type dependent sample times. The next step in the `geolocateGranule()` function is to check the band type setting. If band type is set to Moderate resolution, then the function `calcModFromImg()` is called to calculate the Moderate geolocation products (ellipsoid, terrain corrected and unaggregated). If the band type is set to DNB or Imagery, the function `createInterpRctngls()` is called to define a subset of pixels based on rectangles that span across the scan and do not cross the aggregation zone boundaries. Next, `geolocateDecim()` is called to perform the full geolocation on the decimated set of points, and then `geolocateFullFromDecim()` is called to calculate the geolocation of the remaining pixels using quadratic interpolation. The final step of the `geolocateGranule()` function is to store the geolocation data to memory using the function called `storeGranule()`. If the band type is Imagery, the terrain corrected product is produced in `storeGranule()`, and then saved to memory. The flow diagram for `geolocateGranule()` is shown in Figure 8.

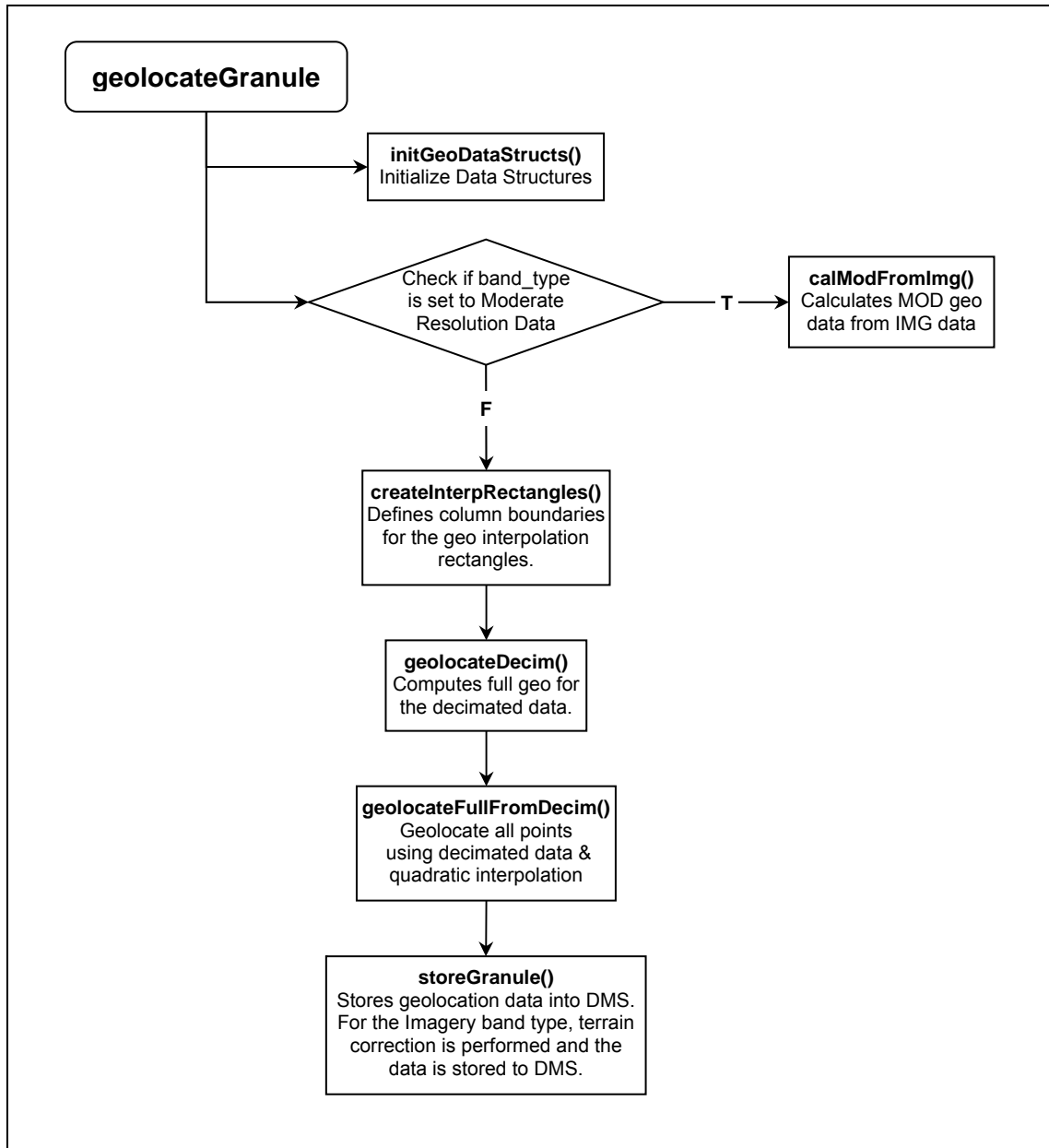


Figure 8 geolocateGranule() Flow Diagram

2.2.2.2 GEO_absolute_limit_check()

GEO_absolute_limit_check() validates a set of input data samples against absolute limits. Flags are set to BAD_DATA for all samples that are not within limits.

2.2.2.3 GEO_determine_DNB_sample_time_offsets()

GEO_determine_DNB_sample_time_offsets() determines the set of relative sample times for all pixels for the DNB. It uses the sample index range to determine the aggregation zone and the number of samples and photosites per zone.

The scan starts at DNB aggregation zone 32, moves through the decreasing side of nadir from zone 32 through to zone 1, crosses nadir, and continues through the increasing side of nadir from zone 1 through to zone 32 where it ends. (i.e. 32, 3, ..., 2, 1, 1, 2, ..., 31, 32).

The sample time determined is the time relative to the scan start. The scan start time is not added, as the GEO software already does this. The relative time is also used independently in several locations.

2.2.2.4 GEO_determine_sample_time_offsets()

GEO_determine_sample_time_offsets() determines the set of relative sample times for all pixels for the requested resolution. It uses the sample index range to determine the aggregation zone and the number of samples (or observations) to be aggregated into a pixel.

The sample time for the first pixel is determined using the latch-to-center time and a time factor for the appropriate resolution. Subsequent sample times use the preceding sample time.

The sample time determined is the time relative to the scan start. The scan start time is not added, as the GEO software already does this. The relative time is also used independently in several locations.

2.2.2.5 GEO_determine_thermal_corrections()

GEO_determine_thermal_corrections() determines the temperature dependent corrections to apply to the granule's geolocation.

Note: The delivered routine of the science VIIRS geolocation code contained an untested or unverified version of temperature correction. All of the delivered test data had the routine 'turned off' by an indicator flag in the test data set. Rather than commenting out the sections of unverified code, it was determined to be better to replace the routine with a stubbed version that was always 'turned on' and returned zero correction for temperature. It is recognized that this routine is to be replaced once actual thermal correction testing verification has occurred. As the routine is currently implemented it should be easy to plug in a new routine into the existing code.

2.2.2.6 GEO_determine_view_vectors()

GEO_determine_view_vectors() calculates object space view vectors in the instrument coordinate system for each along-track detector in a sample. See Figure 9 below.

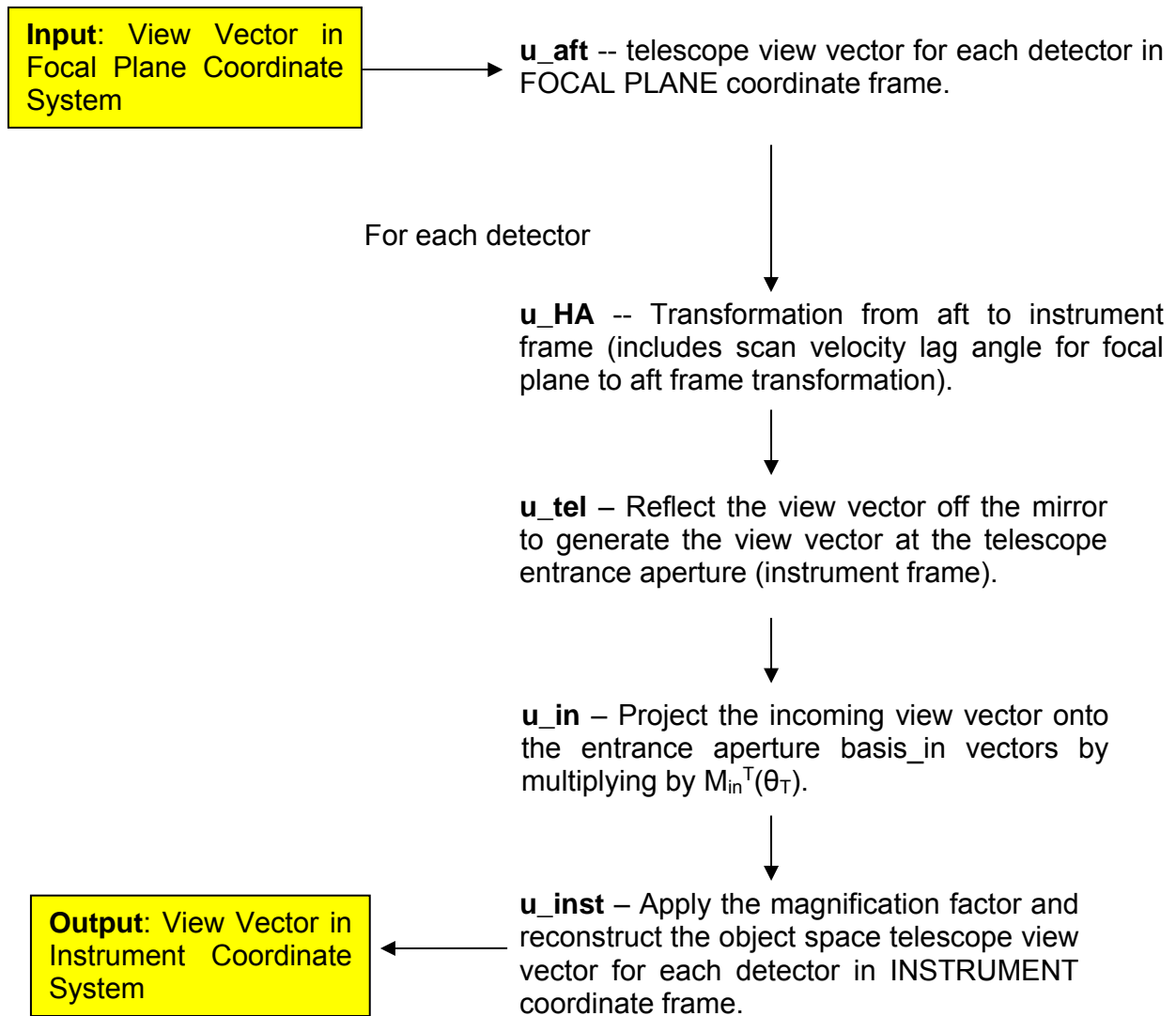


Figure 9 GEO_determine_view_vectors() Block Diagram (Geolocation)

2.2.2.7 GEO_evaluate_polynomial()

GEO_evaluate_polynomial() uses the input parameters to evaluate a polynomial.

2.2.2.8 GEO_find_next_flag()

GEO_find_next_flag() finds the next unflagged sample in a flag array.

2.2.2.9 GEO_get_grid()

GEO_get_grid() generates a grid product.

2.2.2.10 GEO_interp_mod_unagg()

GEO_interp_mod_unagg() uses a quadratic interpolation method to calculate GEO from the values already calculated for the aggregated Moderate resolution, then stores per scan data into output structures based on resolution.

2.2.2.11 GEO_interpolate_mirror_encoder()

GEO_interpolate_mirror_encoder() interpolates the mirror encoder number using a linear interpolation method to interpolate the encoder data to the sample time, using the identified encoder times as bounding variables.

2.2.2.12 GEO_interpolate_telescope_encoder()

GEO_interpolate_telescope_encoder() interpolates the telescope encoder number using a linear interpolation method to interpolate the encoder data to the sample time, using the encoder times as bounding variables.

2.2.2.13 GEO_process_parameters()

GEO_process_parameters() processes input parameter files to extract key values used in GEO processing.

2.2.2.14 GEO_relative_limit_check()

GEO_relative limit check() validates a set of data samples by comparing differences between successive samples against a limit. Previously flagged values are not checked. Flags are set to BAD_DATA for all samples not within limits.

2.2.2.15 GEO_validate_scan_encoder_data()

GEO_validate_scan_encoder_data() unpacks the telescope and mirror encoder data from the encoder and sector start segments. For each scan, it unpacks mirror encoder times from the encoder data, computes encoder values from the sector start and mirror side, and validates the data.

2.2.2.16 geolocatePixel()

This function performs full geolocation for a specific pixel. It uses the ProSdrCmnGeo class to calculate the ellipsoid intersection latitude, longitude and the azimuth, zenith angles to the spacecraft, sun, and moon.

2.2.2.17 geolocateDecim()

This function generates geolocation data for the subset of points that define the interpolation rectangles.

2.2.2.18 geolocateFullFromDecim()

This function uses quadratic interpolation to provide geolocation data for all pixels in the interpolation rectangles.

2.2.2.19 calcModFromImg()

This function calculates the geolocation data for the aggregated Moderate band type by averaging the four Imagery pixels that surround each Moderate pixel. The Imagery pixels are still in the default projection. Due to small satellite zenith values, the code performs full geolocation for pixels that are near nadir. This region is defined by pixel column (1531 through 1670 zero based). The function also generates the terrain corrected product from the ellipsoid for each lat/long pixel.

2.2.2.20 createInterpRctngls()

This function defines the start, middle, and end row/column numbers for each interpolation rectangle.

2.2.2.21 initGeoDataStructs()

This function initializes structures and setup data necessary for geolocation.

2.2.2.22 storeGranule()

This function copies the geolocation data for each band type into DMS. For the Imagery band type, terrain correction occurs here.

2.2.2.23 fixSatAngles()

This function corrects satellite azimuth angles. When the satellite zenith angle gets very small, the satellite azimuth angle changes rapidly. Because quadratic interpolation was used, the satellite azimuth angles need to be recalculated.

2.2.2.24 quadInterp()

This function performs quadratic interpolation.

2.2.2.25 geolocateAllRecPix()

This function performs full geolocation calculations for every pixel in an interpolation rectangle. These calculations are done only if an error does not occur in any of the nine points in the interpolation rectangle.

2.2.2.26 interpLocations()

This function interpolates the latitude and longitude values. The function converts the lat/long values to polar stereographic projection and performs the quadInterp function. The results of this are then converted back to lat/long values.

2.2.2.27 interpAngles()

This function interpolates the satellite, sun, and moon azimuth and zenith angles.

2.2.2.28 Geolocation Quality Flag Logic

Every output product has one pixel level quality flag. The pixel quality flag is an eight-bit field for each pixel indicating the status of the invalid input, bad pointing, bad terrain, invalid solar angles, and a spare unused bit. See Table 14. Any pixel level quality flag with a value of zero contains good data and a pixel level quality flag value other than zero contains anomalous data.

Each output also has two scan level quality flags. The first scan quality flag is an 8-bit field representing the Interpolation Stage, HAM impulse flag, SAA, Solar Eclipse, Lunar Eclipse flags and HAM side. The second quality flag is an 8-bit field representing the Scan Encoder Electronics side. See Table 13. Details of the logic used to set these quality flags can be learned by examining the geolocation functions along with the geolocatePixel() and geolocateGranule() functions.

2.2.2.29 Create Degree GEO Products

After geolocation and calibration processing have been completed then the delivered GEO products, with angles in degrees, are created by calling createDegreeProducts() and convertToDegrees(). This process is performed for all six non-gridded geolocation products.

Angle-values such as latitude, longitude, and satellite and solar azimuth and zenith angles are stored as radians for the internal GEO products and as degrees for the delivered GEO products. The DNB output GEO has no corresponding radian (internal) form, and reports all of the angle-values previously mentioned, with the addition of lunar azimuth and zenith angles and moon phase, in degrees.

2.2.3 Graceful Degradation

The VIIRS SDR Geolocation procedure contains no graceful degradation.

2.2.3.1 Graceful Degradation Inputs

None.

2.2.3.2 Graceful Degradation Processing

None.

2.2.3.3 Graceful Degradation Outputs

None.

2.2.4 Exception Handling

The error handling concept used produces a product if at all possible. This is accomplished by using error fill values to fill data structures at the scan and pixel levels, setting flags and continuing with processing to recover from minor errors and still be able to produce a product. Error handling has been implemented at the granule, scan, and pixel levels of the code.

At the granule level, invalid function arguments, out-of-bound arrays, and failed function calls result in error messages being sent via the INF log mechanism and exiting the function by returning a fail value (with the exception of a failed call to `GEO_get_Gring_points()` which causes an error message to be sent and fill values to be used). When this occurs, no GEO product for that granule is produced. If missing scans are detected, an error message is sent, the scans are filled with fill values, and processing continues.

At the scan level, invalid function arguments and out-of-bound arrays result in error messages being sent via the infrastructure log mechanism and exiting the function by returning a fail value to the granule level function. For invalid IET time, invalid satellite attitude and ephemeris, or invalid mirror side, a flag is set, the entire scan is filled with the appropriate fill values and processing continues with the next scan. For invalid satellite ephemeris and attitude data, invalid sun or moon angles, no ellipse intersect, failed terrain correction, or failure in determining view vectors, a flag is set, the sample is filled with the appropriate fill values, and processing continues with the next sample in the scan.

At the pixel level, invalid function arguments, out-of-bound arrays, and failed function calls result in error messages being sent via the infrastructure log mechanism and exiting the function by returning a fail value. The returned "fail values" are caught by the scan level calling functions resulting in the pixel being filled with the error fill value, a flag being set, and processing continuing with the next pixel.

2.2.5 Data Quality Monitoring

No data quality monitoring is performed by the VIIRS SDR Geolocation procedure.

2.2.6 Computational Precision Requirements

All internal calculations are done at double precision, and they need to be done this way as small scan angle errors lead to large GEO errors. The geodetic Latitude and Longitude fields are output

as floats, which can introduce an uncertainty no larger than two meters in Earth location. Sensor, sun and lunar angles are output as floats.

2.2.7 Algorithm Support Considerations

The DMS and INF must be running before the algorithm is executed.

2.2.8 Assumptions and Limitations

2.2.8.1 Sci2Ops Issues

From the examination and exercising of the accompanying code, several considerations about possible implementation modifications have been identified. Some of the following comments incorporate insights provided by one of the code developers, Mark Kowitt.

- Thermal correction from S/C attitude to mounting matrix.
- The thermal compensation mechanism for the VIIRS sensor has been implemented as an error in effective attitude (roll, pitch and yaw) of the spacecraft. If a common module is implemented, the thermal “error” term should be used to modify the instrument-to-spacecraft effective alignment, rather than the spacecraft attitude.

Note: The delivered routine of the science VIIRS GEO code contained an untested or unverified version of temperature correction. All of the delivered test data had the routine ‘turned off’ by an indicator flag in the test data set. Rather than commenting out the sections of unverified code, it was determined to be better to replace the routine with a stubbed version that was always ‘turned on’ and returned zero correction for temperature. It is recognized that this routine is to be replaced once actual thermal correction testing verification has occurred. As the routine is currently implemented it should be easy to plug in a new routine into the existing code.

2.2.8.2 Numerical Computation Considerations

Several of the inputs in the parameters LUT have to be updated when results from SBRS testing become available and during CalVal. These values are modified to eliminate most of the static and slowly varying biases affecting GEO uncertainty. The methodology to determine these changes has been developed for other sensors, but it has not yet been adapted to VIIRS and no software in its support has been written.

2.2.8.3 Additional Assumptions

It is assumed that the Verified VIIRS RDR and the Verified spacecraft E&A RDR is available for processing. The VIIRS flight model identifier and the RTA and HAM encoder data are assumed to be present in the RDR and of good quality.

2.2.8.4 Additional Limitations

Refer to Section 4.2 of the Geolocation Algorithm Theoretical Basis Document, D43776, for the limitations associated with the algorithm.

2.3 VIIRS SDR Calibration Description

The purpose of the Radiometric CAL Component is to convert the VIIRS digital counts to radiance fields at the top of atmosphere (TOA), as well as brightness temperature and reflectance values. The algorithm used for radiometric CAL has been derived from first principles and then simplified through judicious specifications of algorithm input parameters. The Radiometric CAL Component processes the Verified VIIRS Raw Data Records (RDRs) to produce VIIRS SDRs, VIIRS On-board Calibrator (OBC) Intermediate Product (IP), and VIIRS Calibrated Dual Gain IP². The output SDR data fields include TOA radiances, reflectances, and brightness temperature fields, in addition to quality information. The prototype science code consists of two independent, executable units: Earth View (EV) Radiometric CAL Unit and a Reflective Solar Band Automated Calibration (RSB AutoCal) Processing Unit. The EV Radiometric CAL Unit is executed on a near real-time basis, whereas the RSB AutoCal Processing Unit is executed once per orbit. Outputs from the EV Radiometric CAL Unit are the VIIRS SDRs for each resolution, the Dual Gain IP, and the OBC IP. The RSB AutoCal Processing Unit produces scale factors, F, that are used as a multiplier to the CAL lookup tables (LUTs) used by the EV Radiometric CAL Unit. Refer to Section 2.3.1.2 for details on output SDRs and IPs. The Calibration Processing Chain is shown in Figure 10.

² For dual gain bands only: M1 – M5, M7 and M13.

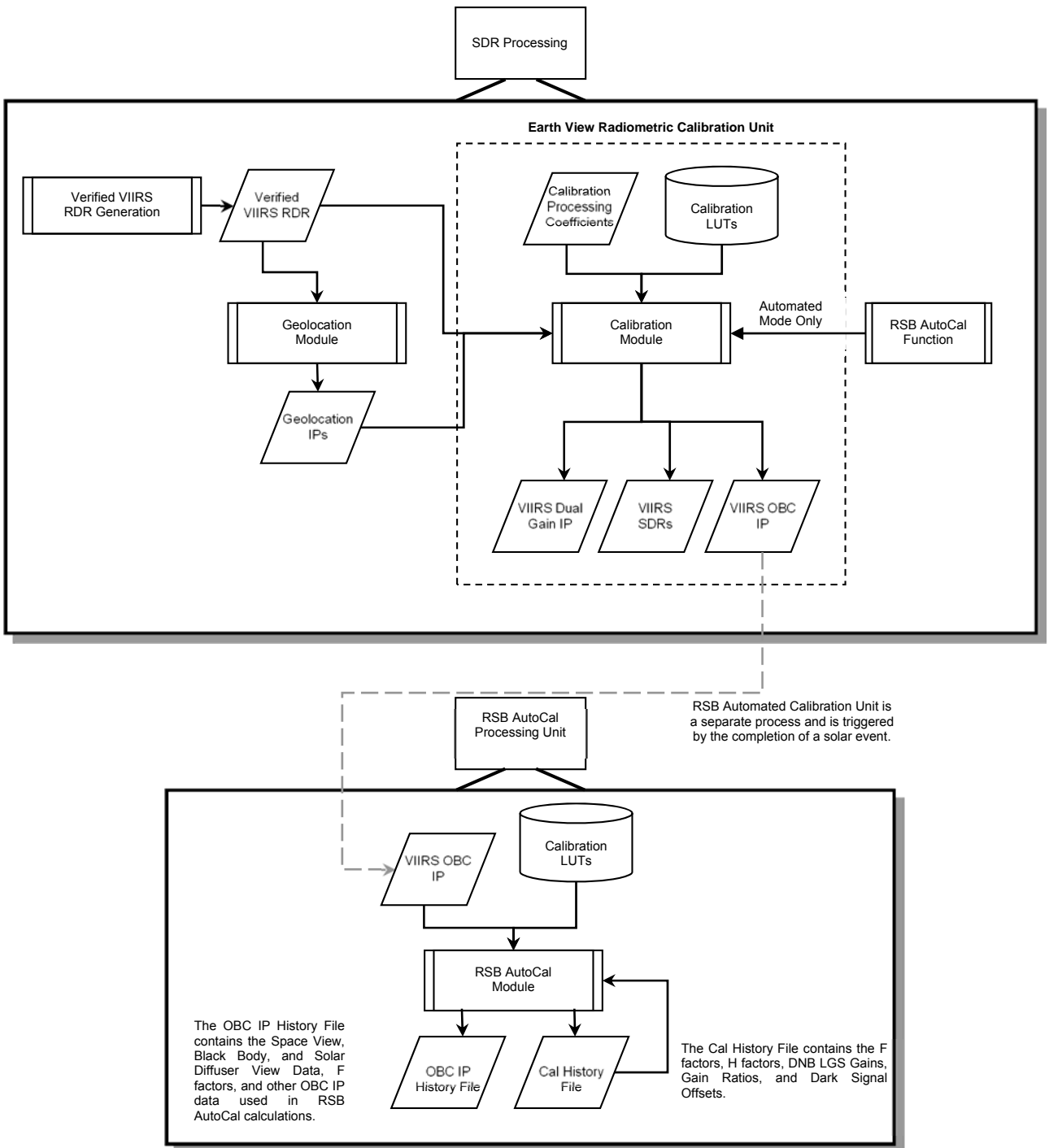


Figure 10 Calibration Processing Chain

2.3.1 Interfaces

2.3.1.1 Inputs

The inputs to the Earth View Radiometric Calibration Unit of the VIIRS Radiometric CAL Component are the Verified VIIRS RDRs, the VIIRS GEO IPs, and a suite of CAL parameter files that include LUTs, CAL coefficients and CAL run-time parameters. The input files are summarized in Tables 18 and 19.

Several of the LUT input items contain platform dependent values. Each platform must have a separate LUT associated with that specific sensor. During the input phase of the algorithms IPO processing model, the spacecraft ID provided in the tasking information is used as search metadata in order to ensure the correct LUT is retrieved from DMS.

Table 18 Earth View Radiometric Calibration Unit Inputs

Input	Description
Verified VIIRS RDR	Data containing digital numbers for earth view, onboard calibrator view and space view data, as well as engineering data, health and safety data. This is raw satellite data that has been reformatted, pre-processed, and verified prior to processing.
VIIRS Geolocation Products	Data containing terrain corrected solar zenith and azimuth angles, satellite zenith and azimuth angles, as well as latitudes and longitudes for each VIIRS grid point for each of the three VIIRS resolutions. (375m, 750m, and DNB)
VIIRS Geolocation OBC-IP	The VIIRS On Board Calibrator IP file contains solar diffuser observations, the associated gain state and HAM side information, and all engineering and housekeeping data, including unscaled data from the Solar Diffuser Stability Monitor (SDSM)/VIIRS Earth View Radiometric Calibration Unit and the Solar Diffuser GEO angles.
VIIRS SDR Calibration Processing Coefficients	Configurable coefficients required for processing. (Scale and Offset Values etc.)
VIIRS SDR Calibration LUTs	Look up tables required for VIIRS SDR Calibration processing.

Table 19 Earth View Radiometric Calibration Parameter & LUT Inputs

Input	Description/Source
DeltaCTempLUT	Contains Delta C Temperature response values.
DetectorResponseLUT	VIIRS Detector Response Coefficient LUT.
DnbCCoeffLUT	DayNight Band C coefficients.
DnbDN0LUT	Contains DN (Digital count) 0 values for DNB calibration.
DnbFPredictedTableLUT	Time-dependent F Coefficients for DNB calibration as calculated from Solar Diffuser data
DnbFrameToZoneLUT	DayNight Band Frame to Zone LUT.
RvfDnbLUT	Day Night Band response versus frame LUT
EmissiveLUT	This file contains various LUTs for emissive band calibration.
FPredictedTableLUT	Time-dependent F Coefficients as calculated from Solar Diffuser data
GainTableLUT	Table containing gain values for each of the bands.
HAMERLUT	Contains the LUT for calculating the emitted radiance of the half angle mirror (HAM) based on its temperature.
ElectronicsResponseLUT	VIIRS Electronics Response LUT.
LtoEBBLUT	Contains the LUTs for converting radiance to brightness temperature.

Input	Description/Source
OBCERLUT	Contains LUTs for calculating the emitted radiance of the blackbody based on the temperature.
OBCRRLUT	Contains LUTs for calculating the reflected radiance of the blackbody based on the temperature.
ObsToPixelsLUT	Contains the dual gain band along-scan samples to aggregated pixel frame number mapping table.
QALUT	Contains LUTs related to quality assurance. Consists of the following SDSs: Detector Quality Flags, Moon Offset Limits.
RMPParametersLUT	Radiometric Parameters LUT.
RSRLUT	Relative Spectral Response table for reflective bands (M1-M11 and I1-I3).
RTAERLUT	Rotating telescope assembly emissive radiance tables for each VIIRS emissive band (I4-I5), (M12-M16).
RVFLUT	Response Vs. Frame LUT for all imagery and moderate resolution bands.
ReflectiveLUT	Contains values for calibrating reflective bands. Values include: first frame to use for OBC average, number of frames to use for OBC average and RSB moon include.
SolarIradLUT	Solar power table needed for calculation of d coefficients, which are used in reflectance algorithm.
TeleCoeffLUT	Calibration coefficients for VIIRS thermistors as provided by Raytheon SBRS. Default values for thermistors.
SDSM Volt	Volt Scale values
VIIRS Imagery Even/Odd Parity	Array of Boolean values for setting whether first, second sub-frame calibration averages are swapped to correct sub-frame timing offset.
DNB Stray Light Correction LUT	Contains DNB stray light correction offsets and the corresponding spacecraft (S/C) solar zenith angle grids. This LUT also contains the maximum radiance limit for which the stray light correction is performed.
DG anomaly DN limits	List of min/max DN values for which the DG anomaly quality flag will be set
RSBAutoCalDnbGainRatiosAutomateLUT	Contains parameters used in DNB gain ratios calculations.
RSBAutoCalDnbLgsGainAutomateLUT	Contains parameters used in DNB LGS gain calculations.
RSBAutoCalDarkSignalAutomateLUT	Contains parameters used in dark signals offsets calculations.
RSBAutoCalHAutomateLUT	Contains parameters used in H factor calculations.
RSBAutoCalRsbFAutomateLUT	Contains parameters used in RSB F factor calculations.
CalAutomateLUT	Contains moon angle threshold and flags to turn on automated calibration.
Cal History	Contains information about past calibration runs.

2.3.1.2 Outputs

The VIIRS EV Radiometric CAL Unit produces 22 SDRs and two IPs, as shown in Table 20. A separate SDR is output for each band in each resolution: Imagery (I1-I5), Moderate (M1-M16), and DNB. All Imagery resolution SDRs and Moderate resolution SDRs contain the full resolution geolocated calibrated TOA radiances. In addition, reflective band SDRs (bands I1-I3 and M1-M11) contain full resolution calibrated reflectances and emissive band SDRs (bands I4-I5 and M12-M16) contain full resolution calibrated TOA brightness temperatures. The DNB SDR contains the full resolution geolocated calibrated TOA radiances for the DNB. The OBC IP contains sensor calibrator view data (space view, blackbody, and solar diffuser) from all VIIRS bands arranged by scan and unprocessed engineering and housekeeping data. The OBC IP is

the input to the Reflective Solar Band Automated Calibration Processing Unit and is also the primary input to offline Cal/Val analysis. The Calibrated Dual Gain IP contains unaggregated TOA radiances for each dual gain band for the nadir (aggregation by three) and the near-nadir (aggregation by two) aggregation zones.

Table 20 Outputs from the Earth View Radiometric Calibration Unit (Calibration)

Output	Description
VIIRS_I1_SDR	The VIIRS 375m I1 band SDR contains TOA radiances, reflectances for each VIIRS pixel.
VIIRS_I2_SDR	The VIIRS 375m I2 band SDR contains TOA radiances, and reflectances for each VIIRS pixel.
VIIRS_I3_SDR	The VIIRS 375m I3 band SDR contains TOA radiances, and reflectances for each VIIRS pixel.
VIIRS_I4_SDR	The VIIRS 375m I4 band SDR contains TOA radiances, and brightness temperatures for each VIIRS pixel.
VIIRS_I5_SDR	The VIIRS 375m I5 band SDR contains TOA radiances, and brightness temperatures for each VIIRS pixel.
VIIRS_M1_SDR	The VIIRS 750m M1 band SDR contains TOA radiances, reflectances for each VIIRS pixel.
VIIRS_M2_SDR	The VIIRS 750m M2 band SDR contains TOA radiances, reflectances for each VIIRS pixel.
VIIRS_M3_SDR	The VIIRS 750m M3 band SDR contains TOA radiances, reflectances for each VIIRS pixel.
VIIRS_M4_SDR	The VIIRS 750m M4 band SDR contains TOA radiances, reflectances for each VIIRS pixel.
VIIRS_M5_SDR	The VIIRS 750m M5 band SDR contains TOA radiances, reflectances for each VIIRS pixel.
VIIRS_M6_SDR	The VIIRS 750m M6 band SDR contains TOA radiances, reflectances for each VIIRS pixel.
VIIRS_M7_SDR	The VIIRS 750m M7 band SDR contains TOA radiances, reflectances for each VIIRS pixel.
VIIRS_M8_SDR	The VIIRS 750m M8 band SDR contains TOA radiances, reflectances for each VIIRS pixel.
VIIRS_M9_SDR	The VIIRS 750m M9 band SDR contains TOA radiances, reflectances for each VIIRS pixel.
VIIRS_M10_SDR	The VIIRS 750m M10 band SDR contains TOA radiances, reflectances for each VIIRS pixel.
VIIRS_M11_SDR	The VIIRS 750m M11 band SDR contains TOA radiances, reflectances for each VIIRS pixel.
VIIRS_M12_SDR	The VIIRS 750m M12 band SDR contains TOA radiances, brightness temperatures for each VIIRS pixel.
VIIRS_M13_SDR	The VIIRS 750m M13 band SDR contains TOA radiances, brightness temperatures for each VIIRS pixel.
VIIRS_M14_SDR	The VIIRS 750m M14 band SDR contains TOA radiances, brightness temperatures for each VIIRS pixel.
VIIRS_M15_SDR	The VIIRS 750m M15 band SDR contains TOA radiances, brightness temperatures for each VIIRS pixel.
VIIRS_M16_SDR	The VIIRS 750m M16 band SDR contains TOA radiances, brightness temperatures for each VIIRS pixel.
VIIRS_DNB_SDR	The VIIRS Day/Night Band SDR contains TOA radiances for each VIIRS pixel.
VIIRS OBC IP	The VIIRS On Board Calibrator IP file contains space view, solar diffuser, on-board calibrator blackbody (OBCBB) view observations, the associated gain state and HAM side information, and all engineering and housekeeping data, including unscaled data from the Solar Diffuser Stability Monitor (SDSM)/VIIRS Earth View Radiometric Calibration Unit and the Solar Diffuser GEO angles.

Output	Description
VIIRS Calibrated Dual Gain IP	The Calibrated Dual Gain IP file contains unaggregated, calibrated TOA radiances for those VIIRS sub-pixel samples that are aggregated along-scan during post-calibration ground processing. In other words, this file contains the calibrated M1 – M5, M7 and M13 dual gain band data from the nadir and near-nadir zones that would otherwise be discarded following post-calibration aggregation/Earth View Radiometric Calibration Unit.

2.3.1.2.1 Definitions of the Calibration VIIRS SDR Outputs

The contents of the VIIRS SDR outputs are described in Tables 18 through 24. The fields specific to a given resolution SDR are indicated in the Description column. The VIIRS SDR CAL routine outputs two structures for each band in the Moderate (750m) resolution, and Imagery (375m) resolution: a scaled version and an unscaled version of the SDR. The scaled versions of the bands are identified for long term storage, and the non scaled full floating point versions are used for immediate processing of EDRs and IPs. These full floating point versions are removed by the storage system after an amount of time, post creation. All relevant Metadata associated with these output items is defined in the CDFCB-X, Volume IV.

Table 21 Imagery Resolution SDR

Field	Type	Dimensions	Description	Units
Radiance	Float32	VIIRS_IMG_COLS x VIIRS_IMG_ROWS	TOA radiances	W/(m ² -sr-μm)
Reflectance or BrightnessTemperature	Float32	VIIRS_IMG_COLS x VIIRS_IMG_ROWS	Reflectances or brightness temperatures determined by band	NA for reflectance K for brightness temperature
Header	VIIRS_HDR_TYPE	NA	VIIRS SDR HDR Type	See Table 30
Actual Scan Count	Int	NA	Number of actual scans in granule	Unitless
numOfMissingPkts	Int32	VIIRS_RDR_SCANS	Missing Packets in Scan	Count
numOfBadChecksum	Int32	VIIRS_RDR_SCANS	Packets with bad CRC in Scan	Count
numOfDiscardedPkts	Int32	VIIRS_RDR_SCANS	Discarded Packets in Scan	Count
Scan Quality	UInt8	VIIRS_RDR_SCANS	Scan level quality information	See Table 26
Pixel Quality	UInt8	VIIRS_IMG_COLS x VIIRS_IMG_ROWS	Pixel level quality information	See Table 27
RDR Scan Quality	Int	VIIRS_RDR_SCANS x RDR_SCAN_FLAGS	Scan level rdr quality information	See Table 28
Reduced Quality Flag	UInt8	VIIRS_IMG_ROWS	Detector x scan level quality flag	See Table 29
Bad Detector	Int	NA	1 bit per scan 0 = detector good 1 = detector bad	Unitless

Table 22 Moderate Resolution SDR

Field	Type	Dimensions	Description	Units
Radiance	Float32	VIIRS_MOD_COLS x VIIRS_MOD_ROWS	TOA radiances	W/(m ² -sr-μm)

Field	Type	Dimensions	Description	Units
Reflectance or BrightnessTemperature	Float32	VIIRS_MOD_COLS x VIIRS_MOD_ROWS	Reflectances or brightness temperatures determined by band	NA for reflectance K for brightness temperature
Header	VIIRS_HDR_TYPE	NA	VIIRS SDR HDR Type	See Table 30
numOfMissingPkts	Int32	VIIRS_RDR_SCANS	Missing Packets in Scan	Count
numOfBadChecksum	Int32	VIIRS_RDR_SCANS	Packets with bad CRC in Scan	Count
numOfDiscardedPkts	Int32	VIIRS_RDR_SCANS	Discarded Packets in Scan	Count
Actual Scan Count	Int	NA	Number of actual scans in granule	Unitless
Scan Quality	UInt8	VIIRS_RDR_SCANS	Scan level quality information	See Table 26
Pixel Quality	UInt8	VIIRS_MOD_COLS x VIIRS_MOD_ROWS	Pixel level quality information	See Table 27
RDR Scan Quality	Int	VIIRS_RDR_SCANS x RDR_SCAN_FLAGS	Scan level rdr quality information	See Table 28
Reduced Quality Flag	UInt8	VIIRS_MOD_ROWS	Detector x scan level quality flag	See Table 29
Bad Detector	Int	NA	1 bit per scan 0 = detector good 1 = detector bad	Unitless

Table 23 Day/Night Band SDR

Field	Type	Dimensions	Description	Units
Radiance	Float32	VIIRS_DNB_COLS x VIIRS_DNB_ROWS	TOA radiances	W/(cm ² -sr)
Header	VIIRS_HDR_TYPE	NA	VIIRS SDR HDR Type	See Table 30
Actual Scan Count	Int	NA	Number of actual scans in granule	Unitless
Scan Quality	UInt8	VIIRS_RDR_SCANS	Scan level quality information	See Table 26
Pixel Quality	UInt8	VIIRS_DNB_COLS x VIIRS_DNB_ROWS	Pixel level quality information	See Table 27
RDR Scan Quality	Int	VIIRS_RDR_SCANS x RDR_SCAN_FLAGS	Scan level rdr quality information	See Table 28
Reduced Quality Flag	UInt8	VIIRS_DNB_ROWS	Detector x scan level quality flag	See Table 30

Table 24 Imagery Resolution Scaled SDR

Field	Type	Dimensions	Description	Units
Radiance	UInt16	VIIRS_IMG_COLS x VIIRS_IMG_ROWS	Scaled TOA radiances	W/(m ² -sr-μm ⁴)
Reflectance or BrightnessTemperature	UInt16	VIIRS_IMG_COLS x VIIRS_IMG_ROWS	Reflectances or brightness temperatures determined by band	NA for reflectance K for brightness temperature
RadianceOffset	Float32	NA	Offset value of the scaled Radiances	W/(m ² -sr-μm ⁴)
RadianceScale	Float32	NA	Scaling factor for the scaled Radiances	NA
ReflectanceOffset or BrightnessTempOffset	Float32	NA	Offset value of the scaled Reflectances or Brightness Temperatures depending on band	NA / K

Field	Type	Dimensions	Description	Units
ReflectanceScale or BrightnessTempScale	Float32	NA	Scaling factor for the scaled Reflectances or Brightness Temperatures depending on band	NA
Header	VIIRS_HDR_TYPE	NA	VIIRS SDR HDR Type	See Table 31
Actual Scan Count	Int	NA	Number of actual scans in granule	Unitless
numOfMissingPkts	Int32	VIIRS_RDR_SCANS	Missing Packets in Scan	Count
numOfBadChecksum	Int32	VIIRS_RDR_SCANS	Packets with bad CRC in Scan	Count
numOfDiscardedPkts	Int32	VIIRS_RDR_SCANS	Discarded Packets in Scan	Count
Scan Quality	UInt8	VIIRS_RDR_SCANS	Scan level quality information	See Table 26
Pixel Quality	UInt8	VIIRS_IMG_COLS x VIIRS_IMG_ROWS	Pixel level quality information	See Table 27
RDR Scan Quality	Int	VIIRS_RDR_SCANS x RDR_SCAN_FLAGS	Scan level rdr quality information	See Table 28
Reduced Quality Flag	UInt8	VIIRS_IMG_ROWS	Detector x scan level quality flag	See Table 29
Bad Detector	Int	NA	1 bit per scan 0 = detector good 1 = detector bad	Unitless

Table 25 Moderate Resolution Scaled SDR

Field	Type	Dimensions	Description	Units
Radiance	UInt16	VIIRS_MOD_COLS x VIIRS_MOD_ROWS	Scaled TOA radiances	W/(m ² -sr-μm)
Reflectance or BrightnessTemperature	UInt16	VIIRS_MOD_COLS x VIIRS_MOD_ROWS	Reflectances or brightness temperatures determined by band	NA for reflectance K for brightness temperature
RadianceOffset	Float32	NA	Offset value of the scaled Radiances	W/(m ² -sr-μm)
RadianceScale	Float32	NA	Scaling factor for the scaled Radiances	NA
ReflectanceOffset or BrightnessTempOffset	Float32	NA	Offset value of the scaled Reflectances or Brightness Temperatures depending on band	NA / K
ReflectanceScale or BrightnessTempScale	Float32	NA	Scaling factor for the scaled Reflectances or Brightness Temperatures depending on band	NA
Header	VIIRS_HDR_TYPE	NA	VIIRS SDR HDR Type	See Table 30
Actual Scan Count	Int32	NA	Number of actual scans in granule	Unitless
numOfMissingPkts	Int32	VIIRS_RDR_SCANS	Missing Packets in Scan	Count
numOfBadChecksum	Int32	VIIRS_RDR_SCANS	Packets with bad CRC in Scan	Count
numOfDiscardedPkts	Int32	VIIRS_RDR_SCANS	Discarded Packets in Scan	Count
Scan Quality	UInt8	VIIRS_RDR_SCANS	Scan level quality information	See Table 26

Field	Type	Dimensions	Description	Units
Pixel Quality	UInt8	VIIRS_MOD_COLS x VIIRS_MOD_ROWS	Pixel level quality Information	See Table 27
RDR Scan Quality	Int	VIIRS_RDR_SCANS x RDR_SCAN_FLAGS	Scan level rdr quality information	See Table 28
Reduced Quality Flag	UInt8	VIIRS_MOD_ROWS	Detector x scan level quality flag	See Table 29
Bad Detector	Int	NA	1 bit per scan 0 = detector good 1 = detector bad	Unitless

Table 26 Scan Quality Byte

Bit	Flag Description	Result
0	Half Angle Mirror Side	0: A-side 1: B-side
1	Moon in Keep-out-box	0: Moon not in space view 1: Moon in space view
2	Spare	N/A
3	HAM/RTA Sync Loss	0: No Sync Loss 1: Sync Loss
4	Sector Rotation	0: No Sector Rotation 1: Sector Rotation
5	OBC Blackbody WU/CD state	0: OBC Blackbody normal 1: OBC Blackbody WU/CD state (Emiss only)
6	LWIR FPA Temperature Note: This bit is only set for LWIR emissive bands.	0: LWIR FPA Temp OK 1: LWIR FPA Temp Not Nominal
7	DNB Stray Light Correction Flag	0: No stray light correction 1: Stray light correction

Table 27 Pixel Quality Byte

Bit	Flag Description	Result
0-1	SDR Quality	0: Good 1: Poor 2: No calibration
2-3	Saturated Pixel	0: None saturated 1: Some saturated 2: All saturated
4-5	Missing Data	0: All data present 1: EV RDR data missing 2: Cal data missing 3: Thermistor data missing
6-7	Out of Range	0: All data within range 1: Radiance out of range 2: Reflectance or EBBT out of range 3: Radiance & Reflectance/EBBT out of range

Table 28 RDR Scan Quality Int

Bit	Flag Description	Result
-----	------------------	--------

Bit	Flag Description	Result
0-5	Checksum	0: Did verify 1: Did not verify
6	Scan Data Present	2.4 0: Some valid data 2.5 1: No valid data

Table 29 Reduced Quality Flag Byte

Bit	Flag Description	Result
0-255	Detector per band quality flag	0: Good 255: Reduced quality flag

Table 30 VIIRS SDR Header

Field	Type	Dimensions	Description	Units
numScans	Int32	NA	Number of complete scans in the granule	NA
scanMode	UInt8*	16	Day/night indicator per scan	NA
mode	UInt8	NA	Day/night indicator per granule	NA

2.3.1.2.2 VIIRS On-Board Calibrator Intermediate Product

Table 31 summarizes the contents of the VIIRS OBC IP output. The OBC IP contains the same granule metadata as the output SDR.

Table 31 OBC IP Output

Output	Type/ Dimensions	Description	Units/ Valid Range	Fill Value
Scan Number	int32/ (nscans)	VIIRS RDR scan number	Unitless/ [1 – nscans]	-999
SD_375m	Float32/ (nscans*32,5,96)	Digital counts from the Solar Diffuser for imagery resolution bands. Table Note 1	Counts/ [0 – 4095]	MISS_FL OAT32_FI LL
SD_750m_SG	Float32/ (nscans*16,11,48)	Digital counts from the Solar Diffuser for single gain moderate resolution bands. Table Note 1	Counts/ [0 – 4095]	MISS_FL OAT32_FI LL
SD_750m_DG	Float32/ (nscans*16,7,48)	Digital counts from the Solar Diffuser for dual gain moderate resolution bands. Table Note 1	Counts/ [0 – 4095]	MISS_FL OAT32_FI LL
SD_DNB	Float32/ (nscans*16,64)	Digital counts from the Solar Diffuser for Day/Night band.	Counts/ [0 – 4095]	MISS_FL OAT32_FI LL
BB_375m	Float32/ (nscans*32,5,96)	Digital counts from the Blackbody for imagery resolution bands. Table Note 1	Counts/ [0 – 4095]	MISS_FL OAT32_FI LL
BB_750m_SG	Float32/ (nscans*16,11,48)	Digital counts from the Blackbody for single gain moderate resolution bands. Table Note 1	Counts/ [0 – 4095]	MISS_FL OAT32_FI LL
BB_750m_DG	Float32/ (nscans*16,7,48)	Digital counts from the Blackbody for dual gain moderate resolution bands. Table Note 1	Counts/ [0 – 4095]	MISS_FL OAT32_FI LL

Output	Type/ Dimensions	Description	Units/ Valid Range	Fill Value
BB_DNB	Float32/ (nscans*16,64)	Digital counts from the Blackbody for Day/Night band.	Counts/ [0 – 4095]	MISS_FL OAT32_FI LL
SV_375m	Float32/ (nscans*32,5,2*48)	Digital counts from the Space View for imagery resolution bands. Table Note 1	Counts/ [0 – 4095]	MISS_FL OAT32_FI LL
SV_750m_SG	Float32/ (nscans*16, 11,48)	Digital counts from the Space View for single gain moderate resolution bands. Table Note 1	Counts/ [0 – 4095]	MISS_FL OAT32_FI LL
SV_750m_DG	Float32/ (nscans*16,7,48)	Digital counts from the Space View for dual gain moderate resolution bands. Table Note 1	Counts/ [0 – 4095]	MISS_FL OAT32_FI LL
SV_DNB	Float32/ (nscans*16,64)	Digital counts from the Space View for Day/Night band.	Counts/ [0 – 4095]	MISS_FL OAT32_FI LL
DN_obc_avg_375m	float32 (nscans*32,5,2)	Average digital counts from the Blackbody for imagery resolution bands.	Counts	FLOAT32 _FILL
DN_obc_avg_750m_s g	float32 (nscans*16,9)	Average digital counts from the Blackbody for single gain moderate resolution bands.	Counts	FLOAT32 _FILL
DN_obc_avg_750m_d g	float32 (nscans*16,7)	Average digital counts from the Blackbody for dual gain moderate resolution bands.	Counts	FLOAT32 _FILL
DN_obc_375M_outlier _mask	uint64/ (nscans*32,5,2)	Number of pixels rejected in calculating the average Blackbody counts for imagery resolution bands.	Counts	MISS_64_ FILL
DN_obc_750M_SG_ou tlier_mask	uint64/ (nscans*16,9,2)	Number of pixels rejected in calculating the average Blackbody counts for single gain moderate resolution bands.	Counts	MISS_64_ FILL
DN_obc_750M_DG_ou tlier_mask	uint64/ (nscans*16,7,2)	Number of pixels rejected in calculating the average Blackbody counts for dual gain moderate resolution bands.	Counts	MISS_64_ FILL
DN_obc_avg_first_fra me_to_use	Int32	Average First Frame to Use Digital Number	Unitless	MISS_INT 32_FILL
DN_obc_avg_number_ of_frames_to_use	Int32	Average Number of Frames to Use Digital Number	Unitless	MISS_INT 32_FILL
OBC Gain States	UInt16 / (7*16 * nscans)	Gain States for the Dual Gain Moderate bands for each calibrator view, for each detectors for each scan.	0 or 1	0
Moon in keep-out-box	Int8 (nscans,22)	Indicates if the moon was found in the keep-out-box for each scan and each band. The keep-out-box is a region including and near to the SV port.	Unitless/ [0 – 1]	-999
dp_reg_tbl_rev	UInt8 / nscans	Indicates which table revision you are on for the DPP register table.	Counts / [0- 255]	NONE
dp_state_tran_tbl_rev	UInt8 / nscans	Indicates which table revision you are on for the DPP state transition table.	Counts / [0- 255]	NONE
dp_band_proc_tbl_rev	UInt8 / nscans	Indicates which table revision you are on for the DPP band processing table.	Counts / [0- 255]	NONE
dp_heat_ctrl_tbl_rev	UInt8 / nscans	Indicates which table revision you are on for the PWM heater control table.	Counts / [0- 255]	NONE

Output	Type/ Dimensions	Description	Units/ Valid Range	Fill Value
dp_macro_cmd_tbl_rev	UInt8 / nscans	Indicates which table revision you are on for the macro command table.	Counts / [0-255]	NONE
dp_crit_tele_tbl_rev	UInt8 / nscans	Indicates which table revision you are on for the critical telemetry table.	Counts / [0-255]	NONE
dp_stor_cmd_tbl_rev	UInt16 / nscans	Indicates which table revision you are on for the stored command table.	Counts / [0-65535]	NONE
dp_dn_m_l_gain_pkt	UInt8 / nscans	Indicates occasional selection to 0=NOT_SEND, 1=SEND DNB Middle Gain Stage (MGS) and Low Gain Stage (LGS) Pkts	Unitless/ [0 – 1]	MISS_UIN T8_FILL
dp_hrd_pkt_norm_test	UInt8 / nscans	PKT_Norm_Test state 0=NORMAL, 1= TEST unique value for all FPA channels except DNB. Valid in Oper and Diag modes.	Unitless/ [0 – 1]	MISS_UIN T8_FILL
dp_nonrdt_fpie_pwr	UInt8 / nscans	0=PS1, 1=PS2; If FPIE Ok connect to active PS. If fault condition, connect to inactive PS	Unitless/ [0 – 1]	MISS_UIN T8_FILL
dp_servo_in_use	UInt8 / nscans	FSW echo of C_DP04, 0=SERVO_A, 1=SERVO_B	Unitless/ [0 – 1]	MISS_UIN T8_FILL
ps_sec_b_apfp_on	UInt8 / nscans	PS_SEC_B 0=OFF, 1=ON	Unitless/ [0 – 1]	MISS_UIN T8_FILL
ps_sec_c_se_on	UInt8 / nscans	PS_SEC_C 0=OFF, 1=ON	Unitless/ [0 – 1]	MISS_UIN T8_FILL
ps_sec_d_csog_on	UInt8 / nscans	PS_SEC_D 0=OFF, 1=ON	Unitless/ [0 – 1]	MISS_UIN T8_FILL
ps_sec_e_isog_on	UInt8 / nscans	PS_SEC_E 0=OFF, 1=ON	Unitless/ [0 – 1]	MISS_UIN T8_FILL
se_a_anlg_pwr_on	UInt8 / nscans	Analog Pwr present on SE_A	Unitless/ [0 – 1]	MISS_UIN T8_FILL
se_a_mtr_coil_driver	UInt8 / nscans	Driver source for SE_A Mtr Coil.	Unitless/ [0 – 1]	MISS_UIN T8_FILL
se_a_mtrs_stopped	UInt8 / nscans	SE_A Motor state	Unitless/ [0 – 1]	MISS_UIN T8_FILL
se_a_tele_pos_known	UInt8 / nscans	Telescope position_A, Known covers Static Case (Stowed) and Dynamic Case (Servo up to speed and controlled)	Unitless/ [0 – 1]	MISS_UIN T8_FILL
se_b_anlg_pwr_on	UInt8 / nscans	Analog Pwr present on SE_B	Unitless/ [0 – 1]	MISS_UIN T8_FILL
se_b_mtr_coil_driver	UInt8 / nscans	Driver source for SE_B Mtr Coil	Unitless/ [0 – 1]	MISS_UIN T8_FILL
se_b_mtrs_stopped	UInt8 / nscans	SE_B Motor state	Unitless/ [0 – 1]	MISS_UIN T8_FILL
se_b_tele_pos_known	UInt8 / nscans	Telescope position_B, Known covers Static Case (Stowed) and Dynamic Case (Servo up to speed and controlled),	Unitless/ [0 – 1]	MISS_UIN T8_FILL
dp_dn_aggreg_mod	UInt8 / nscans	Earth view DNB Aggregation Mode	Unitless/ [0 – 36]	MISS_UIN T8_FILL
cp_blk_pwr_sel	UInt8 / nscans	1=XSTRAP, 0=NORMAL; XS1 NORMAL connects PS1_A_PWR to CP_BLK_A (CP, DP, CT and SI) and PS2_A_PWR to CP_BLK_B; XSTRAP connects PS2_A_PWR to CP_BLK_A and PS1_A_PWR to CP_BLK_B; also by SC pt-pt T_SC02	Unitless/ [0 – 1]	MISS_UIN T8_FILL

Output	Type/ Dimensions	Description	Units/ Valid Range	Fill Value
dp_ap_m16_tdi_on	Uint8 / nscans	Indicates ASP M16 TDI state	Unitless/ [0 – 1]	MISS_UIN T8_FILL
dp_scan_encdr_delta	Uint16 / nscans	Scan Encoder Delta shift from normal value	Counts / [0-32767]	MISS_UIN T16_FILL
dp_ap_self_test	Uint8 / nscans	DP_AP Self Test State	Unitless/ [0 – 1]	MISS_UIN T8_FILL
se_servo_pwr_sel	Uint8 / nscans	1=XSTRAP, 0=NORMAL. XS2 NORMAL connects PS1_A_PWR and PS1_C_PWR to Servo_A; and PS2_A_PWR and PS2_C_PWR to Servo_B. XS2 XSTRAP connects PS2_A_PWR and PS1_C_PWR to Servo_A; and PS1_A_PWR and PS1_C_PWR to Servo_B; also by SC pt-pt.	Unitless/ [0 – 1]	MISS_UIN T8_FILL
dp_dnb_1a_1b_stage	Uint8 / nscans	What DNB stage 1 data is sent	Unitless/ [0 – 2]	MISS_UIN T8_FILL
dp_dnb_tmng_mode	Uint8 / nscans	DNB Timing mode	Unitless/ [0 – 1]	MISS_UIN T8_FILL
dp_dnb_dark_sub_cal	Uint8 / nscans	Dark pixel subtraction for cal views	Unitless/ [0 – 1]	MISS_UIN T8_FILL
dp_dnb_dark_sub_earth	Uint8 / nscans	Dark pixel subtraction for Earth views	Unitless/ [0 – 1]	MISS_UIN T8_FILL
ap_dc_fast_restor	Uint8 / nscans	1 = Fast_Low_Resolution Restore Algorithm 0 = Slow_High_Resolution Algorithm	Unitless/ [0 – 1]	MISS_UIN T8_FILL
se_a_ham_mir_side	Uint8 / nscans	SE_A Mirror Side	Unitless/ [0 – 1]	MISS_UIN T8_FILL
se_b_ham_mir_side	Uint8 / nscans	SE_B Mirror Side	Unitless/ [0 – 1]	MISS_UIN T8_FILL
se_a_ham_mtr_curr	Int16 / nscans	SE_A Half Angle Mirror Motor Current	Unitless/ [-8192–8191]	NONE
se_a_tele_mtr_curr	Int16 / nscans	SE_A Telescope Motor Current	Unitless/ [-8192–8191]	NONE
se_b_ham_mtr_curr	Int16 / nscans	SE_B Half Angle Mirror Motor Current	Unitless/ [-8192–8191]	NONE
se_b_tele_mtr_curr	Int16 / nscans	SE_B Telescope Motor Current	Unitless/ [-8192–8191]	NONE
ct_prec_tref_mux1ca1	Int16 / nscans	Precision Thermistor Cal Ref Resistor = 4.42Kohm	Unitless/ [-8192–8191]	NONE
ct_prec_tref_mux1ca2	Int16 / nscans	Precision Thermistor Cal Ref Resistor =2.87Kohm	Unitless/ [-8192–8191]	NONE
ct_prec_tref_mux1ca3	Int16 / nscans	Precision Thermistor Cal Ref Resistor =1.47Kohm	Unitless/ [-8192–8191]	NONE
ft_adc_ref	Int16 / nscans	FT ADC Ref 5V	Unitless/ [-8192–8191]	NONE
ft_adc_ref_lw_stpt	Int16 / nscans	FT ADC Ref LW Setpoint Volt Ref	Unitless/ [-8192–8191]	NONE
ft_ckt_gnd	Int16 / nscans	FT Circuit Gnd	Unitless/ [-8192–8191]	NONE

Output	Type/ Dimensions	Description	Units/ Valid Range	Fill Value
ft_lw_cfpa_htr_pwr	Int16 / nscans	FT LW Heater volts	Unitless/ [-8192– 8191]	NONE
ft_lw_setpt_ref	Int16 / nscans	FT LW SETPT Ref	Unitless/ [-8192– 8191]	NONE
ft_sm_cfpa_htr_pwr	Int16 / nscans	FT SM Heater volts	Unitless/ [-8192– 8191]	NONE
ft_sm_setpt_ref	Int16 / nscans	FT SM SETPT Ref	Unitless/ [-8192– 8191]	NONE
se_a_ham_rate_error	Int16 / nscans	SE_A Half Angle Mirror Rate Error	Unitless/ [-8192– 8191]	NONE
se_a_tele_rate_error	Int16 / nscans	SE_A Telescope Rate Error	Unitless/ [-8192– 8191]	NONE
se_b_ham_rate_error	Int16 / nscans	SE_B Half Angle Mirror Rate Error	Unitless/ [-8192– 8191]	NONE
se_b_tele_rate_error	Int16 / nscans	SE_Btelescope Rate Error	Unitless/ [-8192– 8191]	NONE
EV start time	float64/ (nscans)	The Earth View start of scan trigger time in IET	Seconds/ [min-max]	NONE
HAM side	int16/ (nscans)	Mirror side in optical path – “0” for side 1 and “1” for side 2.	Unitless [0 1]	NONE
SDSM – position data	Uint8/(nscans)	Solar Diffuser sensor monitor (SDSM) data of the ENG packet. 0=home, 1=SD view and 2=sun view	Unitless [0 2]	NONE
SDSM – sample data	Float32/(nscans, n_sdsm_detectors(8), n_sdsm_samples(5))	Solar Diffuser sensor monitor (SDSM) data of the ENG packet.	Volts [-2.5 to 2.5]	FLOAT32 _FILL
BB Temps	Int16/ (nscans,6)	Black Body Temperatures	Counts	-999
ap_lw_cca	int16/ (nscans)	Long wave IR CCA Information stored in the Engineering packet.	Counts	-999
ap_sm_cca	int16/ (nscans)	Short/Med wave IR CCA information stored in the Engineering packet.	Counts	-999
ap_vn_cca	int16/ (nscans)	Visible/Near IR CCA information stored in the Engineering packet	Counts	-999
mf_scan_cavity_nxp	int16/	Mainframe Scan Cavity NX PZ Thermistor 46	Counts	-999
mf_scan_cavity_baf_nz	(nscans)	Mainframe Scan Cavity Baffle NZ Precision Thermistor 10	Counts	-999
mf_scan_cavity_baf_pz	int16/ (nscans)	Mainframe Scan Cavity Baffle PZ Precision Thermistor 9	Counts	-999
dp_dnb_cca	int16/ (nscans)	Digital Preprocessor DNB Circuit Card Assembly Thermistor 60	Counts	-999
ft_lw_cfpa_hi_rsl	int16/ (nscans)	FT LW CFPA high resolution temperature	Counts	-999
ft_lw_cfpa_lo_rsl	int16/ (nscans)	FT LW CFPA wide range temperature	Counts	-999
ft_sm_cfpa_hi_rsl	int16/ (nscans)	Focal Plane Array Temperature Controller Long Wave IR High Resolution Temperature	Counts	-999

Output	Type/ Dimensions	Description	Units/ Valid Range	Fill Value
ft_sm_cfpa_lo_rsl	int16/ (nscans)	Focal Plane Array Long Wave Wide Range Temperature	Counts	-999
ft_vis_nir_fpa	int16/ (nscans)	Focal Plane Temperature Controller Visual/Near IR FPA Temperature	Counts	-999
ham_tmp1	int16/ (nscans)	Half Angle Mirror T1 Precision Thermistor 07, Radiatively Coupled Temperature	Counts	-999
ham_tmp2	int16/ (nscans)	Half Angle Mirror T2 Precision Thermistor 08, Radiatively Coupled Temperature	Counts	-999
mf_tel_blkhd_py	int16/ (nscans)	Mainframe Telescope Bulkhead Therm 33, RT16 (Node 1022 in Radiometry Model)	NONE	-999
mf_ao_blkhd_px_nz	int16/ (nscans)	MF_AO_BLKHD_PX_NZ Therm 44	NONE	-999
mf_ao_blkhd_nx_pz	int16/ (nscans)	MF_AO_BLKHD_NX_PZ Therm 45	NONE	-999
mf_stopassy_baff_nz	int16/ (nscans)	On Baffle NZ of Apert Stop Assy between HAM and FM2 Therm 14	NONE	-999
mf_fold_mir_blkhd_ct	int16/ (nscans)	MF_FOLD MIRROR BLKHD Center Therm 6	NONE	-999
mf_ham_blkhd	int16/ (nscans)	MF HAM Bulkhead Therm 43	NONE	-999
ev_ct_prec_tref_mux1c a1	int16/ (nscans)	Precision Thermistor Cal Ref Resistor 1	NONE	-999
ev_ct_prec_tref_mux1c a2	int16/ (nscans)	Precision Thermistor Cal Ref Resistor 2	NONE	-999
ev_ct_prec_tref_mux1c a3	int16/ (nscans)	Precision Thermistor Cal Ref Resistor 3	NONE	-999
DNB_sequence	uint8/ (nscans)	DNB Sequence number	Unitless/ 1 to 36	255
dp_dnb_ccd	int16/ (nscans)	DNB CCD Temperature	Counts	-999
mf_tel_blkhd_nypz	int16/ (nscans)	On Tel Blkhd NYPZ Therm 11	Counts	-999
sdsdmpreamp	int16/ (nscans)	SDSM Preamp Thermistor 57	Counts	-999
South Atlantic Anomaly Flag	uint8/ (nscans)	Lowest 48 bits, one bit for each scan, set to 1 if scan is over the South Atlantic Anomaly	Unitless	None
x_Detector Offsets x = [1 to nbands]	int16/(nscans,nham, ndetectors)	Detector offsets for each scans for each band for each mirror side for each detector.	Unitless	-999
Solar	float32 (nscans x 3)	The solar vector in instrument coordinates, computed at the center time of the Solar Diffuser View sector.	Meters/ Range for each component: [-1.53E11 – 1.53E11]; Range for vector magnitude: [1.46E11 – 1.53E11]	-999
Lunar	float32 (nscans x 3)	Moon unit vector in instrument centered coordinates at center of space view sector.	Unitless/ -1<= Moon Vector <= 1	-999

Output	Type/ Dimensions	Description	Units/ Valid Range	Fill Value
sunZen	Float32/(nscans)	The S/C sun zenith angle with respect to the Solar Diffuser (SD) Reference Frame z-axis, where the positive SD z-axis is defined as the normal to the SD surface.	Radians/ [0 – π]	-999.9
earthSunDistance	Float32/(nscans)	Earth sun distance calculated from the Solar Vector at center of Space View scan.	Meters/1.35 E11 – 1.65E11	-999.9

Note: The field is divide by 4 and truncated.

2.3.2 Algorithm Processing

This is the derived algorithm for the Earth View Radiometric CAL Unit algorithm and is a subclass of the AutoGeneratedProSdrViirsCal and ProCmnAlgorithm classes. The derived algorithm class creates a list of input data items read from DMS and passes required data into the algorithm. All output data items are written to DMS once the algorithm finishes processing this data.

The objective of the Radiometric CAL algorithm is to produce TOA radiances, reflectances (reflective bands only), and brightness temperatures (emissive bands only) for each pixel in an imagery, ideal moderate or day/night band. The radiometric CAL equations are derived from first principles. The equations that are implemented in the code have been simplified through extensive modeling and analysis and careful specification of the algorithm input parameters.

The Earth View Radiometric CAL Unit plus functions for the Reflective Solar Band Automated Calibration Processing Unit are described functionally in the following sections. Figure 11 shows the Earth View Radiometric Calibration Flow. Figure 12 shows the Reflective Solar Band Automated Calibration processing flow. For details on the structure of the various functions, please refer to embedded code comments and the function descriptions located in Section 2.2.2. For variable and structure definitions please refer to embedded code comments and the data dictionary in Rose.

The logic flow of the main program for the Earth View Radiometric CAL algorithm is provided in Figure 11. The core of the CAL algorithm occurs in the functions: `Calibrate_Emissive_Bands()`, `Calibrate_Reflective_Bands()`, and `Calibrate_DayNight_Band()`. Core equations for the reflective and emissive radiometric CAL algorithms are specified in Table 37 through Table 40. A summary of the symbols and units used in these equations can be found in Table 36. For a complete derivation of the radiometric CAL equations used in the science code and used for generating the CAL LUTs and coefficients, refer to the VIIRS Radiometric Calibration Equations Document, D36966, and the Radiometric Calibration ATBD, 474-00027.

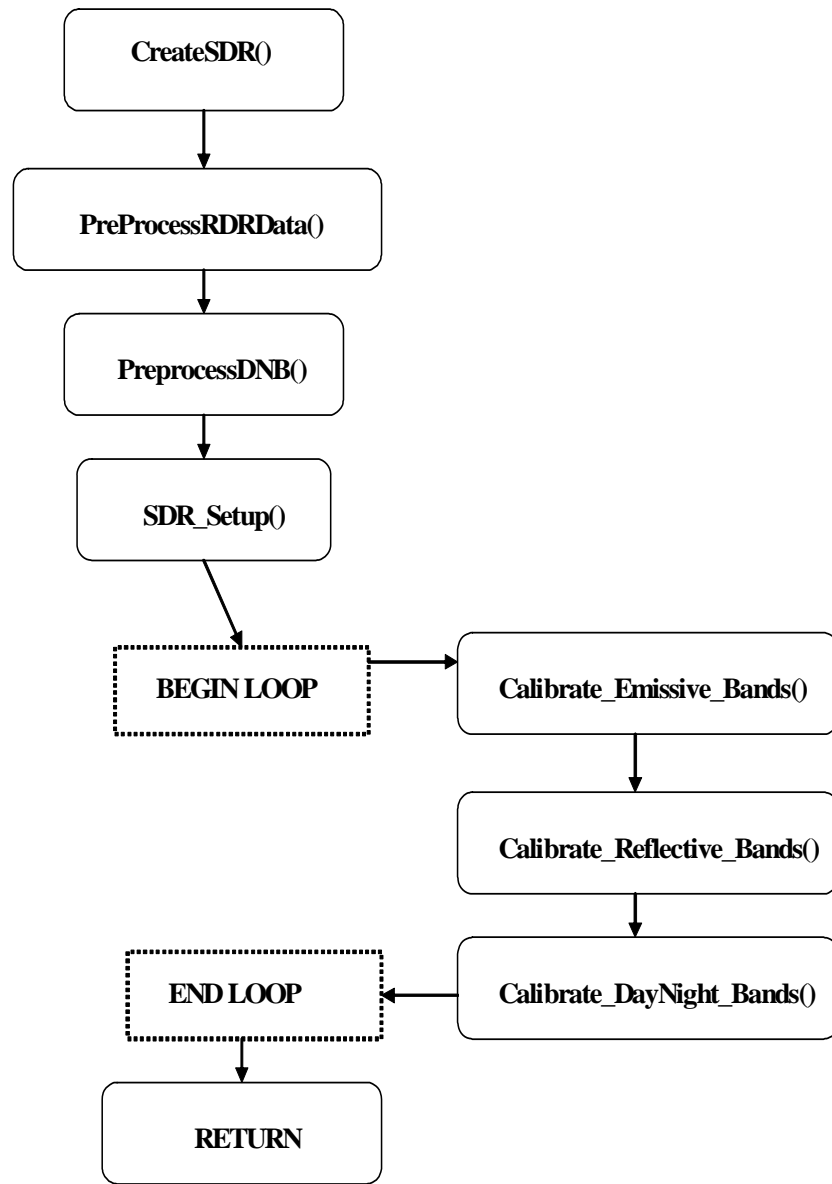


Figure 11 Radiometric Calibration Main Program Flow

2.3.2.1 Sub-frame Offset Compensation

It has been determined that in imagery band samples there is a consistent offset difference between the 1st (odd) and 2nd sub-frames (even). This anomaly is apparent in both space view and black body samples. In order to compensate for this difference, averages are computed for each sub-frame of each offset type, space view or black body. These subframe averages are then swapped per even/odd detector according to the swapEvenOdd arrays and are then used in calibration. Note that this swapping does not occur for the data written out to the OBC IP. For a complete description of the offset difference anomaly see NP-EMD-2007.510.0009_VIIRS_Even_odd_subframe_design and NP-EMD-2009.510.0041 SDR Calibration Imagery Even Odd Parity Fix Code Update.

2.3.2.2 Robust Algorithm Design

Each scan contains data from four views: earth, solar diffuser, space, and black body. In addition each scan contains data regarding DC restore voltage for each detector and thermistor temperatures. These data are used in the calibration algorithm. Since calibration is dependent on all of these inputs, when any input is invalid then an alternate data source is used to replace the invalid data and calibration continues. For a listing of alternate data sources see NP-EDM.2007.510.0010_VIIRS_SDR_Robust_Alg_design. Scans calibrated using an alternate data source are indicated by a non-zero value in the SDR reduced quality flag field. See Table 29.

2.3.2.3 Earth View Radiometric Calibration Error Handling

When the radiometric metrics cannot be computed due to missing input data, dead detectors, invalid electronic background digital numbers, invalid computed CAL coefficients, saturated earth view pixels, or a solar zenith angle greater than 89 degrees (reflectance values only) then the pixel quality flag is set to the appropriate value. The dual gain band pixel quality flags are set according to the convention outlined in Table 27.

2.3.2.4 calibrateSDR()

This is the main driver for the science processing of the EV Radiometric CAL algorithm. It controls each of the calls to the separate modules described below, and is responsible for handling stop calls and processing failures.

2.3.2.5 PreprocessRDR() and PreprocessDNB()

These routines are pre-process parameters needed for scan by scan calibration. Temperatures are determined from VIIRS engineering data. These functions calculate frame-averaged SV counts and standard deviation with outlier rejection for reflective bands. Calibrator gain states are extracted and telemetry and calibrator data are copied to the OBC_IP output item.

2.3.2.6 SDRSetup()

This routine performs a variety of functions in preparation for EV calibration. It calculates radiance and reflectance coefficients, sets up data structures used by CAL routines, as well as initializes QA parameters.

2.3.2.7 Combine_Reduced_Quality_Flags()

This routine calculates and stores the SDR reduced quality flag data in the SDR.

2.3.2.8 Calibrate_Emissive_Bands()

This function calculates emissive band calibrated TOA radiance and brightness temperature for a scan.

2.3.2.9 Find_SV_Scan_Index()

When a dual gain band undergoes either emissive or reflective calibration, the space view with corresponding mirror side and gain state to the current pixel must be used to correctly calibrate the dn value. Due to a dcr state change every four scans, only the space view with the corresponding parameters that is also within the dcr grouping should be used for calibration. At the beginning and end of a granule, it is possible the space view scan required is located within the previous or following granule. This routine determines the correct granule and scan number to use for accurate dual gain calibration.

2.3.2.10 Calibrate_Reflective_Bands()

This function calculates reflective band calibrated TOA radiance and reflectance for a scan.

2.3.2.11 Calibrate_DayNight_Bands()

This function calculates DNB calibrated TOA radiance for a scan. The first frame of a scan line for each of the 16 DNB detectors is filled with zero integer for the Earth View and the three calibration views (Space View, Blackbody View and Solar Diffuser View) in the RDR. This process of zeroing out the first frame for the DNB scan lines is implemented for sensor FU1 to fix an anomaly with hardware.

2.3.2.12 Aggregate_750M_DG()

This function aggregates the dual bands into the single gain resolution. It is responsible for storing the aggregated values in the SDR outputs and the unaggregated values in the Dual Gain IP product.

2.3.2.13 viirs_decmp()

This code decompresses VIIRS earth view packet data. See code headers for copyright and redistribution restrictions.

2.3.3 Graceful Degradation

The VIIRS SDR Calibration procedure contains no graceful degradation.

2.3.3.1 Graceful Degradation Inputs

None.

2.3.3.2 Graceful Degradation Processing

None.

2.3.3.3 Graceful Degradation Outputs

None.

2.3.4 Exception Handling

The code primarily checks for invalid reference values for input and output structures, division by epsilon, and invalid array indexes. These conditions are handled on a case by case basis depending on the purpose of the function they are located within. In all cases an error or debug message is logged. For the dual-gain bands, multiple RDR pixels are aggregated (two or three) together to produce a single output SDR pixel. This creates the possibility of an SDR output pixel where there is a mix of good and bad quality RDR pixels. The dual-gain SDR products therefore have a special quality flag that indicates an aggregated mix of good and bad quality identified as NON_NOMINAL (see Table 11). Problems with CAL cause quality flags to be applied to all SDR pixels that derive from the CAL computation. If CAL source data is missing (space view, solar diffuser, or OBC BB) then a CAL exception occurs and this is applied as a quality flag to all earth view SDR output pixels that require that calibration. Since CAL applies over a whole scan or over multiple scans, this causes a quality flag to be issued for the entire scan.

2.3.5 Data Quality Monitoring

Table 32 shows the VIIRS SDR Calibration data quality monitoring.

Table 32 VIIRS SDR Calibration Data Quality Monitoring

Name	Value	Description
Summary VIIRS SDR Quality	0 – 100 %	Percentage of good quality pixels in granule
Scan Quality Exclusion	0 – 48	Number of scans in granule excluded from processing (including partial scans)

2.3.6 Computational Precision Requirements

The VIIRS SDR CAL routine outputs two structures for each band in the Moderate (750m) resolution, and Imagery (375m) resolution: a scaled version and a non-scaled version of the SDR. The scaled versions of the bands are identified for long term storage, and the non-scaled full floating point versions are used for immediate processing of EDRs and IPs. These full floating point versions are removed by the storage system after an amount of time, post creation.

2.3.7 Algorithm Support Considerations

The DMS and INF must be running before the algorithm is executed.

2.3.8 Assumptions and Limitations

2.3.8.1 I/O Timeliness

Dual gain bands require calibration space view data from the previous granule and next granule. From this, one-granule latency occurs for the dual gain bands.

2.3.8.2 Sci2Ops Issues

The CAL code expects that the Verified VIIRS RDR data follows the “product order” convention for detector numbering, which requires that the highest number detector in scan N lies adjacent to detector number 1 in scan N+1 (see Section 2.2.2.3 of the ATBD, 474-00027).

2.3.8.3 Numerical Computation Considerations

The scientific SDR and EDR algorithms must be convertible into operational code that is compatible with data latency requirements. This essentially means that most EDRs must be completely processed from VIIRS raw data, including CAL and georeferencing, within 28 minutes from the time the raw data are available. The complexity of the calculations used for VIIRS radiometric CAL is similar to those in routine MODIS processing and are therefore expected to perform within a reasonable allocation of the operational timeline.

Here are optimization considerations. The current version of the operational algorithm is deemed to fall within acceptable processing timeline. Should it become necessary then additional optimization can be achieved by threading the algorithm to multiprocess each scan, or multiprocess each CAL step (Reflective, Emissive, DayNight).

2.3.8.4 Additional Assumptions

It is assumed that Verified RDR data are provided in correct time sequence and that complete scans are provided (missing data within a scan is to be filled). It is also assumed that RDR data are reconstructed to remove any coding, compression, and band referencing that was performed on-board.

It is assumed that the time and spacecraft parameters provided in the downlinked data and extracted by the VIIRS Build RDR module are present and correct unless a quality flag is set.

It is assumed that the VIIRS GEO IPs are available at the time of execution of the science code.

It is assumed that sufficient resources are available to support operational processing using the VIIRS Build SDR radiometric CAL algorithm.

It is assumed that the required coefficients and look up tables are complete and provided in the correct format.

Refer to Section 4.0 of the Calibration Algorithm Theoretical Basis Document, D43777, for assumptions made with respect to the on-board processing, input data content, and inputs from pre-launch CAL testing.

2.3.8.5 Additional Limitations

Refer to Section 4.0 of the VIIRS Radiometric Calibration Algorithm Theoretical Basis Document ATBD, 474-00027.

2.4 VIIRS SDR Reflective Solar Band (RSB) Automated Calibration (RSBAutoCal) Description

2.4.1 Interfaces

2.4.1.1 Inputs

The inputs for the Reflective Solar Band Automated Calibration (RSBAutoCal) Data Processing Unit are the VIIRS OBC IP and a suite of Calibration parameter files that include LUTs and CAL coefficients. The input files are summarized in Table 33 and Table 34.

Table 33 RSBAutoCal Data Processing Unit Inputs (Calibration)

Input	Description/Source
VIIRS OBC IP Equivalent Data	The VIIRS On Board Calibrator IP file contains space view, solar diffuser, on-board calibrator blackbody (OBCBB) view observations, the associated gain state and HAM side information, and all engineering and housekeeping data, including raw data from the Solar Diffuser Stability Monitor (SDSM)/VIIRS Earth View Radiometric Calibration Unit. The OBC IP also includes geolocation outputs such as the S/C solar and lunar vectors, the S/C solar zenith angle, and the earth-to-sun distance needed by the SD View Data Processing Unit.

Table 34 RSBAutoCal Data Processing Unit Calibration Parameter Input Files

Input	Description
VIIRS-SDR-SOLAR-IRAD-LUT	See CDFCB-X VIII
VIIRS-SDR-RELATIVE-SPECTRAL-RESPONSE-LUT	Relative spectral response table for day/night, moderate and imagery resolution bands, containing wavelengths and corresponding response values. See CDFCB-X VIII
VIIRS-SDR-DELTA-C-LUT	See CDFCB-X VIII
VIIRS-SDR-TELE-COEFFS-LUT	Thermistor coefficients used to convert thermistor counts to temperature. For more details see CDFCB-X VIII. See CDFCB-X VIII
VIIRS-SDR-RADIOMETRIC-PARAM-LUT	Thermistor weights used for computing the temperatures for the 2 focal planes and Telec. Telect_Therm_Weights[5] Tfpsm_Weights Tfplw_Weights For more details see CDFCB-X VIII.
VIIRS-SOLAR-DIFF-SDSM-TIME-LUT	Scan fractions of SDSM sample times, array of 5 floats
VIIRS-SOLAR-DIFF-ROT-MATRIX-LUT	Solar diffuser rotation matrix, 3x3 array of floats and Solar diffuser stability monitor screen rotation matrix, 3x3 array of floats
VIIRS-SDR-GEO-MOD-PARAM-LUT	Transformation matrix into Solar Diffuser coordinates, 3x3 array of floats
VIIRS-RSBAUTOCAL-BRDF-SCREEN-TRANSMISSION-PRODUCT-RTA-VIEW-LUT	See CDFCB-X VIII
VIIRS-RSBAUTOCAL-BRDF-SCREEN-TRANSMISSION-PRODUCT-SDSM-VIEW-LUT	See CDFCB-X VIII
VIIRS-RSBAUTOCAL-DNB-DARK-SIGNAL-AUTOMATE-LUT	See CDFCB-X VIII
VIIRS-RSBAUTOCAL-DNB-GAIN-RATIOS-AUTOMATE-LUT	See CDFCB-X VIII
VIIRS-RSBAUTOCAL-DNB-LGS-GAIN-AUTOMATE-LUT	See CDFCB-X VIII
VIIRS-RSBAUTOCAL-DNB-MOON-ILLUMINATION-LUT	See CDFCB-X VIII
VIIRS-RSBAUTOCAL-H-AUTOMATE-LUT	
VIIRS-RSBAUTOCAL-H-LUT	Array of float values for minimum elevation, maximum elevation, minimum azimuth, maximum azimuth in SDSM screen coordinates (0 deg elevation and azimuth is perpendicular to SDSM attenuation screen, positive elevation is towards negative Z, positive azimuth is towards negative Y)
VIIRS-RSBAUTOCAL-RSB-F-AUTOMATE-LUT	See CDFCB-X VIII
VIIRS-RSBAUTOCAL-RVF-LUT	See CDFCB-X VIII
VIIRS-RSBAUTOCAL-SDSM-SOLAR-SCREEN-TRANS-LUT	See CDFCB-X VIII
VIIRS-SDR-CAL-AUTOMATE-LUT	See CDFCB-X VIII
VIIRS-SDR-DNB-GAIN-RATIOS-LUT	See CDFCB-X VIII
VIIRS-SDR-DNB-LGS-GAINS-LUT	See CDFCB-X VIII
VIIRS-SDR-DNB-FRAME-TO-ZONE-LUT	See CDFCB-X VIII

Input	Description
VIIRS-SDR-QA-LUT	Contains LUTs related to quality assurance. Consists of the following SDSs: Detector Quality Flags, Moon Offset Limits.

2.4.1.2 Outputs for RSBAutoCal Data Processing Unit

The RSBAutoCa Data Processing Unit has two output files, as described in Table 35. The OBCIP History file contains the RSB F table as well as a collection of useful information from OBCIPs processed. The Cal History file contains the last 20 updates of the RSB F, H, DNB LGS gain, DNB dark signal, DNB gain ratios, and solar processing data.

Table 35 RSBAutoCal: Table Output

Note - This is broken out by Static and Dynamic Section for the same output.

Output	Type	Description/Source	Units	Valid Range
VIIRS-RSBAUTOCAL-OBCIP-HISTORY-AUX	Binary	Field 1: Aggregate Sequence	Field 1: index	Field 1: 1 to 36
		Field 2: HAMside	Field 2: index	Field 2: 0 or 1
		Field 3: Solar Zenith Angle	Field 3: degrees	Field 3: 0 to 360
		Field 4: Night Flag	Field 4: integer	Field 4: 0 or 1
		Field 5: Black Body View Data	Field 5: unitless	Field 5: real
		Field 6: Solar Diffuser View Data	Field 6: unitless	Field 6: real
		Field 7: Space View Data	Field 7: unitless	Field 7: real
		Field 8: Granule ID	Field 8: index	Field 8: 0 to 255
		Field 9: Granule Version	Field 9: index	Field 9: 0 to 255
		Field 10: Orbit	Field 10: index	Field 10: 0 to 4294967297
		Field 11: EV Start Time of First Scan	Field 11: microseconds	Field 11: Int64
		Field 12: numScans	Field 12: index	Field 12: Int32
		Field 13: Solar Event EV Start Time	Field 13: microseconds	Field 13: Int64
		Field 14: RSB F	Field 14: microseconds	Field 14: real
		Field 15: HAM for RSB F	Field 15: unitless	Field 15: Int8
		Field 16: Gain for RSB F	Field 16: unitless	Field 16: Int8
		Field 17: DNB LGS Gains	Field 17: unitless	Field 17: Float32
		Field 18: numSolarEventScans	Field 18: unitless	Field 18: 0 to 127
		Field 19: sdsMValidDataScanEVStartTime	Field 19: index	Field 19: Int64
		Field 20: sdsMValidPosition	Field 20: microseconds	Field 20: 0 to 2
		Field 21: sdsMValidSample	Field 21: unitless	Field 21: Float32
		Field 22: Solar Vector	Field 22: unitless	Field 22: Float32
		Field 23: numSdsMScans	Field 23: unitless	Field 23: 0 to 127
		Field 24: Solar Processine EV Start Time First Scan in First Granule	Field 24: index	Field 24: Int64
		Field 25: Solar Processing Orbit	Field 25: microseconds	Field 25: UInt32
		Field 26: Solar Processing Granule ID	Field 26: unitless	Field 26: 0 to 255
		Field 27: Solar Processing Granule Version	Field 27: index	Field 27: 0 to 255

Output	Type	Description/Source	Units	Valid Range
VIIRS-RSBAUTOCAL-HISTORY-AUX	Binary	Field 1: Orbit Field 2: Solar Event Ref IET Time Field 3: RSB F Field 4: RSB F trend Field 5: RSB F sigma Field 6: RSB F replaced Field 7: H Field 8: H trend Field 9: H sigma Field 10: H replaced Field 11: DNB LGS gain Field 12: DNB LGS gain trend Field 13: DNB LGS gain sigma Field 14: DNB LGS gain replaced Field 15: DNB dark signal Field 16: DNB dark signal trend Field 17: DNB dark signal sigma Field 18: DNB dark signal replaced Field 19: DNB gain ratios Field 20: DNB gain ratios trend Field 21: DNB gain ratios sigma Field 22: DNB gain ratios replaced Field 23: Solar Event Data Valid Field 24: Full Orbit DNB Data Valid	Field 1: index Field 2: microseconds Field 3: unitless Field 4: unitless Field 5: unitless Field 6: integer Field 7: unitless Field 8: unitless Field 9: unitless Field 10: integer Field 11: unitless Field 12: unitless Field 13: unitless Field 14: integer Field 15: unitless Field 16: unitless Field 17: unitless Field 18: integer Field 19: unitless Field 20: unitless Field 21: unitless Field 22: integer Field 23: integer Field 24: integer	Field 1: 0 to 4294967297 Field 2: Int64 Field 3: Float32 Field 4: Float32 Field 5: Float32 Field 6: 0 or 1 Field 7: Float32 Field 8: Float32 Field 9: Float32 Field 10: 0 or 1 Field 11: Float32 Field 12: Float32 Field 13: Float32 Field 14: 0 or 1 Field 15: Float32 Field 16: Float32 Field 17: Float32 Field 18: 0 or 1 Field 19: Float32 Field 20: Float32 Field 21: Float32 Field 22: 0 or 1 Field 23: Int8 Field 24: Int8

2.4.2 Algorithm Processing

This is the derived algorithm for the RSBAutoCal Unit algorithm and is a subclass of the ProCmnAlgorithm class. The derived algorithm class creates a list of input data items read from DMS and passes required data into the algorithm. All output data items are written to DMS once the algorithm finishes processing this data.

2.4.2.1 Automated Reflective Solar Band Calibration Data Processing Logic

The logic flow of the main program for the RSBAutoCal Data Processing algorithm is provided in Figure 12. The core of the RSBAutoCal Data occurs inside processSolarEventFromInto() and processDnbCalDataInto(CalHistory), where RSB F, H, DNB LGS gain, DNB dark signal, and DNB gain ratios are calculated. The outputs are stored in Cal History file.

Core equations used for the Automated Reflective Solar Band Calibration Data Processing algorithm are specified in Table 18. For a complete derivation of the radiometric calibration equations used in the science code for generating the RSB F, H, DNB LGS gain, DNB dark signal offsets, and DNB gain ratios, refer to the VIIRS Radiometric Calibration Equations document, D36966, and the Radiometric Calibration ATBD, 474-00027.

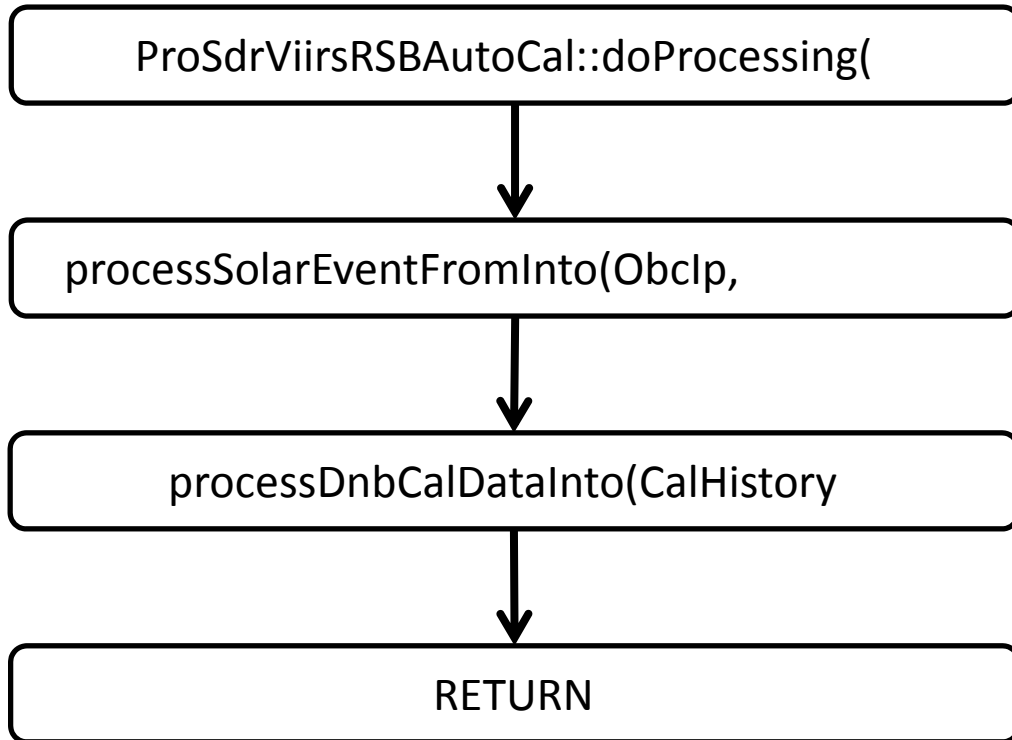


Figure 12 High level RSBAutoCal Data Processing Main Program Flow

2.4.2.2 Calibration Symbols and Units

Table 36 Calibration Symbols and Units

Symbol	Un-notated Indices ³	Description	Units
$a_1(T_{det})$	B, d, g, m	Temperature dependent first order (linear) coefficient of the response function of a detector circuit. This is the effective capacitance of the detector circuit.	Photoelectrons/V
$a_2(T_{det})$	B, d, g, m	Temperature dependent second order coefficient of the response function of a detector circuit.	Photoelectrons/V ²
$agg(N_F)$	N/A	Along-scan aggregation zone for DNB.	Unitless
B	N/A	Band number.	Unitless
$b_1(T_{elec})$	B, d, m	Temperature dependent first order (linear) coefficient of the response function of electronics. This is the inverse of the gain of the combined ADC & ASP circuits.	V/count
$b_2(T_{elec})$	B, d, m	Temperature dependent second order coefficient of the response function of electronics.	V/count ²
$BRDF(\phi_h, \phi_v, \lambda, t)$	B, d	Bi-directional reflectance distribution function of solar diffuser expressed in terms of lab angles.	1/sr
c_0	B, d, g, m	0 order coefficient of the radiance response function.	W/(m ² μm sr)

³ In order to reduce complexity of the notation some indices are dropped in the equations in this document. The following abbreviations are used in this column. B=band number; d=detector number; g=gain state; m=mirror side; n=cross-track pixel number

Symbol	Un-notated Indices ³	Description	Units
$c_1(T_{det}, T_{elec})$	B, d, g, m	Temperature dependent first order (linear) coefficient of the response function for radiance.	W/(m ² μm sr cnts)
$c_2(T_{det}, T_{elec})$	B, d, g, m	Temperature dependent second order coefficient of the response function for radiance.	W/(m ² μm sr cnts ²)
$c_j(T_{det}, T_{elec})$	B, d, g, m	Temperature dependent jth order coefficient of the response function after calibration update.	W/(m ² μm sr cnts ^j)
$c[agg(N_F, N_P, N_G)]$		Pre-determined DNB calibration coefficients, dependent on N_F , N_P , and N_G .	W/(m ² μm sr cnts ^j)
ΔC_j	B, d, g, m	Adjustment to coefficient of the response function.	W/(m ² μm sr cnts ^j)
$d_j(T_{det}, T_{elec})$	B, d, g, m	Temperature dependent jth order coefficient of the response function for reflectance.	1/counts ^j
$d_{se}(t)$		Distance from sun to earth at time t .	Meter
$\overline{d_{se}}$		Distance from sun to earth averaged over a year.	Meter
$dn_{sd}(t)$	B, d, g, m, n	Differential detector counts at solar diffuser with space view subtracted.	Counts
$\overline{dn_{sd}}(t_n)$	B, d, g, m	Differential detector counts at solar diffuser averaged over the acquisition at time t_n .	Counts
$dn_{obc}(t)$	B, d, g, m, n	Differential detector counts at OBCBB with space view subtracted at time t .	Counts
$\overline{dn_{obc}}(t_n)$	B, d, g, m	Differential detector counts at OBCBB averaged over the acquisition at time t_n .	Counts
DN	B, d, g, m, n	Total detector counts.	Counts
DN_{DNB}		Total DNB detector counts.	Counts
$DN_{SV_DNB}[N_F, N_P, N_G]$		DNB space view offset LUT, as a function of N_F , N_P , and N_G .	Counts
dn_{ev}	B, d, g, m, n	Differential detector earth view counts with space view subtracted.	Counts
dn_{DNB}		Differential DNB detector counts with space view subtracted.	Counts
\overline{DN}_{sv}	B, d, g, m	Total detector counts per frame averaged over space view.	Counts
$E_{sun}(\lambda, t), E_{sun}(\lambda, d_{se})$		Irradiance from the sun upon a surface with normal pointing toward the sun.	W/(m ² μm)
F	B, d, g, m	Factor for update of the radiance coefficients.	Unitless
F_{cav}	B	Factor describing the effective solid angle of the cavity as seen by the OBD BB.	sr
F_{sh}	B	Factor describing the effective solid angle of the shield as seen by the OBD BB.	sr
F_{tele}	B	Factor describing the effective solid angle of the telescope as seen by the OBD BB.	sr
G	B	Gain converting detector electron counts to radiance.	W/(m ² μm sr) /photoelectron
$\Delta L_{det}(\theta, B)$	d, m	Differential band-averaged detected spectral radiance at field stop for angle θ relative to space view.	W/(m ² μm sr)
$\overline{L}_{ap}(\theta, B)$	d	Band-averaged spectral radiance at the aperture for scan angle θ .	W/(m ² μm sr)
$\overline{L}_{nsd}(\phi_h, \phi_v, B)$	d	Band-averaged normalized solar diffuser spectral radiance.	W/(m ² μm sr)
\overline{L}_{DNB}		Band-averaged spectral radiance at the aperture for Day Night Band.	W/(m ² μm sr)
$L(T, \lambda)$		Blackbody spectral radiance according to Planck's function.	W/(m ² μm sr)
$L_{obc_rfl}(T_{sh}, T_{cav}, T_{tele}, \lambda)$	B, d, n	Spectral radiance emissive background from shield, cavity and telescope, and reflected off the OBCBB.	W/(m ² μm sr)
N_{acq}		Number of scans over which solar diffuser is observed	Unitless
N_{cal}	B	Number of frames per scan while observing OBCBB.	Unitless

Symbol	Un-notated Indices ³	Description	Units
N_F		Along-scan frame number.	Unitless
N_G		DNB Gain stage.	Unitless
N_H		HAM side index.	Unitless
N_P		Along-track pixel.	Unitless
N_{SDfrm}	B	The number of frames per scan over which the solar diffuser calibration counts are recorded.	Unitless
$RVS(\theta, B)$	d, m	Response Versus Scan function at scan angle θ for band B .	Unitless
$RVS[N_F, N_P, N_H]$		Pre-determined Response Versus Scan for DNB, as a function of N_F , N_P , and N_H .	Unitless
t		Time.	Seconds
t_n		Time of scan n of an acquisition.	Seconds
Δt_{frame}	B	Time between frames or samples for detectors.	Seconds
T_{cav}		Temperature of cavity contributing to reflection off OBCBB.	K
T_{det}		Temperature of FPA detector circuits.	K
T_{elec}		Temperature of electronics module.	K
T_{ham}		Temperature of HAM.	K
T_{obc}		Temperature of OBCBB.	K
T_{rta}		Temperature of RTA.	K
T_{sh}		Temperature of shield contributing to reflection off OBCBB.	K
T_{tele}		Temperature of telescope contributing to reflection off OBCBB.	K
V_{dcr}	B, d	Analog DC restore voltage signal with respect to some nominal dark condition.	V
$\epsilon_{obc}(\lambda)$		Spectral emissivity of the OBCBB	Unitless
θ_{inc}		Incidence angle onto solar diffuser relative to normal.	Radians
θ_{obc}		Scan angle of OBCBB.	Radians
θ_{sd}		Scan angle at solar diffuser.	Radians
θ_{ev}		Scan angle at earth view.	Radians
θ_{sun_earth}		Solar incidence angle of the sun on the earth.	Radians
λ		Wavelength.	μm
$\overline{\rho_{ev}}(\theta_{ev}, B)$		Band-averaged earth view spectral reflectance.	Unitless
$\rho_{rta}(\lambda)$		Spectral reflectance of RTA.	Unitless
$\tau_{sds}(\phi_h, \phi_v, \lambda)$	d	Spectral transmittance of solar diffuser screen.	Unitless
$\phi(t)$		Vertical incidence angle of solar illumination upon SD in laboratory coordinates.	Radians
$\phi_h(t)$		Horizontal incidence angle of solar illumination upon SD in laboratory coordinates.	Radians
ϕ_{inc}		Azimuthal incidence angle onto solar diffuser relative to x-axis.	Radians
$\Phi_{sun}(\lambda, t)$		Spectral output power of the sun.	W/ μm

2.4.2.3 Reflective Calibration Core Equations

Table 37 Reflective Calibration Core Equations (Calibration)

Equations	ATBD Eqn
-----------	----------

Equations	ATBD Eqn
$\overline{L_{ap}}(\theta_{ev}, B) = \frac{\overline{\Delta L_{det}}(\theta_{ev}, B)}{RVS(\theta_{ev}, B)} = \frac{F \cdot \sum_{j=0}^2 c_j \cdot dn_{ev}^j}{RVS(\theta_{ev}, B)} = \frac{\sum_{j=0}^2 c'_j \cdot dn_{ev}^j}{RVS(\theta_{ev}, B)}$	70
$\overline{\rho_{ev}}(\theta_{ev}, B) = \frac{\pi \cdot \sum_{j=0}^2 c'_j dn_{ev}^j}{RVS(\theta_{ev}, B) \cdot \cos(\theta_{sun_earth}) \cdot \overline{E_{sun}}(\lambda, d_{se})}$ $= \frac{\sum_{j=0}^2 d_j dn_{ev}^j}{RVS(\theta_{ev}, B) \cdot \cos(\theta_{sun_earth})}$	81
$dn_{ev} = DN - \overline{DN}_{sv}$	28
$c'_j = F \cdot c_j$	65
$d_j = \frac{\pi}{\overline{E_{sun}}(\lambda, d_{se})} \cdot c'_j$	76
$C_0(T_{det}, T_{elec}) = \Delta C_0(T_{det}, T_{elec})$	Table 18
$C_1(T_{det}, T_{elec}, V_{dcr}) = G \cdot b_1(T_{elec}) \cdot [a_1(T_{det}) + 2a_2(T_{det}) \cdot V_{dcr}] + \Delta C_1(T_{det}, T_{elec})$	Table 18
$C_2(T_{det}, T_{elec}, V_{dcr}) = G \cdot [a_1(T_{det}) + 2a_2(T_{det}) \cdot V_{dcr}] \cdot b_2(T_{elec}) + a_2(T_{det}) \cdot b_1(T_{elec})^2 + \Delta C_2(T_{det}, T_{elec})$	Table 18

2.4.2.4 Emissive Calibration Core Equations

Table 38 Emissive Calibration Core Equations (Calibration)

Equations	ATBD Eqn
$\overline{L_{ap}}(\theta_{ev}, B) = \frac{(1 - RVS(\theta_{ev}, B)) \cdot \left[\left(\frac{1}{\rho_{rta}(\lambda)} - 1 \right) \cdot \overline{L(T_{rta}, \lambda)} - \frac{\overline{L(T_{ham}, \lambda)}}{\rho_{rta}(\lambda)} \right] + F \cdot \sum_{j=0}^2 c_j(T_{det}, T_{elec}) \cdot dn_{ev}^j}{RVS(\theta_{ev}, B)}$	115
$F = RVS(\theta_{obc}) \cdot \frac{\left\{ \left(1 - \frac{1}{RVS(\theta_{obc})} \right) \cdot \left[\left(\frac{1}{\rho_{rta}(\lambda)} - 1 \right) \cdot \overline{L(T_{rta}(t), \lambda)} - \frac{\overline{L(T_{ham}(t), \lambda)}}{\rho_{rta}(\lambda)} \right] \right\} + \overline{\varepsilon_{obc}}(\lambda) \cdot \overline{L(T_{obc}(t), \lambda)} + \overline{L_{obc_rfl}}(T_{sh}(t), T_{cav}(t), T_{tele}(t), \lambda)}{\sum_{j=0}^2 c_j \cdot \overline{dn_{obc}}(t)^j}$	112
$\overline{L_{obc_rfl}}(T_{sh}, T_{cav}, T_{tele}, \lambda) = \left[\begin{array}{l} F_{cav} \cdot (1 - \varepsilon_{obc}(\lambda)) \cdot \overline{L(T_{cav}, \lambda)} + F_{sh} \cdot (1 - \varepsilon_{obc}(\lambda)) \cdot \overline{L(T_{sh}, \lambda)} \\ + F_{tele} \cdot (1 - \varepsilon_{obc}(\lambda)) \cdot \overline{L(T_{tele}, \lambda)} \end{array} \right]$	114
$\overline{dn_{obc}}(t) = \frac{1}{N_{cal}} \sum_{m=0}^{N_{cal}} dn_{obc}(t + m \cdot \Delta t_{frame})$	106
<p>Same c_j values as in Table 37</p>	

2.4.2.5 Day Night Band Calibration Core Equations

Table 39 Day Night Band Calibration Core Equations (Calibration)

Equations	ATBD Eqn
$\overline{L}_{DNB} = \frac{\sum_{i=0}^2 c_i [agg(N_F), N_P, N_G] \cdot dn_{DNB}^i}{RVS[N_F, N_P, N_H]}$	119
$dn_{DNB} = DN_{DNB} - DN_{sv_DNB}[N_F, N_P, N_G]$	120

2.4.2.6 Solar Diffuser View Data Processing Core Equations

Table 40 Solar Diffuser View Data Processing Core Equations (Calibration)

Equations	ATBD Eqn
$F = \frac{RVS(\theta_{sd}, B)}{N_{acq}} \cdot \left(\frac{\overline{d}_{se}}{d_{se}}\right)^2 \cdot \sum_{n=0}^{N_{acq}-1} \left(\frac{\cos(\theta_{inc}(t_n)) \cdot \overline{L}_{nsd}(\phi_h(t_n), \phi_v(t_n), B)}{\sum_{j=0}^2 c_j \cdot \overline{dn}_{sd}(t_n)^j} \right)$	68
$\begin{aligned} \overline{L}_{nsd}(\phi_h, \phi_v, B) &= \overline{(\tau_{sds}(\phi_h, \phi_v, \lambda) \cdot E_{sun}(\lambda, \overline{d}_{se}) \cdot BRDF(\phi_h, \phi_v, \lambda))} \\ &= \frac{1}{4\pi \cdot \overline{d}_{se}^2} \cdot \overline{(\tau_{sds}(\phi_h, \phi_v, \lambda) \cdot \Phi_{sun}(\lambda) \cdot BRDF(\phi_h, \phi_v, \lambda))} \end{aligned}$	67
$\overline{dn}_{sd}(t_n) = \frac{1}{N_{SDfrm}} \sum_{m=0}^{N_{SDfrm}} dn_{sd}(t_n + m \cdot \Delta t_{frame})$	69
$\phi_v = \arctan\left(\frac{\tan \theta_{inc}}{\sqrt{\tan^2 \phi_{inc} + 1}}\right)$	104
$\phi_h = \arctan\left(\frac{\tan \theta_{inc} \tan \phi_{inc}}{\sqrt{\tan^2 \phi_{inc} + 1}}\right)$	105

2.4.2.7 Event Processing

Calibration of the reflective solar bands of the VIIRS instrument happens once per orbit, when the orbit geometry allows it to be illuminated by the sun. Equations describing the calculations of the H factor, F factors, DNB LGS Gains, DNB Dark Signal Offsets, and DNB Gain Ratios are located in the VIIRS Radiometric Calibration Algorithm Theoretical Basis Document (ATBD).

2.4.2.7.1 Solar Event Processing Flow

Figure 13 shows the SDSM Processing Block diagram.

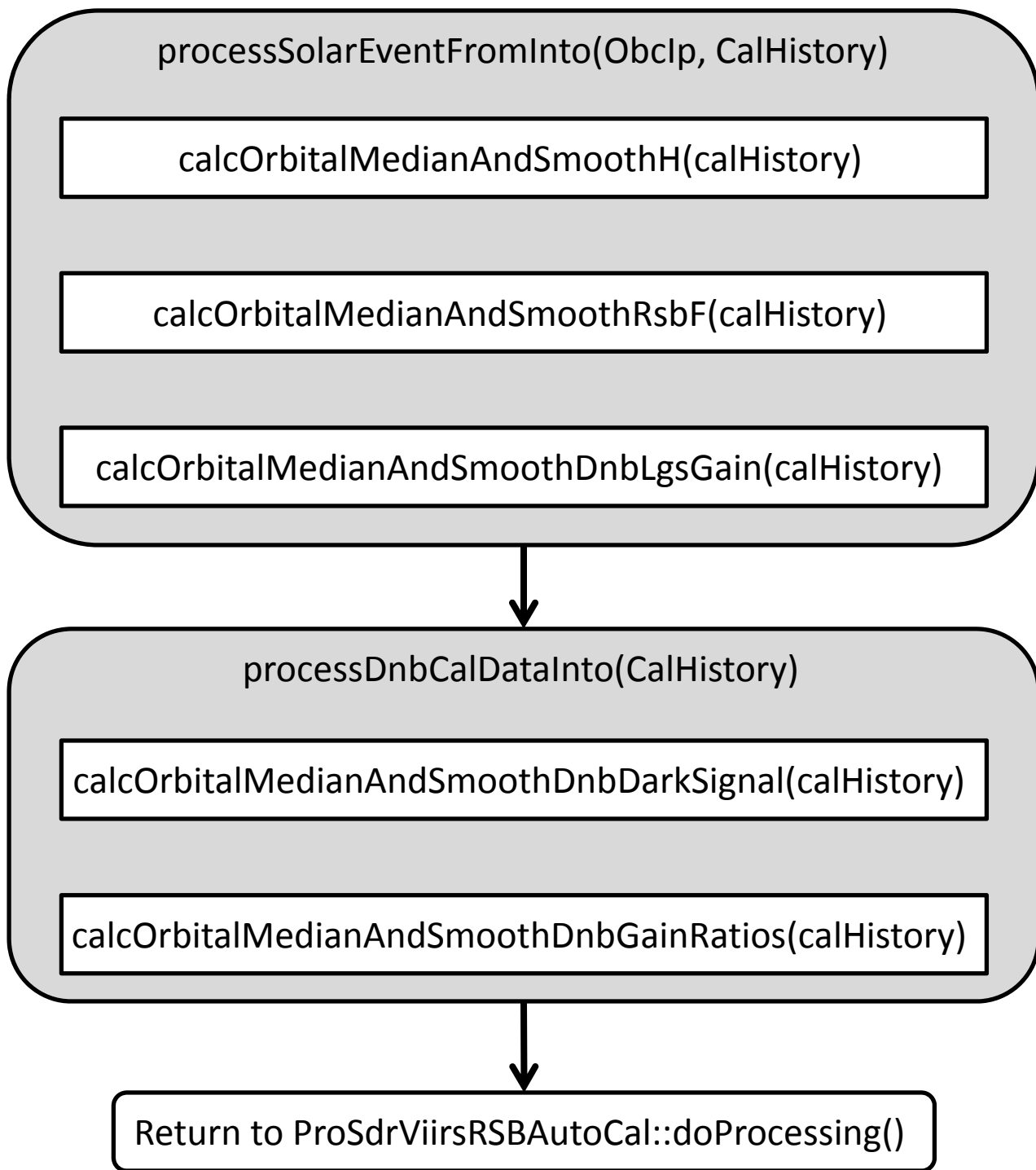


Figure 13 Detailed Solar Event Processing Program Flow

2.4.2.7.1.1 calcOrbitalMedianAndSmoothH

The Solar Diffuser BRDF degradation factors, or “H” factors, are calculated as described in VIIRS Radiometric Calibration ATBD, section 3.3.3.1 for the eight SDSM detectors. The H factors are updated every orbit using measured data from the most recent operation of the SDSM.

2.4.2.7.1.2 calcOrbitalMedianAndSmoothRsbF

The RSB calibration scale factors, or F factors, are calculated as described in VIIRS Radiometric Calibration ATBD, section 3.3.3. The F factors are computed every orbit shortly after the solar calibration data are acquired.

2.4.2.7.1.3 calcOrbitalMedianAndSmoothDnbLgsGain

The DNB LGS gain is calculated as described in VIIRS Radiometric Calibration ATBD, section 3.3.5.3 for each aggregation zone, detector, and mirror side. The gains are computed every orbit in this algorithm shortly after the solar calibration data are acquired.

2.4.2.7.1.4 calcOrbitalMedianAndSmoothDnbDarkSignal

The DNB dark signal offsets are determined from Earth View (EV) data acquired during new moon periods when the instrument is viewing dark, uniform ocean scenes and from calibration sector data acquired every scan (Solar Diffuser (SD), On-Board Calibrator Blackbody (OBC BB), and Space View (SV)). The EV dark scene data are used to generate offsets for every detector, every sample across the EV scan, both Half Angle Mirror (HAM) sides and all three DNB gain stages.

2.4.2.7.1.5 calcOrbitalMedianAndSmoothDnbGainRatios)

DNB LGS gain ratios are calculated from the calibration sector data acquired over the terminator region. Pairs of unsaturated signals for successive gain states, e.g., MGS and LGS, MGS and HGA, or MGS and HGB, are identified and captured. For pairs of dark signals that pass through both filters, gain ratios are calculated as follows:

$$\frac{c_{MGS}}{c_{LGS}} = \frac{dn_{LGS}}{dn_{MGS}}$$

$$\frac{c_{HGA}}{c_{MGS}} = \frac{1}{2} \frac{dn_{MGS}}{dn_{HGA}}$$

$$\frac{c_{HGB}}{c_{MGS}} = \frac{dn_{MGS}}{dn_{HGB}}$$

where:

- c_{MGS} = MGS gain for 13 bit EV data
- c_{LGS} = LGS gain for 13 bit EV data
- c_{HGA} = HGA gain for 14 bit EV data
- c_{HGB} = HGB gain for 14 bit EV data
- dn_{LGS} = LGS offset corrected cal sector counts at 14 bits
- dn_{MGS} = MGS offset corrected cal sector counts at 14 bits
- dn_{HGA} = HGA offset corrected cal sector counts at 14 bits
- dn_{HGB} = HGB offset corrected cal sector counts at 14 bits

Once the gain ratios have been calculated for a given orbit for each calibration sector, detector, sequence order, and mirror side, the values for different calibration sectors are pooled together

into a common set, depending upon the value of a flag in a LUT. Any subset of the three calibration sectors can be selected for use in dark signal determination. The median of the pooled set is calculated as the representative value of the gain ratio for the given orbit.

2.4.3 Graceful Degradation

The VIIRS SDR Solar Diffuser process contains no graceful degradation.

2.4.3.1 Graceful Degradation Inputs

None.

2.4.3.2 Graceful Degradation Processing

None.

2.4.3.3 Graceful Degradation Outputs

None.

2.4.4 Exception Handling

No exception handling is performed in the VIIRS SDR Solar Diffuser process.

2.4.5 Data Quality Monitoring

No data quality monitoring is performed.

2.4.6 Computational Precision Requirements

The VIIRS SDR Solar Diffuser process uses double precision values in order to ensure the required accuracy.

2.4.7 Algorithm Support Considerations

The DMS and INF must be running before the algorithm is executed.

2.4.8 Assumptions and Limitations

The Reflective Solar Band Automated Calibration Processing Unit needs the inputs identified in the two tables of Section 2.4.1.1 before the execution of the code.

2.5 VIIRS SDR Bright Pixel Description

Scattered light can contaminate pixels in the vicinity of bright objects in VIIRS scenes. Also, bright objects can lose light that is scattered to darker areas. Although the fraction of scattered light is low, for a sufficiently bright source near a dim nearby pixel, the scattered contribution can dominate the radiometric uncertainty. This condition is easily understood by considering the

ocean’s color and VIIRS ability to determine that color with a bright cloud in the nearby scene. Several EDRs (ocean color, land albedo, and sea-surface temperature) have exclusion conditions in the NPOESS System Spec around bright pixels, and call for a flag to indicate when scattering is above an acceptable level.

2.5.1 Interfaces

2.5.1.1 Inputs

VIIRS Bright Pixel Inputs are listed in Table 41.

Table 41 VIIRS Bright Pixel Algorithm Inputs

Input	Type	Description
VIIRS 750m (Moderate) SDR	Binary	The VIIRS 750m SDR contains TOA radiances, reflectances (for reflective ‘M’ bands only) and brightness temperatures (emissive ‘M’ bands only) for each VIIRS pixel
Point Spread Functions (PSF) LUT	Binary	The VIIRS point spread functions (PSF) resolved to the resolution of the unaggregated samples for each bands.
Band Replacement LUT	Binary	This file contains proxy (substitution) bands to be used for saturated pixels, scale factor, and alternative maximum radiance. It also inputs the threshold limits for the 4-bit flags.
Bright Pixel Threshold LUT	Binary	This file contains the threshold table by band for flag data to floating point translation.

2.5.1.2 Outputs

The output of this algorithm will be a 4-bit flag for each pixel in each band that characterizes the level of contamination of signal by scattered light.

The percentage of scattered light is defined to be:

$$\% \text{ scattered light} = \left| \frac{S_{scat}}{S_{meas}} \right| * 100$$

4-bit state flag:

- 0000 0.0 - 0.01% scattered light
- 0001 0.01 - 0.02% scattered light
- 0010 0.02 - 0.05% scattered light
- 0011 0.05 – 0.1% scattered light
- 0100 0.1 – 0.2% scattered light
- 0101 0.2 – 0.5% scattered light
- 0110 0.5 - 1.0% scattered light
- 0111 1.0 - 2.0% scattered light
- 1000 2.0 – 5.0% scattered light
- 1001 5 – 10% scattered light
- 1010 >10% scattered light
- 1111 calculation unreliable

VIIRS Bright Pixel Output is listed in Table 42.

Table 42 VIIRS Bright Pixel Output Files

Output	Type	Description
VIIRS 750m (Moderate) Bright Pixel ID	Binary	This data contains all Moderate band Flag data for Bright Pixel at pixel resolution.

2.5.2 Algorithm Processing

2.5.2.1 Estimating % Scattered Light

Scattered light distribution is a property of the telescope & focal plane and is referred to as the near-field scattering. Bright Pixel Algorithm models the scattering with a point-spread function that is composed of a delta function with small epsilon tails. The measured scene is the true scene convolved with the PSF.

Definitions:

- S_{true} = true scene
- S_{meas} = measured scene including scattered light
- P_{true} = true PSF
- P_{meas} = measured PSF
- δ = Dirac Delta Function
- $\delta(i, j) = \begin{cases} 1 & \text{if } i = i_{center} \text{ \& } j = j_{center} \\ 0 & \text{otherwise} \end{cases}$
- i = in-track sample index
- j = in-scan sample index

$$S_{meas} = P_{true} * S_{true}$$

The PSF here is a full optical PSF, including all the effects of Near-Field Scattering (NFS). This is sometimes also referred to as a Point Source Transmittance (PST), but it will be referred to as PSF here. The effect of NFS can be considered as a perturbation, ϵ , with respect to the Dirac Delta function

$$P_{true} = \delta + \epsilon_{true}$$

$$P_{meas} = \delta + \epsilon_{meas}$$

The following normalization conditions apply to both the measured and the true PSF.

$$\sum_i \sum_j P(i, j) = 1$$

$$\sum_i \sum_j \epsilon(i, j) = 0$$

The true scattering in the scene is the difference between the measured scene and the true scene.

$$\begin{aligned} S_{scat} &= S_{meas} - S_{true} = P_{true} * S_{true} - \delta * S_{true} \\ &= (P_{true} - \delta) * S_{true} \\ &= \epsilon_{true} * S_{true} \end{aligned}$$

If the measured scene is convolved again with the PSF, it is found:

$$\begin{aligned} S_{double\ conv} &= P_{meas} * S_{meas} \\ &= (\delta + \epsilon_{meas}) * (\delta + \epsilon_{true}) * S_{true} \\ &= (\delta * \delta + \epsilon_{meas} * \epsilon_{true} + \epsilon_{meas} + \epsilon_{true}) * S_{true} \end{aligned}$$

Subtracting the measured scene from this gives what will be referred to as S'_{scat} .

$$\begin{aligned} S'_{scat} &= S_{double\ conv} - S_{meas} = P_{meas} * S_{meas} - \delta * S_{meas} \\ &= (\delta + \epsilon_{meas} - \delta) * S_{meas} \\ &= \epsilon_{meas} * S_{meas} \\ &= \epsilon_{meas} * (\delta + \epsilon_{true}) * S_{true} \end{aligned}$$

Then it can be written:

$$\begin{aligned} S'_{scat} - S_{scat} &= (\epsilon_{meas} + \epsilon_{meas} * \epsilon_{true} - \epsilon_{true}) * S_{true} \\ \text{or} \\ S'_{scat} &= S_{scat} + (\epsilon_{meas} - \epsilon_{true} + \epsilon_{meas} * \epsilon_{true}) * S_{true} \end{aligned}$$

which reduces to $S'_{scat} = S_{scat}$ when $\epsilon_{true} \cong \epsilon_{meas}$ and $\epsilon_{true} * \epsilon_{meas} * S \cong 0$.

As long as the measured NFS is a good estimate of the true NFS, and NSF is a small contribution to the whole PSF, then the difference between the doubly convolved scene and the measured scene is a good estimate of the scattering. Our estimate of scattered light then is:

$$\% \text{ scattered light} = \frac{S_{scat}}{S_{meas}} * 100 \cong \frac{S'_{scat}}{S_{meas}} * 100 \cong \frac{\epsilon_{meas} * S_{meas}}{S_{meas}} * 100$$

In addition to the above requirements that the measured scattering distribution be close to the real one and much smaller than one, there is another requirement here, that $S_{meas} \gg S'_{scat}$. Very close to a bright object, where the % scattered light is close to or greater than one, the exact value will become very uncertain. However, there is no uncertainty that the scattering is large, but the only thing that is uncertain is how large the scattering is going to be. Since it has been chosen that highest threshold of 10% for the flags, anything above this is flagged as >10% scattered light, so it will not matter whether it is, say, 20% or 40%. Either way, it is much too large an error to provide a meaningful EDR.

\mathcal{E}_{meas} as an estimate of \mathcal{E}_{true}

SBRS measures the LSF and Near-Field scattering. Until such measurements become available for the flight unit, the in-track and cross-track NFS contribution to the PSF will be based on a fit to a Harvey-Shack (H-S) BRDF model. H-S BRDF is translated into \mathcal{E}_{meas} , using the angular separations in the BRDF to describe the scattering to adjacent samples in the in-track and in-scan direction.

$$PSF = \delta + \mathcal{E}_{meas}$$

The true scattering function, \mathcal{E}_{true} , is expected to differ from this, especially over the life of VIIRS as optical surfaces degrade with time, and SBRS has models to estimate this impact. So that our flags are conservatively pessimistic, end-of-life (EOL) estimates are to be used over the entire mission.

2.5.2.2 “Calculation Unreliable” Flag

The tails of the scattering distribution are notoriously difficult to measure since they are several orders of magnitude lower than the peak. The VIIRS near-field response (NFR) test FP-14 uses bright sources that saturate the central pixels to measure the tails and therefore it is expect to know \mathcal{E}_{meas} over several orders of magnitude. There will be some point, however, when the measured tails become unreliable. Computing the scattering fraction becomes problematic when both S_{meas} and S'_{scat} become very small, since the uncertainty of both is inversely related to the value.

A reasonable approach is to set minimum thresholds for each. The flag is then set if both S_{meas} and S'_{scat} are below their associated thresholds. For S_{meas} , a dim pixel threshold S_{lo_thresh} is defined for each band. A reasonable choice for S_{lo_thresh} is L_{min} or, for the emissive bands, is the black body radiance associated with T_{min} .

For S'_{scat} a threshold, S_{scat_thresh} , will be based on test data. Determine the minimum \mathcal{E}_{meas} that is reliable and flag possible conditions where a reference bright target could scatter significant light beyond the measured tails. The bright target, as defined by the spec is at L_{max} and has an angular extent of 12 by 12 milliradians per the System Spec. If θ is the angle which defines the limit of the measurement of the NFS, then $S_{scat_thresh} = S'_{scat}(\theta)$ where $S'_{scat}(\theta)$ is computed for the bright target.

2.5.2.3 Creation of Non-Saturated Scene

Determining the % scattered light using the measured scene and a PSF has been considered; however, there is a difference between the scene needed to do this computation and a VIIRS SDR. The SDR is not a continuous field of radiance, which is what is necessary to do the

convolution described above. Therefore, there are several features of the VIIRS SDR which need to be addressed to produce a continuous scene from the SDR.

- **Saturated radiance**

Values are assigned from a proxy band that has highly correlated radiances and substitute scaled radiances of the proxy band in place of the saturated data in cases where the pixel is saturated. Which proxy bands to use and the scale factors are controlled by a changeable LUT.

If no suitable proxy band is found, or if the radiance in the proxy band is saturated or missing, then default radiance based on maximum reflectance or brightness temperature are used when available. This would be higher than Tmax or Lmax values and lead to a conservative upper estimate of the scattering.

- **In-scan angular resolution and Aggregation**

The PSF is a function of uniformly spaced pixels on the focal plane. Because of the size of the scattering PSF it is faster to convolve using an FFT. Computationally an FFT convolution requires a regular sample interval. Because the in-scan angular resolution changes across an aggregation zone boundary, each aggregation zone has a different angular resolution in-scan. To overcome this problem the aggregated pixels are “de-aggregated” by repeating them by the number of samples that were used in the original aggregation. A guard band would be added that would avoid aliasing of the FFT.

- **Bowtie and Edge of scan effects**

Re-pixelize is needed between the scans because of the “bowtie” overlap with adjacent scans. IDPS uses a common adjacency implementation to correct bowtie and edge of scan effects. This implement is not the same as is used in the science grade code which causes difference the outputs of the science algorithm to the science and operational implementation.

- **Missing radiance**

If the gap in radiance data is small, such as a single pixel, or a row of pixels, then the pixels are estimated by interpolating the nearest neighbors. If the gap is large, then it is filled in with proxy bands.

- **Scan & Granule limits**

The PSF is created to be as wide as or wider than a scan in the in-track direction. Reliable convolution depends on having guard regions around the scene that are about the size of the PSF. Granules are processed so that the granule before and the granule after is always available, so that scans adjacent to the first and last scan of the granule are available.

- **Scene edges**

In the usual processing mode, there is always a granule before and after the current granule. In the case where the process is just starting up, the IDPS algorithm should create a guard region by reflecting the first or last granule in the processing chain so that the flags can be calculated. The alternative is to set the “calculation unreliable” flag until the 2nd or 3rd scan. This is not part of the Science Grade Code. The IDPS Ops code uses the Common

adjacency solution to pad the data with the previous and next scans providing all needed data for calculation.

2.5.2.4 Common Adjacency Use In Bright Pixel

On Board Pixel trim in the SDR data must be replaced in order to provide for continuous data in on board pixel trim regions of each scan before convolution with the point spread function for calculation of the stray light percentages can be done. This replacement was described in the TM as being an area that must be modified by the IDPS operational baseline to use a modified version of the common IDPS operation method of on board bowtie deleted pixel replacement.

The provided implementation uses a spline average replacement as done with the bad data replacement. The TM NP-EMD-2007.510.0011.Rev.A describes this implementation as flawed and as an area that must be fixed in the IDPS operational solution. The method used was described in detail in the TM and has been the subject of a few meetings between IDPS and NGST. Because this has been a point of confusion in the past, a detailed explanation at this point of how this algorithm works has been included.

The first step in the replacement is to find the nearest neighbor for the bowtie deleted pixels in the previous or next scan as needed. The nearest neighbor once identified is then copied into the bowtie area, along with the in-track neighbors to the identified replacement pixel filling all missing bowtie pixels in the in-track direction in current scan being processed. This process is repeated for each cross-track (column) for all onboard bowtie deleted pixels. This is then continued for all scans of data being processed.

2.5.2.5 Data Convolution

In the TM provided, along with explaining the needed changes for the on board pixel trim replacement, it also described a new approach for doing the point spread function convolution to replace the existing science implementation. The new approach is meant to remove discontinuities that can be produced during the convolution of the data. The science implementation takes the SDR data that has been updated to replace bad pixels, saturated pixels, and bowtie pixels and pads the data with the points spread function data and convolutes it with the PSF (point spread function) data. This is implemented in the science code as a by band calculation done once for each band.

IDPS operational implementation follows the method outlined in the TM by instead convoluting each scan separately in a 5-scan matrix. The 5-scan matrixes are made of the current scan as scan 3 of the 5-scan matrix. Scans 1 and 2 are made up of the previous two scans, and scans 4 and 5 are made using the next two scans. After the convolution is completed, only the current scan (scan 3 in the matrix) is maintained for use after the convolution.

Further differences were needed to implement this approach in the IDPS operational baseline for efficiency reasons. The code was modified to process the bowtie replacement on each matrix instead of the whole granule at once. The modification of the data from aggregated to unaggregated VIIRS space were also modified and moved to be done on the matrix of data to prevent duplication of work. Only the current scan is aggregated at the end to make the code more efficient.

2.5.3 Graceful Degradation

The VIIRS Bright Pixel process contains no graceful degradation.

2.5.3.1 Graceful Degradation Inputs

None.

2.5.3.2 Graceful Degradation Processing

None.

2.5.3.3 Graceful Degradation Outputs

None.

2.5.4 Exception Handling

No exception handling is performed in the VIIRS Bright Pixel process.

2.5.5 Data Quality Monitoring

No data quality monitoring is performed.

2.5.6 Computational Precision Requirements

The VIIRS Bright Pixel process uses double precision values in order to ensure the required accuracy.

2.5.7 Algorithm Support Considerations

The DMS and INF must be running before the algorithm is executed.

2.5.8 Assumptions and Limitations

Bright Pixel implementation is currently limited to Moderate band data processing. Image band support is available with minor updates to the code.

3.0 GLOSSARY/ACRONYM LIST

3.1 Glossary

Table 43 contains terms most applicable for this OAD.

Table 43 Glossary

Term	Description
Algorithm	A formula or set of steps for solving a particular problem. Algorithms can be expressed in any language, from natural languages like English to mathematical expressions to programming languages like FORTRAN. On NPOESS, an algorithm consists of: <ol style="list-style-type: none"> 1. A theoretical description (i.e., science/mathematical basis) 2. A computer implementation description (i.e., method of solution) 3. A computer implementation (i.e., code)
Algorithm Configuration Control Board (ACCB)	Interdisciplinary team of scientific and engineering personnel responsible for the approval and disposition of algorithm acceptance, verification, development and testing transitions. Chaired by the Algorithm Implementation Process Lead, members include representatives from IWPTB, Systems Engineering & Integration IPT, System Test IPT, and IDPS IPT.
Algorithm Verification	Science-grade software delivered by an algorithm provider is verified for compliance with data quality and timeliness requirements by Algorithm Team science personnel. This activity is nominally performed at the IWPTB facility. Delivered code is executed on compatible IWPTB computing platforms. Minor hosting modifications may be made to allow code execution. Optionally, verification may be performed at the Algorithm Provider’s facility if warranted due to technical, schedule or cost considerations.
Ancillary Data	Any data which is not produced by the NPOESS System, but which is acquired from external providers and used by the NPOESS system in the production of NPOESS data products.
Auxiliary Data	Auxiliary Data is defined as data, other than data included in the sensor application packets, which is produced internally by the NPOESS system, and used to produce the NPOESS deliverable data products.
EDR Algorithm	Scientific description and corresponding software and test data necessary to produce one or more environmental data records. The scientific computational basis for the production of each data record is described in an ATBD. At a minimum, implemented software is science-grade and includes test data demonstrating data quality compliance.
Environmental Data Record (EDR)	<p><i>[IORD Definition]</i> Data record produced when an algorithm is used to convert Raw Data Records (RDRs) to geophysical parameters (including ancillary parameters, e.g., cloud clear radiation, etc.).</p> <p><i>[Supplementary Definition]</i> An Environmental Data Record (EDR) represents the state of the environment, and the related information needed to access and understand the record. Specifically, it is a set of related data items that describe one or more related estimated environmental parameters over a limited time-space range. The parameters are located by time and Earth coordinates. EDRs may have been resampled if they are created from multiple data sources with different sampling patterns. An EDR is created from one or more NPOESS SDRs or EDRs, plus ancillary environmental data provided by others. EDR metadata contains references to its processing history, spatial and temporal coverage, and quality.</p>
Model Validation	The process of determining the degree to which a model is an accurate representation of the real-world from the perspective of the intended uses of the model. [Ref.: DoDD 5000.59-DoD Modeling and Simulation Management]
Model Verification	The process of determining that a model implementation accurately represents the developer’s conceptual description and specifications. [Ref.: DoDD 5000.59-DoD Modeling and Simulation Management]
Operational Code	Verified science-grade software, delivered by an algorithm provider and verified by IWPTB, is developed into operational-grade code by the IDPS IPT.
Operational-Grade Software	Code that produces data records compliant with the System Specification requirements for data quality and IDPS timeliness and operational infrastructure. The software is modular relative to the IDPS infrastructure and compliant with IDPS application programming interfaces (APIs) as specified for TDR/SDR or EDR code.

Term	Description
Raw Data Record (RDR)	<p><i>[IORD Definition]</i> Full resolution digital sensor data, time referenced and earth located, with absolute radiometric and geometric calibration coefficients appended, but not applied, to the data. Aggregates (sums or weighted averages) of detector samples are considered to be full resolution data if the aggregation is normally performed to meet resolution and other requirements. Sensor data shall be unprocessed with the following exceptions: time delay and integration (TDI), detector array non-uniformity correction (i.e., offset and responsivity equalization), and data compression are allowed. Lossy data compression is allowed only if the total measurement error is dominated by error sources other than the data compression algorithm. All calibration data will be retained and communicated to the ground without lossy compression.</p> <p><i>[Supplementary Definition]</i> A Raw Data Record (RDR) is a logical grouping of raw data output by a sensor, and related information needed to process the record into an SDR or TDR. Specifically, it is a set of unmodified raw data (mission and housekeeping) produced by a sensor suite, one sensor, or a reasonable subset of a sensor (e.g., channel or channel group), over a specified, limited time range. Along with the sensor data, the RDR includes auxiliary data from other portions of NPOESS (space or ground) needed to recreate the sensor measurement, to correct the measurement for known distortions, and to locate the measurement in time and space, through subsequent processing. Metadata is associated with the sensor and auxiliary data to permit its effective use.</p>
Retrieval Algorithm	<p>A science-based algorithm used to ‘retrieve’ a set of environmental/geophysical parameters (EDR) from calibrated and geolocated sensor data (SDR). Synonym for EDR processing.</p>
Science Algorithm	<p>The theoretical description and a corresponding software implementation needed to produce an NPP/NPOESS data product (TDR, SDR or EDR). The former is described in an ATBD. The latter is typically developed for a research setting and characterized as “science-grade”.</p>
Science Algorithm Provider	<p>Organization responsible for development and/or delivery of TDR/SDR or EDR algorithms associated with a given sensor.</p>
Science-Grade Software	<p>Code that produces data records in accordance with the science algorithm data quality requirements. This code, typically, has no software requirements for implementation language, targeted operating system, modularity, input and output data format or any other design discipline or assumed infrastructure.</p>
SDR/TDR Algorithm	<p>Scientific description and corresponding software and test data necessary to produce a Temperature Data Record and/or Sensor Data Record given a sensor’s Raw Data Record. The scientific computational basis for the production of each data record is described in an Algorithm Theoretical Basis Document (ATBD). At a minimum, implemented software is science-grade and includes test data demonstrating data quality compliance.</p>
Sensor Data Record (SDR)	<p><i>[IORD Definition]</i> Data record produced when an algorithm is used to convert Raw Data Records (RDRs) to calibrated brightness temperatures with associated ephemeris data. The existence of the SDRs provides reversible data tracking back from the EDRs to the Raw data.</p> <p><i>[Supplementary Definition]</i> A Sensor Data Record (SDR) is the recreated input to a sensor, and the related information needed to access and understand the record. Specifically, it is a set of incident flux estimates made by a sensor, over a limited time interval, with annotations that permit its effective use. The environmental flux estimates at the sensor aperture are corrected for sensor effects. The estimates are reported in physically meaningful units, usually in terms of an angular or spatial and temporal distribution at the sensor location, as a function of spectrum, polarization, or delay, and always at full resolution. When meaningful, the flux is also associated with the point on the Earth geoid from which it apparently originated. Also, when meaningful, the sensor flux is converted to an equivalent top-of-atmosphere (TOA) brightness. . The associated metadata includes a record of the processing and sources from which the SDR was created, and other information needed to understand the data.</p>

Term	Description
Temperature Data Record (TDR)	<p><i>[IORD Definition]</i> Temperature Data Records (TDRs) are geolocated, antenna temperatures with all relevant calibration data counts and ephemeris data to revert from T-sub-a into counts.</p> <p><i>[Supplementary Definition]</i> A Temperature Data Record (TDR) is the brightness temperature value measured by a microwave sensor, and the related information needed to access and understand the record. Specifically, it is a set of the corrected radiometric measurements made by an imaging microwave sensor, over a limited time range, with annotation that permits its effective use. A TDR is a partially-processed variant of an SDR. Instead of reporting the estimated microwave flux from a specified direction, it reports the observed antenna brightness temperature in that direction.</p>

3.2 Acronyms

Table 44 contains acronyms most applicable for this OAD.

Table 44 Acronyms

Acronym	Description
AM&S	Algorithms, Models & Simulations
API	Application Programming Interfaces
ARP	Application Related Product
CDFCB-X	Common Data Format Control Book - External
DMS	Data Management Subsystem
DPIS ICD	Data Processor Inter-subsystem Interface Control Document
DQTT	Data Quality Test Table
E&A	Ephemeris and Attitude
EV	Earth View
FPA	Focal Plane Array
HAM	Half Angle Mirror
H-S	Harvey-Shack
IEO	Instrument Engineering Order
IET	IDPS Epoch Time
IMG	Imagery
INF	Infrastructure
ING	Ingest
IP	Intermediate Product
IPO	Input Processing Output
LOS	Loss of Signal
LUT	Look-Up Table
MBN	Max Band Number
MDFCB	Mission Data Format Control Book
MOD	Moderate
NCSA	National Center for Supercomputing Applications
NFR	Near-Field Response
NFS	Near-Field Scattering
OBC	On-board Calibrator
OBCBB	On-board Calibrator BlackBody
PO	Product Order
PSF	Point Spread Function
PST	Point Source Transmittance
QF	Quality Flag
RTA	Rotating Telescope Assembly
SDR	Sensor Data Record
SDSM	Solar Diffuser Stability Monitor
SI	International System of Units
TBD	To Be Determined
TBR	To Be Resolved
TOA	Top of the Atmosphere
USES	Universal Source Encoder for Space

4.0 OPEN ISSUES

Table 45 List of TBD/TBR

TBX ID	Title/Description	Resolution Date
None		